Technical Report
TR-17-09
April 2018

Nitrogen compounds in groundwater – Assessment of the influence of blasting during tunnel expansion of the Äspö Hard Rock Laboratory

Frédéric Mathurin

SVENSK KÄRNBRÄNSLEHANTERING AB

SWEDISH NUCLEAR FUEL
AND WASTE MANAGEMENT CO

Box 3091, SE-169 03 Solna
Phone +46 8 459 84 00
skb.se

SVENSK KÄRNBRÄNSLEHANTERING

ISSN 1404-0344
SKB TR-17-09
ID 1601554
April 2018

Nitrogen compounds in groundwater – Assessment of the influence of blasting during tunnel expansion of the Äspö Hard Rock Laboratory

Frédéric Mathurin, Skrivarstugan AB

Keywords: Äspö Hard Rock Laboratory, Groundwater, Nitrogen compounds, Nitrate, Nitrite, Ammonia.

This report concerns a study which was conducted for Svensk Kärnbränslehantering AB (SKB). The conclusions and viewpoints presented in the report are those of the authors. SKB may draw modified conclusions, based on additional literature sources and/or expert opinions.

A pdf version of this document can be downloaded from www.skb.se.

© 2018 Svensk Kärnbränslehantering AB

Abstract

Most explosives used for construction contain various nitrogen compounds. Ammonia and nitrite might facilitate stress corrosion cracking of copper canisters if present in sufficient concentrations in groundwater. Potential contamination from blasting on the natural nitrogen concentration in groundwater and bedrock at repository depth is therefore of concern for the safety assessment of a deep repository. After the construction of the Äspö Hard Rock Laboratory (Äspö HRL) in the early 1990's, explosives have only been used during the excavation of the TASS-tunnel (450 m below sea level) during year 2008 and the excavation of the TASU and TASP tunnels (410 m below sea level) during year 2012. This report focuses on the evolution of the concentrations of dissolved nitrogen compounds with time in the hydro-structures located in the near rock volume of these blasted tunnels at the Äspö HRL. The aim of this report is to assess the possible contamination of fracture groundwater with respect to nitrogen compounds induced by the blasting activity.

The dissolved nitrogen compounds in the hydro-structures were investigated from packed-off borehole sections within pilot boreholes (boreholes drilled along the planned perimeter of the tunnels before excavation), boreholes that are part of the long-term hydrochemical monitoring programme and boreholes drilled from the tunnel wall after excavation. The concentration ranges of dissolved nitrogen compounds (i.e. NH_4^+, NO_2^- and NO_3^-) before the blasting activities allow defining the natural variability in the investigated hydro-structures. By contrast, the concentrations during and after blasting may help to identify the trends with time and possible anomalous concentrations (if any) resulting from the blasting.

The measured concentrations of dissolved NH_4^+ – the dominant dissolved nitrogen compound in the fracture groundwater at Äspö – suggest either relatively constant values or an initial increase during the blasting period and then a progressive decrease to the original concentration several years after completion of the TASS excavation. Several packed off-sections close to the blasted rock volumes of the TASU and TASP tunnel showed moderately increased concentrations months or years after the beginning of the excavation (i.e. specific to each packed-off section). However, the enhanced NH_4^+ concentrations remained within the range of the natural concentrations determined before blasting and thus no extreme NH_4^+ concentrations were observed. The tunnel excavations are believed to indirectly contribute to this moderate increase of dissolved NH_4^+ concentrations through the increased drawdown of groundwater of marine origin near the excavated tunnels.

Anomalously high nitrate and nitrite concentrations, i.e. one order of magnitude higher than the upper range of the natural concentrations determined before blasting, were found in the fracture groundwater after the completion of the tunnel expansion. However, there may be several reasons for the high nitrite concentrations, such as microbial activity leading to nitrification in the section or in the samples and, thus, cannot be strictly attributed to contamination from blasting.

It may therefore be concluded, that the existing data from the TASS, TASU and TASP excavations do not suggest any contamination of nitrogen compounds induced by the use of explosives in the fracture groundwaters.

Contents

1 Introduction

The majority of the explosives used in Sweden are nitrate based (Tilly et al. 2006) and the most common explosives consist of ammonium nitrate (NH_4NO_3). The explosives used during the rock blasting (e.g. road construction, mining) have been implicated as source of nitrogen contamination to drainage water at construction sites but only as potential source of nitrogen contamination in groundwater, due to limited direct evidence (e.g. Degnan et al. 2016, Karlsson and Kauppila 2016). The identification of blasting-related nitrogen compounds can be complicated and it may be difficult to differentiate these compounds from other (natural) nitrogen sources in groundwater, especially at great depth, due to hydrogeological, hydrogeochemical and biochemical factors affecting nitrogen transport and stability.

During handling of explosive and charging of blast holes, the major source for nitrogen contamination from rock blasting is spillage of explosives (Tilly et al. 2006). During and after the detonation, nitrogen contamination results from gas and non-detonated explosive residues, as the NH_4NO_3 salt is highly soluble in water and can contribute to leakage of nitrogen to water. Among the nitrogen compounds, ammonia and nitrite might facilitate stress corrosion cracking of copper canisters if present in sufficient concentrations in groundwater (King et al. 2010). In the deep fractured bedrock, the natural nitrogen cycle and fluxes are highly controlled by the microbial activity, as dissolved nitrogen is a substrate and nutrient in the food chain. Accordingly, high concentration of nitrogen compounds at repository depth could, through production of ammonia and nitrite by microbiologically-mediated redox processes, induce corrosion of the copper canister (Arilahti et al. 2000, King et al. 2001, 2013). Potential contamination from blasting on the natural nitrogen concentration in groundwater and bedrock at repository depth is therefore of concern for the safety assessment of a deep repository.

The effect of blasting on the nitrogen contamination has been investigated during the expansion of the Äspö HRL and the excavation of the TASS-tunnel (Håkansson 2016). High levels of nitrogen were observed mainly in the drainage water after blasting operations, reaching concentrations about 2 orders of magnitude higher (1 to 100 mg L^{-1}) compared to the levels in fracture groundwater. Such concentrations suggested that between 1 and 10 % of the nitrogen content of the explosive material ended up in the drain water. With respect to groundwater, the nitrogen concentrations were mainly studied in seeping water from cracks along the tunnel walls and generally, it did not exceed 0.4 mg L^{-1}. No investigation, in terms of qualitative or quantitative contaminations, has been performed in the water bearing fractures connected to the excavated rock volume, although blast fractures and blast induced fractures (Figure 1-1) can be differentiated in the excavated rock volume (Olsson et al. 2009). The capacity of blast fractures to open up sealed natural fractures and connect the natural fractures with the blast hole – containing high pressure gases from the explosive's detonation or unexploded explosives – motivated the assessment of possible contamination induced by the blasting activity in fracture groundwater with respect to nitrogen compounds.

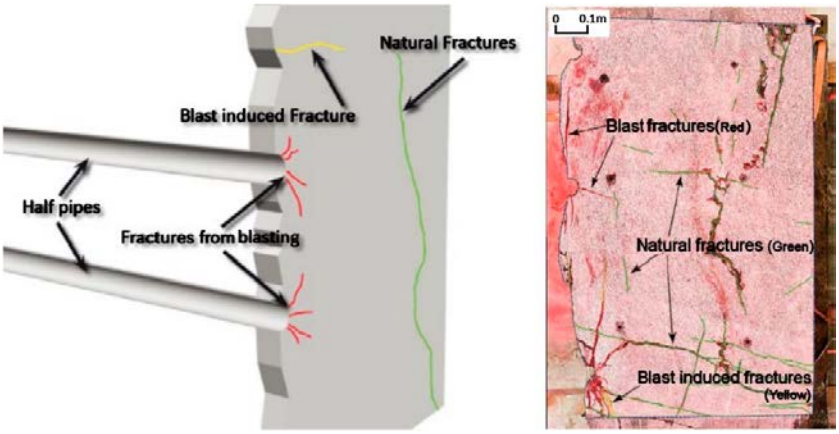

Figure 1-1. *Fracture patterns observed in the rock volume in the vicinity of half pipes drilled for blasting, including natural fractures (green), fracture from blasting (red) and induced by blasting (yellow): (left) schematic representation (Olsson et al. 2004), and (right) photos of digitalized fractures traces from the plane of a rock block (Olsson et al. 2009).*

2 Aim

The aim of this report is to assess the possible contamination of fracture groundwater with respect to nitrogen compounds induced by the blasting activity.

After the construction of the Äspö Hard Rock Laboratory (Äspö HRL) in the early 1990's, explosives have been used during the excavation of the TASS-tunnel (450 m below sea level) year 2008 and the excavation of the TASU and TASP tunnels (410 m below sea level) year 2012. These expansion phases of the Äspö Hard Rock laboratory are the areas of focus for this investigation. Data on the evolution with time of the concentration of nitrogen compounds in groundwater has been evaluated in packed-off borehole sections of boreholes located in the near rock volume of blasted tunnels at Äspö.

Taking into account the natural variability of nitrogen compounds in the fracture groundwater, apparent changes (if any) in the concentrations in response to the tunnel expansion phases are discussed in order to assess whether or not any evidence of contamination from the blasting can be concluded from the existing data. The extent of the evolution (contamination) of the nitrogen concentration with time is also considered of interest in this study in order to obtain a better understanding of the processes involved during the operation phase of a deep repository.

3 Background

3.1 Concern of nitrogen contamination for the KBS-3 system

The KBS-3 system is the concept for disposal of spent nuclear fuel developed and planned to be applied by the Swedish Nuclear Fuel and Waste Management Company (SKB). A KBS-3 repository comprises the rock at the repository site, the canisters containing spent nuclear fuel, the bentonite clay surrounding the canisters, as well as engineered and residual materials that remain in the rock once the underground openings have been backfilled and closed (Figure 3-1).

The canister has a tight, corrosion resistant shell of copper and a load bearing insert of cast iron in which spent nuclear fuel is placed for deposition in the final repository at approximately 500 m depth for at least 100,000 years. The outer copper shell of the canister provides corrosion protection in the deep geosphere, and the canister can be claimed to be immune to stress corrosion cracking (King et al. 2010 and references therein). From a general point of view, the three pre-requisites for stress corrosion cracking are (1) a susceptible material, (2) a tensile stress, and (3) a suitably aggressive environment (King et al. 2010, 2013 and references therein). Ammonia and nitrite in aqueous solution may facilitate stress corrosion cracking. Therefore, the presence of nitrogen compounds in the environment, either by natural occurrence or induced by contamination during the construction and operation of the repository, is of concern for the long term reliability of the canister.

3.2 Tunnel expansion projects

3.2.1 TASS tunnel

The TASS tunnel was excavated from December 2007 to December 2008. It is located at the −450 m level in the Äspö Hard Rock Laboratory and reaches a length of 80.7 m counted from the intersection of the centre line of the TASS tunnel and the centre line of the TASI tunnel from which it emanates (Figure 3-2).

The purpose of the TASS tunnel was mainly to demonstrate the ability of silica sol, an alternative and/or complement to cement-based injection grout, to seal fractures along the tunnel. Different types of explosives, drilling techniques and borehole layouts were tested in a subproject called ‘Excavation’, in order to achieve as good tunnel contours as possible, minimise the damage to the tunnel walls, roof and floor, or, in more general terms, give recommendations on how the final repository for spent nuclear fuel should be excavated.

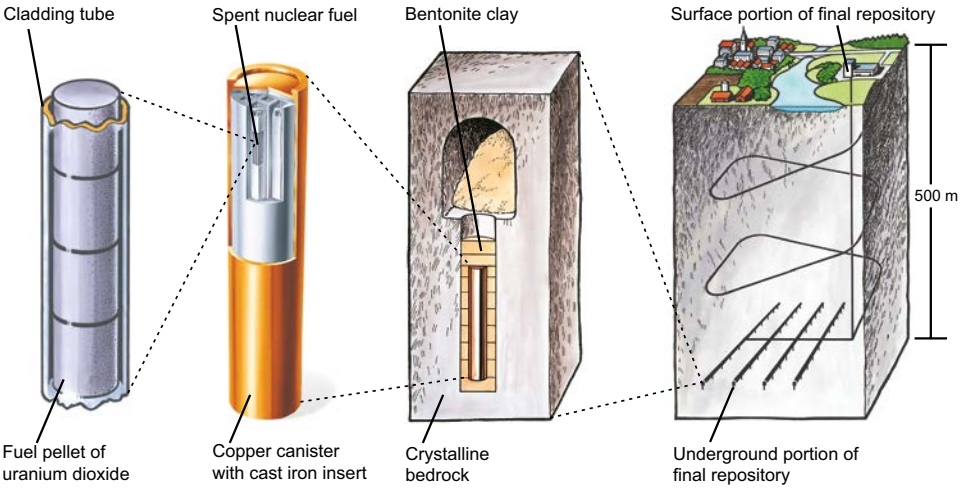

Figure 3-1. *Schematic illustration of the KBS-3 concept for disposal of the spent nuclear fuel (adapted from SKB 2006).*

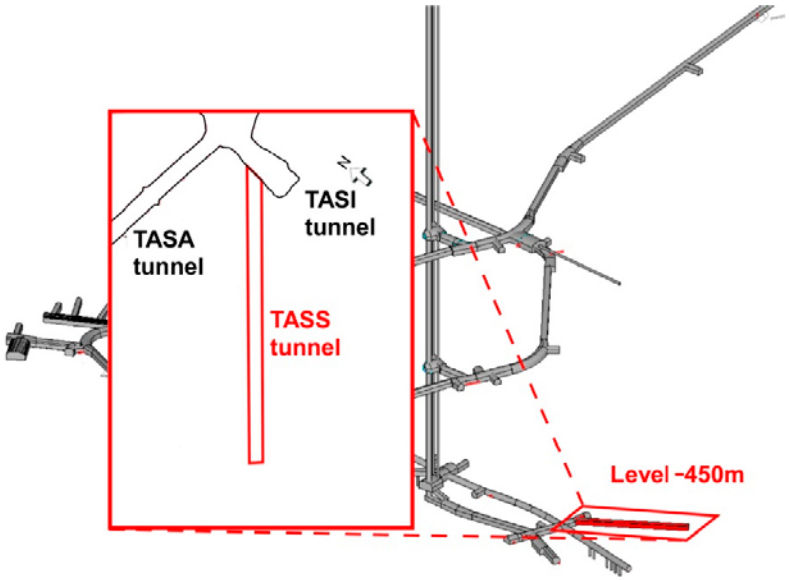

Figure 3-2. *Design of the TASS tunnel in the southwest part of Äspö HRL at the –450 m level. TASS profile (view from above) adapted from Karlzén and Johansson (2010).*

The direction of the tunnel is perpendicular to the zones of water bearing fractures. The area is classified as consisting of fresh Äspö diorite, with steep water bearing fractures in the NW-NNW direction (Olsson et al. 2009).

3.2.2 TASU and TASP tunnels

The TASU and TASP tunnels were constructed with the aim to demonstrate that the methodologies and technologies for the construction according to the KBS-3 design are appropriate for the underground environment. Both tunnels were excavated in the rock volume at the −410 m level, in the northeast part of the Äspö Hard Rock Laboratory. The 65 m long TASU transport tunnel was excavated from March to September 2012, together with three large niches/experimental tunnels (Figure 3-3), while the 80 m long TASP transport tunnel was excavated from March to December 2012, together with four large niches/experimental tunnels (Figure 3-4). The predominant rock types are Ävrö granodiorite and more locally Äspö diorite (Ericsson et al. 2015).

3.3 Use of explosives during blasting

3.3.1 Nitrogen contaminations from explosives

Blasting agents, primarily used in mining operations, are generally composed of a mixture of various components, such as nitroglycerin, nitro glycol, dinitrotoluene and trinitrotoluene (Ekblad 1995). Blasting agents are available in different forms, including plastic, powder and aqueous explosives. The majority of the explosives used in Sweden today are nitrate based (Håkansson 2016), and the most common explosive consist of ammonium nitrate (Tilly et al. 2006), with nitrogen contents ranging between 35 and 65 % of the total mass (Högström and Olin 1990).

Contaminations by nitrogen compounds from explosives may appear in two different ways. First, ammonium nitrate (NH_4NO_3), a highly soluble salt in water, contributes to undetonated explosive leaks of nitrogen to water either during charge or after blasting. Secondly, blasting gives rise to nitrogen gas, N_2. However, in the case of incomplete detonation, toxic nitrogen gases, such as nitric oxide (NO_x) or nitrogen dioxide (NO_2), may also be formed (Ekblad 1995, Håkansson 2016). Some explosives, such as nitroglycerin and nitroglycol, can even give rise to minor N_2(g) amounts during the charge.

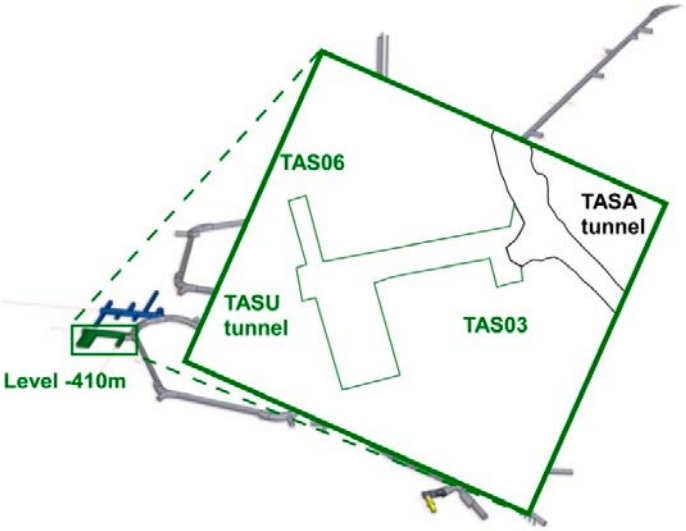

Figure 3-3. *Design of the TASU tunnel and connected niches in the northeast part of Äspö HRL at the –410 m level. The planned TASU design (view from above, adapted from Olofsson et al. 2014) differs slightly from the final design shown on the 3D view.*

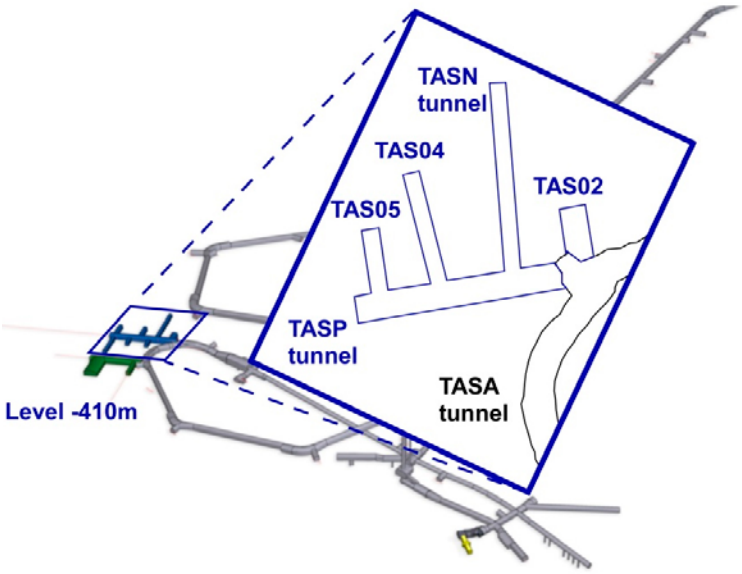

Figure 3-4. *Design of the TASP tunnel and connected niches in the northeast part of Äspö HRL at the –410 m level. The planned TASU design (view from above, adapted from Olofsson et al. 2014) differs slightly from the final design shown on the 3D view.*

Depending on the oxygen supply during the charge, detonation and after blasting, the aqueous nitrogen or gas compounds can be converted to more oxidized or reduced forms. During the explosion both the N_2 and NO gases may react with oxygen:

$N_2(g) + O_2(g) \rightleftharpoons 2\ NO(g)$

$2NO(g) + O_2(g) \rightleftharpoons 2\ NO_2(g)$

Under reduced conditions, such as in water-bearing fractures in the bedrock, ammonia gas (NH_3) can be formed and lead to release of ammonium (NH_4^+) in the aqueous phase:

$NH_3(g) + H^+ \rightleftharpoons NH_4^+$

In a similar way, nitrate and ammonium in the aqueous phase, mainly resulting from the dissolution of unexploded (NH_4NO_3) explosives, can be converted to other forms of nitrogen, depending on the redox environment of the waters. Drainage water present in the tunnel after leaching the blasted rock volume will rapidly reach oxidized conditions favourable to nitrate and nitrite aqueous species. By contrast, reduced conditions prevail in deep water-bearing fractures, i.e. in the undamaged host rock (Auque et al. 2008). Under such conditions, the emitted nitrogen compounds will be subjected to different microbiologically-mediated processes able to convert nitrite and/or nitrate to ammonium in the aqueous phase (Hallbeck and Pedersen 2008a, b).

In his review, Håkansson (2016) concludes that the level of emission of nitrogen compounds to the environment is primarily related to the applied handling and blasting technology, whereas the type of explosive or its nitrogen content is of secondary importance. In other words, the amount of emitted nitrogen to the environment is influenced by the amount of explosive requested by the applied blasting method. Based on his literature search Håkansson concluded that between 1 and 10 % of the total nitrogen content in the explosives is estimated to contaminate the aqueous phase. However, the relative effect of the contamination was found to be strongly related to the natural background concentration of N compounds, which can vary from one site to another. Moreover, such contamination was mainly observed in the drainage water and minor cracks along the tunnel wall related to the excavation damaged zone.

3.3.2 Blasting method for tunnel expansion

Karlzén and Johansson (2010) and Johansson et al. (2015) describe in details the excavation methods applied for the TASS tunnel and for the TASU and TASP tunnels, respectively. The excavation methods are out of scope of this report but some basic information is given here.

The excavation of the TASS tunnel resulted in a total number of 52 blasting events between December 2007 and December 2008. Smooth blasting techniques using cartridge explosives from Orica was applied at all the rounds. An approximated total charge of 3.5 tons of explosives was used for the excavation of the TASS tunnel.

The excavation of the TASU tunnel and the related niches resulted in a total number of 35 blasting events between March and September 2012 and the excavation of the TASP tunnel and the related niches resulted in a total number of 33 blasting events between March and December 2012. Smooth blasting techniques were used primarily with the emulsion explosive Kemiitti 810 and Pentex 25F as blasting caps in all the rounds. The total charge, estimated from the information in Jonsson (2012) and Johansson et al. (2015), was 8.1 and 9.4 tons of explosives for the TASU tunnel and TASP tunnel, respectively. These values exclude the amount of explosive used to excavate the related niches.

4 Description of the rock volumes around the expansion tunnels

Information about the water conductive structures (open rock fractures and fracture zones) is needed when interpreting the hydrogeochemical composition of the groundwater samples. Fractures reaching the tunnels and fractures between boreholes are potential pathways for nitrogen contamination from blasting, and groundwater in these fractures may drain nitrogen compounds (either natural or from blasting events) into the tunnel. The water conductive structures and fractures presented in this section reflect the existing knowledge before the Äspö expansion (TASS, TASU and TASP tunnels). The geological and hydrogeological information were collected from core-drilled pilot boreholes inside the rock volume of the projected contours of the main tunnels and from boreholes drilled prior to the tunnel expansion projects (i.e. for other purposes) and close to the location of the planned excavated rock-volume for the TASA tunnel.

4.1 TASS tunnel

The construction of the TASS tunnel, was preceded by drilling of three pilot boreholes KI0010B01, KI0014B01 and KI0016B01 (each about 100 m long), from the right wall of the TASI tunnel (Hardenby et al. 2008, Hardenby and Sigurdsson 2010). These approximately parallel pilot boreholes within the planned tunnel volume were aimed to give information on the rock quality and possible major deformation/crush zones. Overall parallel to each other and located along the planned perimeter of the TASS tunnel, these pilot boreholes were destructed during the subsequent tunnel excavation (Figure 4-1).

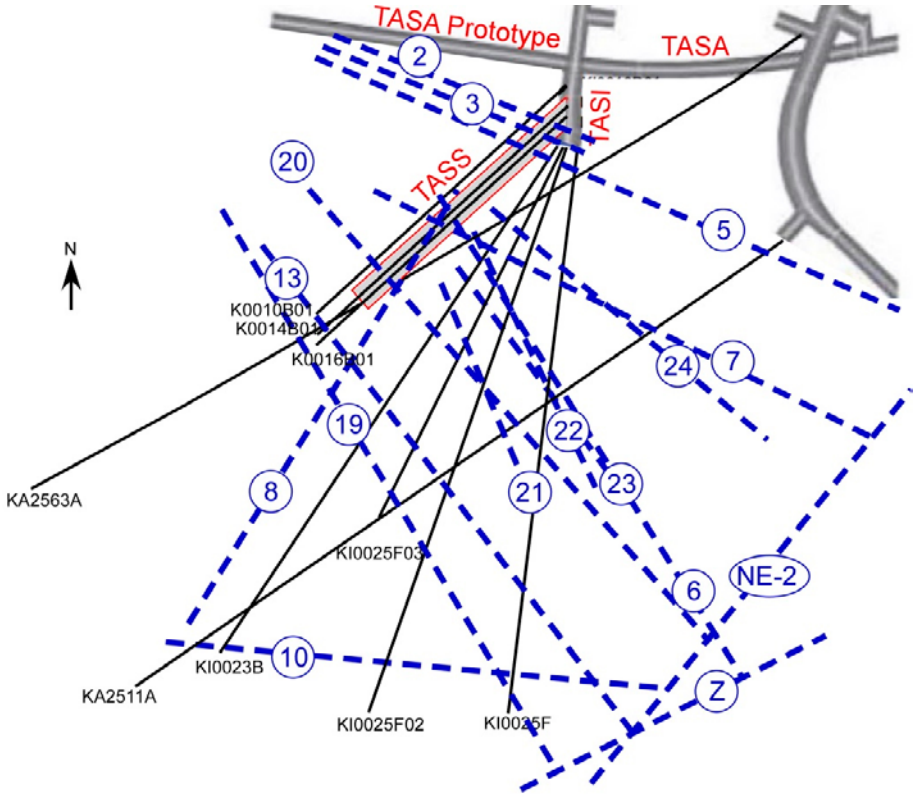

Figure 4-1. *Plan view of the TRUE Block Scale hydro-structural model (adapted from Hardenby and Sigurdsson (2010) and references therein). The approximate outline of the TASS-tunnel has been marked in red, the approximate locations of boreholes K0010B01, K0014B01 and K0016B01 have been indicated as black lines together with existing boreholes KI0025F, KI0025F02, KI0025F03, KA2511A, KA2563A and KI0023B.*

The TASS tunnel was planned in the near proximity of the True Block Scale Experiment site (Figure 4-1). This is a 200x250x100 m rock volume that has been characterised with the purpose of furnishing the basis for tracer transport experiments in a network of conductive structures in the block scale, i.e. 10–100 m (Andersson et al. 2002, Winberg et al. 2003, Andersson et al. 2007). The hydraulic measurements in the three pilot boreholes were compared with the structural Block Scale model defined from already existing boreholes (listed on Figure 4-1). All observed water-bearing structures in the True Block Scale model were mapped and given a structure number (Figure 4-1). Furthermore, they were consistently modelled as flat geometric structures, although in reality they consist of complex and heterogeneous structures. Hydrogeological features were estimated for the most transmissive hydro-structures (Table 4-1).

Points of inflow were identified as possible intersections between boreholes and the extrapolated water conductive structures #5, #7, #8, #20 and #22 from the True Block Scale model (Hardenby et al. 2008, Hardenby and Sigurdsson 2010). Although poorly characterised in term of hydraulic measurements, the water conductive structures #2 #3, and #8 were identified from standard mapping along the TASA Prototype tunnel (Patel et al. 1997).

Table 4-1. Hydrogeological characteristic of the TRUE Block Scale hydro-structural model (compiled from Fox et al. 2005).

Structure ID	Transmissity (m^2 s^{-1})	Aperture (mm)
#5	4.02E-07	0.29
#6	1.91E-07	0.20
#7	9.76E-08	0.14
#10	2.98E-08	0.08
#13	1.38E-08	0.05
#19	1.02E-07	0.15
#20	1.43E-07	0.17
#21	6.02E-08	0.11
#22	2.19E-08	0.07
#23	1.66E-07	0.19
#24	8.51E-08	0.13

4.2 TASU and TASP tunnels

The integrated geological and hydrogeological structural model for the TASU and TASP tunnel was based on information from the pilot boreholes KA3011A01 and KA3065A01 drilled inside the main projected contours of the TASP tunnel and TASU tunnel, respectively (Figure 4-2). In addition, data from the already existing boreholes (KA2050A, KXTT4 and KXTT5) and the newly drilled boreholes (KA2051A01 and KA3007A01) within or close to the rock volume of interest were used to identify and model the extent of the potential continuous water conductive structures in the different boreholes. One example is borehole KA2050A that was drilled from the Äspö spiral (TASA tunnel) during the construction of the Äspö HRL in the early 90's. KA2050A is 211 m long and located above the planned tunnel expansion and penetrates the middle of the pillar separating the TASP and TASU tunnel contours.

A brittle deformation is manifested by two well-defined sub-vertical fracture sets, along with a more scattered group of gently dipping fractures (Ericsson et al. 2015). The predominant set strikes in a NW-SE direction, largely orthogonal to the TASU and TASP tunnels. These water-conductive structures (Morosini M 2012, personal communication), belong – with few exceptions – to the NW-SE deformations zones. Eleven water-conductive structures, representing one or a combination of geological structure(s), were identified (see Figure 4-2 and Table 4-2) from the geological and hydrogeological M2 model (Morosini M 2012, personal communication). These water-conductive structures were consistently modelled as flat geometric structures, although in reality they are complex and heterogeneous structures.

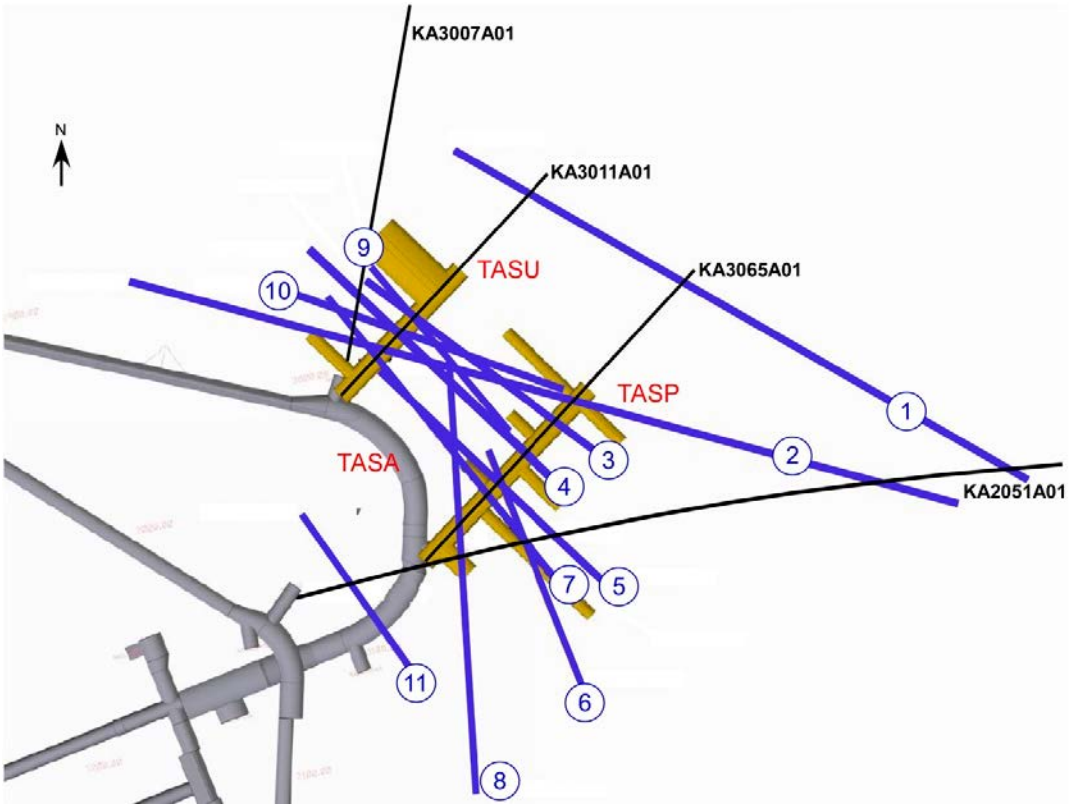

Figure 4-2. *Plan view of the hydro-structural model of the TASU and TASP tunnels (Morosini M 2012, personal communication). The outline of the TASU and TASP-tunnel has been marked in yellow, the locations of the pilot boreholes KA3011A01 and KA3065A01 have been indicated as black lines together with the existing borehole KA2051A01 and KA3007A01.*

Based on the geological and hydrogeological M2 model (Morosini M 2012, personal communication), six water-conductive structures (#2, #3, #4, #5, #7, #10) are interpreted to intersect both the TASU and TASP tunnel (Figure 4-2). One water-conductive structure (#9) and two water-conductive structures (#6, #8) intersect solely the TASU tunnel and the TASP tunnel, respectively. However, they may intercept other water-conductive structures in the middle of the pillar separating the TASP and TASU tunnel contours. The water-conductive structures #1 and #11 were identified at the bottom of the boreholes in the rock volume near the TASA tunnel, located ca. 100 m above the TASU and TASP tunnels, i.e. in the first spiral. The majority of the structures do not terminate against each other into a connected system, but terminate blindly in the rock mass or at the interphase of contact between two different rock types (Ericsson et al. 2015).

Table 4-2. Hydrogeological characteristic of the 11 hydro structures identified from the M2 model (Morosini M 2012, personal communication).

Structure ID (this report)	Borehole	Anomaly ID (M2 model)	Location of the hydraulic feature: (borehole length: m)	Inflow (L min^{-1})	Transmissity (m^2 s^{-1})	Aperture (mm)
#1	KA3065A01	4c				2
#2	KA3007A01	2	12.36	181	8.00E-06	0.5
#3	KA3011A01	4	34.6	34.1	2.04E-07	1
#4	KA3011A01	1a	24.8	12.2	2.00E-07	1
#5	KA2051A01	4	103.32	45	7.00E-06	0.5
#6	KA2051A01	3	82.6	30	6.00E-06	1
#7	KA3065A01	2	24.3	28	4.32E-07	9
#8	KA3065A01	1	10	9.5	5.09E-07	0.5
#9	KA3011A01	3	34.1	4.7	1.08E-07	1
#10	KA3011A01	2a	28.6	10.6	2.63E-07	2
#11	KA2051A01	1a	36.2	7	5.00E-07	7

5 Groundwater sampling

The groundwater data used in this report, with focus on nitrogen compounds, was collected from SKB's quality assured Sicada database. This chapter describes the sampling locations and sampling techniques used for the groundwater sampling.

5.1 Packed-off borehole sections

The packer systems used to isolate sections of boreholes, in order to enable hydrogeological monitoring in the water conductive geological structures of interest, have been gradually optimised by re-instrumentation after the construction of the Äspö HRL. However, possible correlation between hydro-structures and groundwater composition has not been studied so far and the hydraulic situation in the different sampled borehole sections has been poorly characterised in most of the tunnel. Several hydro structural models have been developed near the TASS tunnel (True Block Scale models) and the TASU and TASP tunnels (M2 hydro model). This subchapter presents the isolated borehole sections included in this study and describe the hydro-structures intercepted in the borehole sections in order to integrate the groundwater composition with the current hydrogeological knowledge in the discussion chapter.

5.1.1 Borehole sections near the TASS tunnel

Apart from the pilot boreholes (Figure 5-1; Table 5-1), several other boreholes were located near the planned TASS tunnel. However, only a few boreholes in this part of the tunnel were included in the groundwater chemical (long or short term) monitoring programme carried out at the Äspö HRL during and after the excavation of the TASS tunnel.

The well characterised bedrock volume of the True Block Scale Experiment included only one packed-off borehole section that was sampled on a regular basis (borehole KA2511A) within the long-term monitoring programme for groundwater chemistry before, during and after the excavation of the TASS tunnel (Table 5-1). However, on the other side of the TASS tunnel, six more boreholes (KA3539G, KA3542G01, KA3548A01, KA3554G01, KA3573A, KA3600F; Figure 5-1) were regularly monitored during the period of interest for this project (Table 5-1). In addition, one borehole section in each one of the boreholes KA3548A01 and KA3554G01 was also sampled the year before the excavation of the TASS tunnel (Table 5-1). The data from all these mentioned boreholes should be relatively unaffected by the research experiments performed in the Äspö HRL and therefore suitable for characterisation of the short and long-term impact of the TASS tunnel excavation on the nitrogen compounds.

The borehole sections in borehole KA2511A monitor the groundwater chemistry of the sub-horizontal structure #16 (not shown on Figure 4-1), which turned out to be of minor importance for the connectivity within the True Block Scale rock volume (Andersson 1999). However, hydrogeological responses have been observed during hydraulic interference tests involving the structure #20 (low response), which intercepts the TASS tunnel (Figure 4-1), and the structure #21 (medium response), suggesting a connection between the structure #16 and these two sub-vertical structures (Hermansson 1998, Fox et al. 2005). Although the hydro-structural model in the rock volume located near the TASA prototype tunnel is very limited and poorly described, the packed-off borehole sections in boreholes KA3539G, KA3542G01, KA3548A01, KA3554G01, KA3573A, KA3600F are presumed (in this report) to characterise the groundwater composition in the structure #2, #3 and/or #5, all of them intercepting the TASS tunnel (Figure 4-1).

Table 5-1. Packed-off borehole sections in pilot boreholes of the TASS tunnel and packed-off borehole sections part of the groundwater chemical monitoring program nearby the TASS tunnel. Only sections with available hydrochemical data (n = number of groundwater samples), used for the characterisation and investigation of the evolution of the nitrogen compound concentrations induced by the excavation of the TASS tunnel, are presented.

Borehole ID	Section Up (m)	Section Mid (m)	Section Low (m)	Elevation (m.a.s.l.)	Section (number)	First sampling date	Latest sampling date	n_{tot}	n before tunnel expansion
Packed-off sections in pilot boreholes									
KI0010B01	0.00	50.32	100.64	−446.15		2007-06-26	2007-06-26	1	1
KI0014B01	0.00	50.13	100.27	−447.8		2007-06-26	2007-06-26	1	1
KI0016B01	0.00	50.12	100.24	−446.1		2007-06-26	2007-06-26	1	1
Monitored borehole sections									
KA2511A	103	106.5	110	−394.51	5	1999-04-08	2015-04-28	10	4
KA3539G	15.85	16.73	17.6	−465.66	2	2003-09-24	2010-11-23	5	4
KA3542G01	18.6	19.45	20.3	−462.79	3	2003-09-24	2010-11-23	5	4
KA3548A01	8.8	9.78	10.75	−447.08	3	2003-09-24	2010-11-23	4	3
KA3554G01	22.6	23.38	24.15	−465.34	2	2003-09-24	2010-11-23	5	3
KA3573A	21.0	22.5	24.0	−446.87	2	2002-09-24	2008-05-22	6	5
KA3600F	40.5	41.25	42.0	−445.94	2	2001-10-15	2015-05-27	23	9
KA3600F	43.0	46.55	50.1	−446.94	1	2001-10-15	2015-05-27	19	7
Borehole sections with single sample									
KA3548A01	0.00	15.00	30.00	−447.36		2007-01-09	2007-01-09	1	1
KA3554G01	0.00	15.01	30.01	−459.42		2007-01-09	2007-01-09	1	1

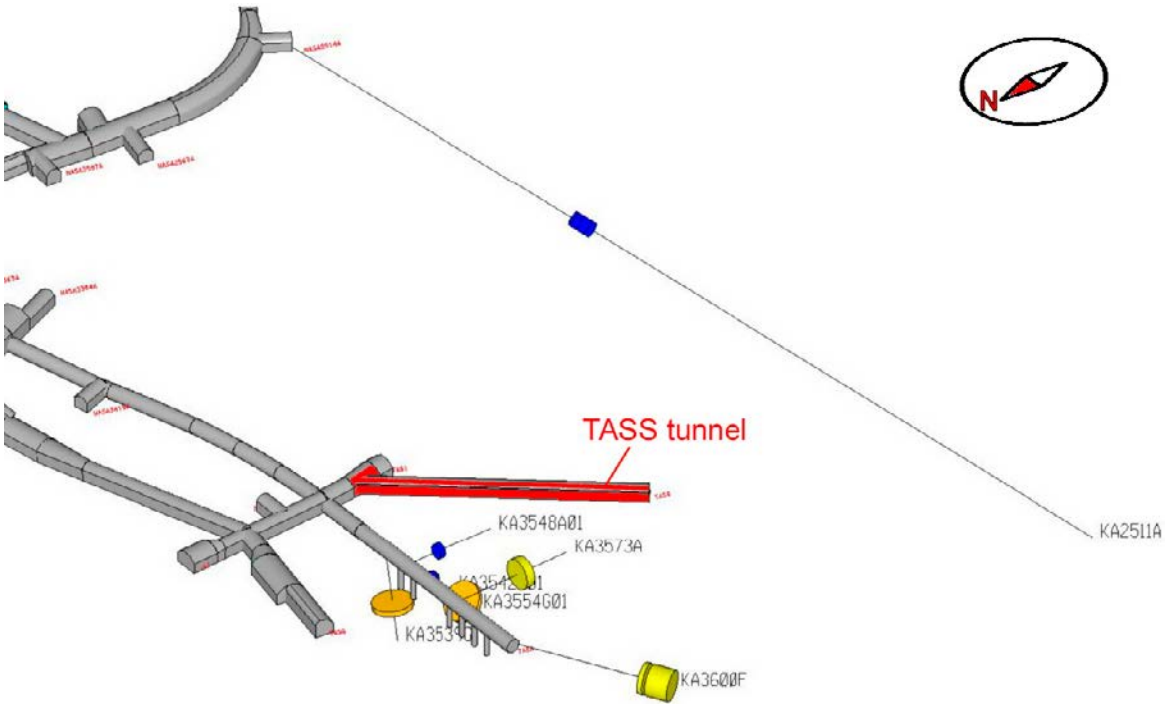

Figure 5-1. *Spatial distribution of the boreholes nearby the TASS tunnel and related borehole sections part of the groundwater chemical monitoring program with analyses of nitrogen compounds. The borehole sections are symbolized by cylinders of different colours and/or diameters mainly for visualisation purpose to distinguish possible overlapping borehole sections.*

5.1.2 Borehole sections near the TASU and TASP tunnels

Pilot boreholes as well as other early or newly drilled boreholes were used for extensive geological, hydrogeological and hydrogeochemical characterization before the expansion and the excavation of the TASP and TASU tunnels. The multidisciplinary characterisation aimed to explore the possibility of developing useful models at different scales for recurrent planning of future construction work and to propose important components to be included in such a modelling methodology. The hydro-geochemical characterisation of nitrogen compounds in this report focuses on the same packed-off borehole sections as used for the development of the local hydro-structural model in the rock volume close to the TASU and TASP tunnel locations (Morosini M 2012, personal communication).

Accordingly, the characterisation and investigation of the evolution of the concentrations of nitrogen compounds induced by the excavation of the TASU and TASP tunnels, are based on packed-off borehole sections from the two pilot boreholes (KA3011A01 and KA3065A01), two boreholes (KA2051A01 and KA3007A01) drilled for the expansion plans and six existing boreholes (KA2050A, KA2858A, KA2862A, KA3067A, KA3105A, KA3110A) drilled at the beginning of the operation phase of the Äspö HRL (Table 5-2). Hydrogeochemical data from the two boreholes (K03009F01 and K08028F01) drilled after the completion of the TASU tunnel (Wallin 2016) were used in this study with a particular focus on the nitrogen compounds in groundwater during drilling and after installation of fixed packed-off borehole sections (Table 5-2). The location of the packed-off borehole sections with respect to the TASU and TASP tunnel are shown in Figure 5-2.

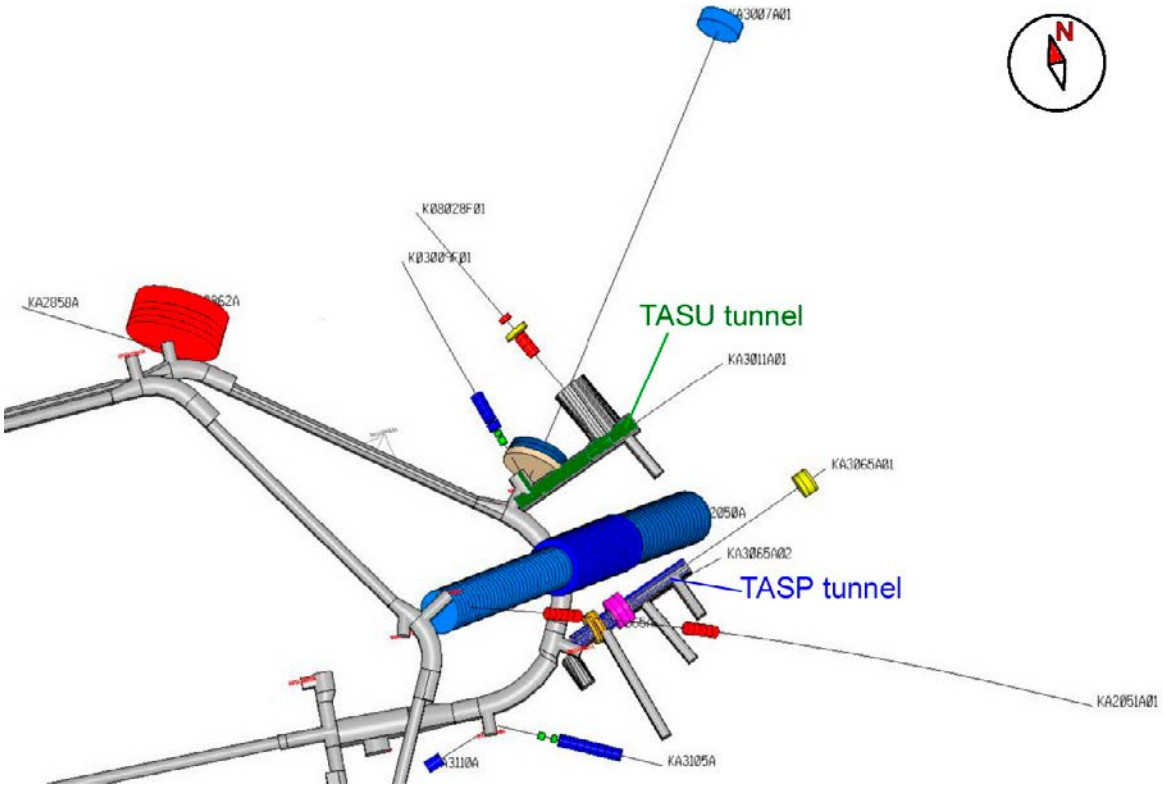

Figure 5-2. *Spatial distribution of the boreholes close to the TASU and TASP tunnels and packed-off borehole sections part of the groundwater chemical monitoring program and including analyses of nitrogen compounds. The packed-off borehole sections are symbolized by cylinders of different colours and/or diameters mainly for visualisation purpose to distinguish overlapping borehole sections.*

Table 5-2. Packed-off borehole sections in pilot boreholes of the TASU and TASP tunnels, packed-off borehole sections part of the groundwater chemical monitoring program nearby the TASU and TASP tunnels and packed-off borehole sections in boreholes drilled along the wall of the TASU tunnel after its completion. Only packed-off borehole sections with available hydrochemical data (n = number of groundwater samples), used for the characterisation and investigation of the evolution of the nitrogen compound concentrations induced by the excavation of the TASU and TASP tunnels, are presented.

Borehole ID	Section Up (m)	Section Mid (m)	Section Low (m)	Elevation (m.a.s.l.)	Section (number)	First sampling date	Latest sampling date	n_{tot}	n before tunnel expansion
Packed-off sections in pilot boreholes									
KA3011A01	28	33.31	38.62	−398.44		2011-11-15	2011-11-15	1	1
KA3011A01	16.38	26.69	37	−398.28		2011-11-16	2011-11-16	1	1
KA3065A01	112	115.06	118.12	−407.32		2012-01-09	2012-01-09	1	1
KA3065A01	19	22.71	26.43	−406.89		2012-01-11	2012-01-11	1	1
KA3065A02	7.5	10.25	13	−409.11	3	2011-10-12	2011-10-12	1	1
Packed-off sections in monitored boreholes									
KA2050A	155	183.28	211.57	−422.81	1	2012-02-28	2014-11-05	8	5
KA2050A	102	128	154	−378.62	2	2012-02-27	2013-03-06	6	4
KA2050A	6	53.5	101	−318.78	3	2012-02-29	2015-05-19	9	1
KA2051A01	120	127.5	135	−349.1	5	2012-02-22	2015-05-19	8	1
KA2051A01	51	59	67	−310.25	9	2012-02-23	2015-05-20	8	1
KA2862A	0	7.99	15.98	−380.63	1	2009-09-23	2015-04-27	15	10
KA3105A	25.51	38.76	52.01	−416.84	2	2013-10-31	2015-05-05	3	0
KA3105A	22.51	23.51	24.51	−415.59	3	2011-10-11	2015-04-27	6	1
KA3105A	17.01	18.26	19.51	−415.16	4	2011-10-10	2015-05-05	2	1
KA3110A	20.05	23.44	26.83	−415.91	1	2009-09-21	2013-05-07	21	14
Packed-off sections in boreholes with single sample									
KA3007A01	9.3	10.83	12.36	−403.37		2011-04-15	2011-04-15	1	1
KA3007A01	12	14.68	17.36	−404.35		2011-05-05	2011-05-05	1	1
KA3007A01	222	224.88	227.76	−456.8		2011-05-18	2011-05-18	1	1
KA2051A01	99.85	109.72	119.59	−339.02		2011-02-16	2011-02-16	1	1
KA2051A01	78	83.5	89	−324.17		2011-02-16	2011-02-16	1	1
KA3067A	30.55	32.05	33.55	−410.98	2	2011-10-07	2011-10-07	1	1
KA3067A	28.05	28.8	29.55	−411.26	3	2011-10-07	2011-10-07	1	1
Packed-off sections in boreholes drilled along the wall of the TASU tunnel									
K03009F01	14.2	15.7	17.2	−399.39		2014-03-03	2014-03-03	1	1
K03009F01	14.5	16	17.5	−399.39	7	2014-10-14	2014-10-14	1	1
K03009F01	17.2	18.7	20.2	−399.42		2014-02-27	2014-02-27	1	1
K03009F01	18.5	19.5	20.5	−399.43	6	2014-10-10	2014-10-10	1	1
K03009F01	21.5	23	24.5	−399.47	5	2014-10-16	2014-10-16	1	1
K03009F01	25.2	26.7	28.2	−391.51		2014-02-25	2014-02-25	1	1
K03009F01	25.5	31.75	38	−399.56	4	2014-10-13	2014-10-13	1	1
K03009F01	30	32	33.99	−399.56		2014-04-15	2014-04-15	1	1
K08028F01	30	31	32	−395.39	6	2014-10-07	2014-10-07	1	1
K08028F01	37	38	39	−395.12	4	2014-10-09	2014-10-09	1	1
Single sample during drilling of the boreholes along the wall of the TASU tunnel									
K03009F01	0.34	1.44	2.55	−399.21		2013-11-12	2013-11-12	1	1
K03009F01	0	7.75	15.5	−399.29		2013-11-29	2013-11-29	1	1

Only a limited number of packed-off borehole sections monitors the groundwater chemistry along the borehole intervals intersected by the identified hydro-structures in the model M2 (Morosini M 2012, personal communication). Among the main 11 hydro-structures, only three of them (#2, #5 and #7) intersect monitored borehole sections in at least two different boreholes (Table 5-3). These three hydro-structures, displaying among the lowest transmissivities measured (Table 4-2), allow studying the spatial evolution or stability of the groundwater chemistry in general and the nitrogen compounds in particular along water conductive structures in both short and long packed-off borehole sections.

Table 5-3. Hydro-structures present in boreholes (based on the M2 model, Morosini M 2012, personal communication) and corresponding packed-off borehole sections with available hydrogeochemical data.

Structure ID	Borehole	Anomaly ID	Location of the hydraulic feature length: [m]	Corresponding borehole sections with hydro-geochemical data (sec up – sec low) [m]	Boreholes with similar structure occurrence	Corresponding bore-hole sections with hydrogeochemical data (sec up – sec low) [m]
#1	KA3065A01	4c	Not identified	–	KA3007A01	KA3007A01 (9.3–12.36)
#2	KA3007A01	2	12.36	KA3007A01 (9.3–12.36)	KA2050A	KA2050A (6–101)
#3	KA3011A01	4	34.6	KA3011A01 (28–38.62)	none	–
#4	KA3011A01	1a	24.8	KA3011A01 (16.38–37)	none	–
#5	KA2051A01	4	103.32	–	KA2050A	KA2050A (102–128)
					KA3065A01	KA3065A01 (19–26.43)
#6	KA2051A01	3	82.6	–	none	–
#7	KA3065A01	2	24.3	KA3065A01 (19–26.43)	KA2050A	KA2050A (102–128)
					KA2051A01	–
#8	KA3065A01	1	10	–	none	–
#9	KA3011A01	3	34.1	KA3011A01 (28–38.62)	none	–
#10	KA3011A01	2a	28.6	KA3011A01 (28–38.62)	none	–
#11	KA2051A01	1a	36.2	–	KA3105A	KA3105A (25.5–52)

In addition to the characterisation of the extent of the hydro-structures within the rock volume, interference tests were performed between pilot boreholes and existing borehole drilled for the expansion plan of the Äspö HRL for most of the hydro-structures. The hydrogeological responses to this set of pressure interference tests were observed in the pressure monitored boreholes in the entire Äspö HRL. The results of the pressure interference test and the corresponding hydrogeochemically monitored packed-off borehole sections are summarised in Table 5-4. Accordingly, the hydrogeochemical continuity or evolution can be followed not only at the scale of the hydro structures, but also extended to the entire network of connected fractures, where interferences were observed, such as the fracture network connected to the structures #4, #7, #9 and #10. In broader terms, a similar approach can be performed within the fracture network connected to the structures #5, #6, #8 and #11, although there is no hydrogeochemistry data available for these structures of interest.

Table 5-4. Connectivity of the hydro- structures with hydrogeological monitored boreholes in the entire Äspö HRL, based on pressure interference test campaign (Morosini M 2012, personal communication) and corresponding packed-off borehole sections with available hydrogeochemical data.

Structure ID	Borehole	Anomaly ID	Borehole length [m]	Borehole sections with hydrogeochemical data sec up – sec low [m]	Hydrogeological response in other borehole sections	Borehole sections with available hydrogeochemical data (sec up – sec low) [m]
#1	KA3065A01	4c			KA3011A01 (bottom) KA2051A01 (bottom)	no
#2	KA3007A01	2	12.36	KA3007A01 (9.3–12.36)	KA3010A KA2051A01	no
#3	KA3011A01	4	34.6	KA3011A01 (28–38.62)	KA2050A KA3010A	KA2050A (155–211)
#4	KA3011A01	1a	24.8	KA3011A01 (16.38–37)	KA2050A	KA2050A (155–211)
#5	KA2051A01	4	103.32		KA2050A KA3065A02 KA3065A03 KA3010A KA3067A KA3068A SA3045A	KA2050A (102–154) KA2050A (6–101) KA3065A02 (7.5–13) KA3010A (8.5–13) KA3067A (30.55–33.55) KA3067A (28.05–29.55) KA3068A (0–16.85)
#6	KA2051A01	3	82.6		KA2050A KA2051A01 SA3045A KA3010A KA3065A02 KA3065A03 KA3067A KA3068A KA3105A	KA2050A (102–154) KA2050A (6–101) KA2051A01 (78–89) SA3045 (6–8) KA3010A (8.5–13) KA3065A02 (7.5–13) KA3067A (30.55–33.55) KA3067A (28.05–29.55) KA3068A (0–16.85)
#7	KA3065A01	2	24.3	KA3065A01 (19–26.43)	KA3065A02 KA2050A	KA2050A (102–154)
#8	KA3065A01	1	10	no	KA2050A KA2051A KA3011A0	KA2050A
#9	KA3011A01	3	34.1	KA3011A01 (28–38.62)	KA2050A KA3010A	KA2050A (155–211) KA2050A (102–154) KA3010A (8.5–13)
#10	KA3011A01	2a	28.6	KA3011A01 (28–38.62)	KA2050A:01 KA3011A01	KA2050A (6–101)
#11	KA2051A01	1a	36.2	no	KA3105A (all sections) KA3110A (all sections) KA3065A02 (all sections) KA2050A (all sections) KA3105A	KA3105A (17.01–19.51) KA3105A (22.51–23.51) KA3105A (25.51–38.76) KA3110A (6.55–19.05) KA3110A (20.05–26.83) KA3065A02 (7.5–13) KA2050A (6–101) KA2050A (102–154) KA2050A (155–211.57)

5.1.3 Groundwater chemical monitoring programme

Considerable amounts of geoscientific data, including hydrogeochemical data have been produced at the Äspö HRL since the start of the pre-investigations in 1986, during the construction phase of the main access tunnel from 1990 to February 1995, and during the operation phase (ongoing since 1995). The entire Äspö hydrogeochemical dataset, covering the period 1986–2014, has been revisited in this study in order to define the natural variability of nitrogen compounds in groundwater at Äspö.

With respect to nitrogen compounds, the dataset includes NO_2-N, NO_3-N, and NH_4-N concentrations from the pre-investigation phase, although the nitrogen compounds, individually or in general, were not systematically analysed in each groundwater sample. Most of the samples collected between 1990 and 2003 included only NH_4-N determinations. Since 2004, also NO_2-N and NO_3-N concentrations were included together with the NH_4-N concentrations in almost all the collected groundwater samples. Accordingly, the data set for nitrogen is relatively limited and most analyses cover only NH_4-N. The number of analyses is still enough to show a clear pattern in terms of the nitrogen compounds.

In general terms, the hydrogeochemical dataset from Äspö indicates an artificially imposed dynamic flow system, with the addition of other anthropogenic effects (e.g. experimental tracer test, pumping test) to the expected gradual changes caused by the presence of the tunnel system. Therefore, the characterisation of the natural variability of nitrogen compounds cannot only be restricted to the concentration ranges, but should be studied over time. To fulfil this requirement, the choice has been made to work with temporal snapshots of the concentrations of the different nitrogen compounds in groundwater samples collected in the entire Äspö HRL.

Six periods have been selected to apply this strategy: (1) the pre-investigation period, (2) year 1995, (3) year 2004, (4) year 2007, (5) year 2011 and (6) year 2014. The snapshot of the pre-investigation period, corresponding to groundwater samples collected from surface boreholes during the years 1988 and 1989, represents the fracture groundwater chemistry under conditions undisturbed from the tunnel construction and operation. The snapshot of the year 1995 represents the hydrogeochemical conditions at the end of the Äspö tunnel construction and the related intense dynamic flow. The snapshot of the year 1999 displays the hydrogeochemical conditions after 5 years of operation phase. The snapshots of the years 2007 and 2011 represent the hydrogeochemical conditions the year before the excavation of the TASS tunnel and before the excavation of the TASU and TASP tunnels, respectively. The snapshot of the year 2014 represents the most recent hydrogeochemical conditions based on the dataset used (i.e. data freeze December 2014) after the excavation of the TASS, TASU and TASP tunnels.

The dataset relies on packed-off borehole sections with determined concentration of at least one of the nitrogen compounds (i.e. NO_2-N, NO_3-N, or NH_4-N). The snapshot of the hydrogeochemical conditions during the pre-investigation period is composed of groundwater observations collected from packed-off borehole sections in five boreholes drilled from the surface (Figure 5-3) and covering a depth range between −64.88 and −914 m.a.s.l. (Table 5-5).

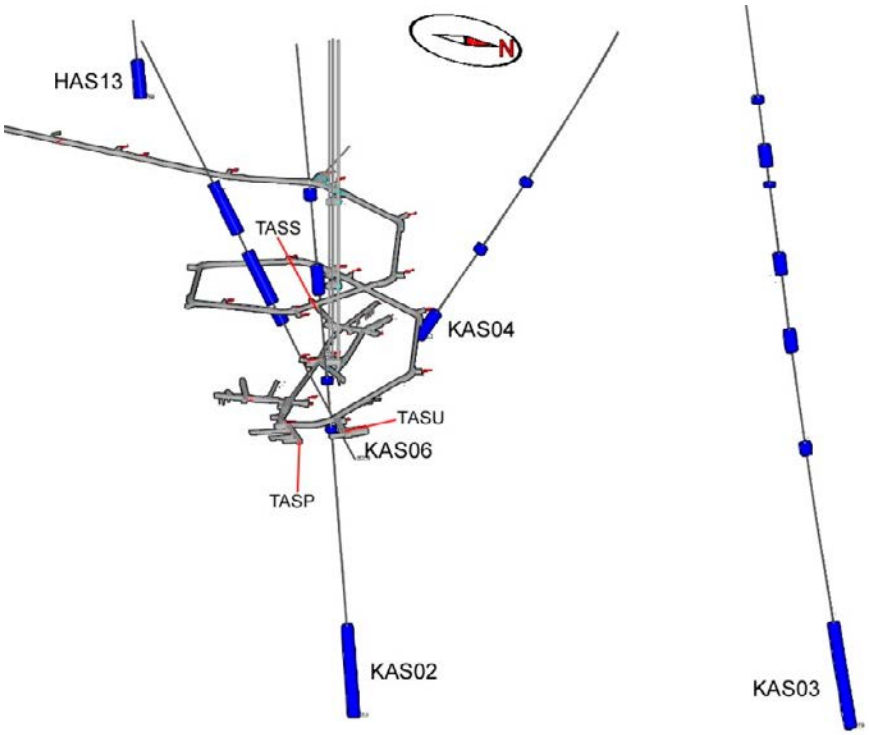

Figure 5-3. 3D distribution of the Äspö HRL and the hydrochemically monitored borehole sections in the surface boreholes close to the Äspö HRL.

Table 5-5. Borehole sections with available hydrochemical data from the pre-investigation in the Äspö area (years 1988–1989) and used in this report for the evaluation of the natural variability of the nitrogen compound concentrations in groundwater before the construction of the Äspö HRL.

Borehole ID	Section Up (m)	Section Mid (m)	Section Low (m)	Elevation (m.a.s.l.)	Sampling date
KAS02	202	208.25	214.5	−199.81	1989-01-11
KAS02	314	316.5	319	−307.69	1988-03-30
KAS02	308	326	344	−317.15	1988-09-27
KAS02	463	465.5	468	−456.16	1988-04-20
KAS02	530	532.5	535	−522.95	1988-05-03
KAS02	802	863.02	924.04	−852.34	1988-09-20
KAS02	860	892.02	924.04	−881.22	1989-01-30
KAS03	129	131.5	134	−121.78	1989-02-21
KAS03	196	209	222	−198.73	1988-08-10
KAS03	248	249.5	251	−238.92	1988-08-28
KAS03	347	360	373	−348.56	1988-08-16
KAS03	453	466.5	480	−454.25	1988-08-21
KAS03	609	616	623	−602.45	1988-09-01
KAS03	860	931.03	1002.06	−914.04	1989-03-14
KAS04	226	230.5	235	−185.15	1989-04-13
KAS04	334	338.5	343	−275.61	1989-04-26
KAS04	440	460.49	480.98	−376.76	1989-03-29
KAS06	204	240.5	277	−200.04	1989-05-31
KAS06	304	340.5	377	−284.37	1989-06-07
KAS06	389	397.5	406	−331.85	1989-06-14
KAS06	439	520.59	602.17	−433.25	1989-06-21
HAS13	51	75.5	100	−64.88	1989-07-03

Snapshots of the hydrogeochemical conditions during years 1995, 1999, 2007, 2011 and 2014 include mainly observations from boreholes drilled along the Äspö HRL tunnel wall. The long-term hydrogeochemical monitoring programme carried out in the tunnel boreholes included 33 packed-off borehole sections (Table 5-6). The groundwater was collected once or twice a year from the packed-off borehole section for at least three consecutive years or more. These packed-off borehole sections intersect deformation zones and fractures at depth between −69 and −566 m.a.s.l. along different parts of the Äspö HRL (Figure 5-4). The other groundwater samples during the years of interest for the snapshots were either collected only for short periods for specific projects or not on regular basis and are therefore considered part of the short term monitoring programme thereafter. The number of packed-off borehole sections within the short term monitoring programme varies from a year to another, including 26 borehole sections during year 1999 (Table 5-7), 16 borehole section during year 2007 (Table 5-8), 15 borehole sections during both year 2011 (Table 5-9) and year 2014 (Table 5-10).

Table 5-6. Borehole sections included in the long term groundwater chemical monitoring programme and used for the characterisation and investigation of the natural variability of the nitrogen compound concentrations in fracture groundwater at Äspö.

Borehole ID	Section Up (m)	Section Mid (m)	Section Low (m)	Elevation (m.a.s.l.)	First sampling date	Lasted sampling date	1995	1999	2007	2011	2014
HA2780A	0.4	21.85	43.3	−380.52	2007-10-05	2014-05-12			y	y	y
HD0025A	0	7.5	15	−415.76	1999-10-04	2014-11-21		y	y	y	y
HG0038B01	1	2.3	3.6	−446.73	2007-10-03	2011-11-10			y	y	
KA1061A	0	104.25	208.5	−143.98	1999-10-01	2011-11-16		y	y	y	
KA1755A	88	124	160	−279.89	1995-10-12	2014-05-09	y	y	y	y	y
KA2050A	155	183.28	211.57	−378.62	1999-04-08	2014-11-05		y	y		y
KA2162B	201.5	244.8	288.1	−353.21	1999-09-30	2011-11-21		y	y	y	
KA2511A	103	106.5	110	−394.51	1999-09-30	2014-05-08		y			y
KA2862A	0	7.99	15.98	−380.63	1999-10-06	2014-04-01		y		y	y
KA3105A	22.51	23.51	24.51	−415.59	2011-10-11	2014-04-07				y	y
KA3110A	20.05	23.44	26.83	−415.91	1999-10-01	2014-04-02		y	y		y
KA3385A	32.05	33.11	34.18	−448.35	1999-09-29	2014-05-14		y	y	y	y
KA3600F	40.5	41.25	42	−446.78	2007-01-09	2014-05-07			y	y	y
KA3600F	43	46.55	50.1	−446.94	2007-10-03	2014-05-07			y	y	y
KAS03	107	179.5	252	−169.44	1999-04-12	2011-05-19		y		y	
KAS03	533	579.5	626	−566.28	1999-10-06	2011-11-03		y		y	
KAS09	116	133	150	−110.56	1995-10-12	2011-11-02	y	y	y	y	
KJ0052F01	44.9	47.48	50.06	−450.81	2007-10-02	2011-01-11			y	y	
KJ0052F02	0	10.71	21.42	−447.35	2007-10-08	2011-05-18			y	y	
KR0012B	5	7.79	10.57	−69.17	1995-05-18	1999-09-27	y	y			
KR0013B	7.05	12	16.94	−69.24	1995-05-18	1999-04-15	y	y			
KR0015B	1.25	25.06	30.31	−69.44	1995-05-18	2014-11-28	y	y	y	y	y
SA0813B	5.6	12.55	19.5	−112.9	1995-10-12	1999-04-15	y	y			
SA1009B	1.7	10.6	19.5	−139.45	1995-10-12	2014-11-05	y	y	y		y
SA1229A	0.85	10.68	20.5	−170.82	1995-10-11	2014-11-20	y	y			y
SA1420A	1.15	25.57	50	−200.14	1995-10-11	2014-05-05	y	y	y	y	y
SA1730A	1.35	10.68	20	−236.65	1995-05-18	2014-11-27	y	y	y	y	y
SA2074A	1.35	20.03	38.7	−281.28	1995-10-11	2007-10-05	y	y	y		
SA2273A	1.35	10.68	20	−305.59	1995-10-11	2014-05-12	y	y	y	y	y
SA2600A	1.35	10.38	19.4	−344.63	1995-05-17	2014-05-08	y	y	y	y	y
SA2783A	5.8	12.85	19.9	−371.33	1995-10-25	1999-04-14	y	y			
SA2880A	0	9.95	19.9	−384.09	1995-10-25	2014-04-09	y	y	y	y	y
SA3045A	6	7	8	−406.66	1995-10-25	2011-10-06	y	y	y	y	

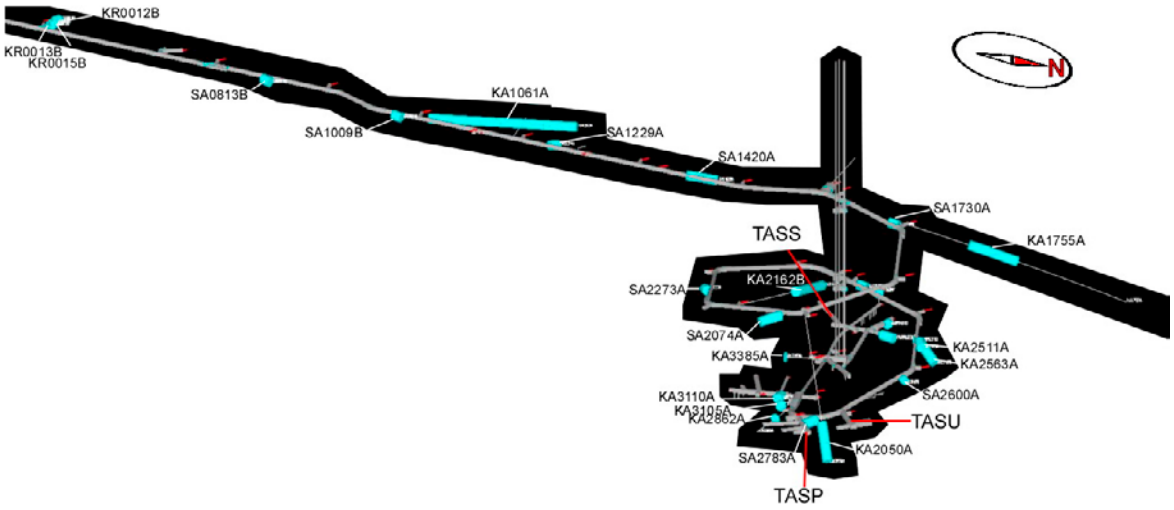

Figure 5-4. *3D distribution of the borehole sections hydrochemically monitored in the boreholes drilled along the tunnel wall of the Äspö HRL.*

Table 5-7. Packed-off borehole sections part of the groundwater chemical programme during year 1999 for a short term period and used in this report for the characterisation and investigation of the natural variability of the nitrogen compound concentrations in fracture groundwater at Äspö.

Borehole ID	Section Up (m)	Section Mid (m)	Section Low (m)	Elevation (m.a.s.l.)	Sampling date
KA1131B	0	101.55	203.1	−178.85	1999-04-09
KA2511A	111	124.5	138	−404.41	1999-09-30
KA2563A	187	188.5	190	−466.54	1999-09-28
KA2563A	206	207	208	−478.63	1999-09-28
KA2563A	242	244	246	−502.62	1999-09-28
KA3385A	7.05	19.05	31.05	−447.33	1999-04-06
KA3566G01	12.2	16	19.8	−459.83	1999-04-09
KA3573A	4.5	10.75	17	−446.43	1999-09-29
KA3573A	18	29.04	40.07	−447.11	1999-04-07
KA3590G02	8.3	12.3	16.3	−456.57	1999-04-13
KA3593G	1.3	4.3	7.3	−452.28	1999-04-15
KA3600F	4.5	12.75	21	−445.94	1999-09-29
KA3600F	22	36.05	50.1	−446.63	1999-04-09
KI0023B	4.6	22.53	40.45	−455.66	1999-04-07
KI0023B	41.45	41.95	42.45	−462.58	1999-04-07
KI0023B	43.45	56.7	69.95	−467.86	1999-09-27
KI0023B	70.95	71.45	71.95	−473.16	1999-09-27
KI0023B	84.75	85.47	86.2	−478.2	1999-09-27
KI0025F	87.5	88.5	89.5	−477.52	1999-09-29
KI0025F	164	166	168	−501.2	1999-04-07
KI0025F	165.5	167.5	169.5	−501.65	1999-09-29
KI0025F02	56.1	59.55	63	−473.58	1999-09-28
KI0025F02	64	68.15	72.3	−477.15	1999-09-28
KI0025F02	73.3	75.28	77.25	−480.1	1999-09-28
KI0025F02	93.35	96.35	99.35	−488.78	1999-09-28
KXTT3	10.92	12.67	14.42	−398.65	1999-10-04

Table 5-8. Packed-off borehole sections part of the groundwater chemical programme during year 2007 for a short term period and used in this report for the characterisation and investigation of the natural variability of the nitrogen compound concentrations in fracture groundwater at Äspö.

Borehole ID	Section Up (m)	Section Mid (m)	Section Low (m)	Elevation (m.a.s.l.)	Sampling date
KA2050A	102	128	154	−378.62	2007-10-24
KA3386A02	0	3.1	6.2	−446.43	2007-10-01
KA3386A03	0	2.78	5.56	−446.36	2007-10-01
KA3386A04	0	2.79	5.59	−446.28	2007-10-01
KA3386A05	0	2.39	4.78	−446.15	2007-10-01
KA3386A06	0	2.79	5.59	−446.22	2007-10-01
KA3539G	15.85	16.73	17.6	−465.66	2007-01-09
KA3542G01	18.6	19.45	20.3	−462.79	2007-01-10
KA3548A01	8.8	9.78	10.75	−447.08	2007-01-09
KA3554G01	22.6	23.38	24.15	−465.34	2007-01-09
KA3573A	26	33.03	40.07	−447.26	2007-09-28
KG0021A01	35	35.5	36	−434.35	2007-01-10
KG0048A01	32.8	33.3	33.8	−436.4	2007-01-10
KJ0044F01	1	9.13	17.26	−447.76	2007-10-08
KJ0050F01	13.84	30.31	46.79	−449.67	2007-10-02
KJ0052F03	10.43	10.52	10.6	−447.66	2007-10-02

Table 5-9. Packed-off borehole sections part of the groundwater chemical programme during year 2011 for a short term period and used in this report for the characterisation and investigation of the natural variability of the nitrogen compound concentrations in fracture groundwater at Äspö.

Borehole ID	Section Up (m)	Section Mid (m)	Section Low (m)	Elevation (m.a.s.l.)	Sampling date
KA1755A	6	46.5	87	−253.47	2011-05-11
KA2051A01	99.85	109.72	119.59	−339.02	2011-02-16
KA2051A01	78	83.5	89	−324.17	2011-02-16
KA3005A	44.78	45.28	45.78	−403.38	2011-10-04
KA3005A	46.78	48.41	50.03	−403.61	2011-10-04
KA3007A01	9.3	10.83	12.36	−403.37	2011-04-15
KA3007A01	12	14.68	17.36	−404.35	2011-05-05
KA3007A01	222	224.88	227.76	−456.11	2011-05-18
KA3010A	8.56	11.81	15.06	−400.84	2011-10-06
KA3065A02	7.5	10.25	13	−409.11	2011-10-12
KA3067A	28.05	28.8	29.55	−410.98	2011-10-07
KA3067A	30.55	32.05	33.55	−411.26	2011-10-07
KA3068A	0	8.43	16.85	−407.94	2011-10-07
KJ0052F01	3.21	22.96	42.7	−448.84	2011-01-11
KJ0052F01	43.7	43.8	43.9	−450.52	2011-05-18

Table 5-10. Packed-off borehole sections part of the groundwater chemical programme during year 2014 for a short term period and used in this report for the characterisation and investigation of the natural variability of the nitrogen compound concentrations in fracture groundwater at Äspö.

Borehole ID	Section Up (m)	Section Mid (m)	Section Low (m)	Elevation (m.a.s.l.)	Sampling date
K03009F01	14.2	15.7	17.2	−399.39	2014-03-03
K03009F01	14.5	16	17.5	−399.39	2014-10-14
K03009F01	17.2	18.7	20.2	−399.42	2014-02-27
K03009F01	18.5	19.5	20.5	−399.43	2014-10-10
K03009F01	21.5	23	24.5	−399.47	2014-10-16
K03009F01	25.2	26.7	28.2	−391.51	2014-02-25
K03009F01	25.5	31.75	38	−399.56	2014-10-13
K03009F01	30	32	33.99	−399.56	2014-04-15
K08028F01	30	31	32	−395.39	2014-10-07
K08028F01	37	38	39	−395.12	2014-10-09
KA2050A	6	53.5	101	−318.78	2014-04-03
KA2051A01	51	59	67	−310.25	2014-11-03
KA2051A01	120	127.5	135	−349.1	2014-11-04
KA3105A	17.01	18.26	19.51	−416.84	2014-04-08
KA3105A	25.51	38.76	52.01	−415.16	2014-04-08

5.2 Groundwater origin and classification

The groundwater composition in the Äspö area is a result of different water origins and a complex history of transport and mixing in the water conductive structures (Smellie et al. 1995, Gascoyne 2004, Laaksoharju et al. 2008b). In the upper 100 m of the fractured bedrock, meteoric (low salinity) groundwater, with near modern and warm-climate isotopic signature, circulates through the sub-horizontal shallow fractures interconnected to the sub-vertical fracture zones. At greater depth, from 100–200 m to approximately 1 km (depending on local topography), a transition zone is observed in which groundwater evolves from fresh to brackish composition (Cl: 1–8 g L^{-1}). Remnants of glacial melt-water, and occasionally (coastal bedrock) marine water in the brackish groundwater are suggested by the isotopic signature, that is either low or high in $\delta^{18}O$, respectively. Old saline-to-highly saline groundwater (Cl: 10–50 g L^{-1}) resides in the fractured crystalline bedrock below this transition zone (Fritz, 1997, Louvat et al. 1999). The saline to highly saline groundwater, of uncertain origin, is believed to result from preservation of allochthonous shield brines, through vertical salinity-induced density gradients, and continuous water–rock interactions in the deep bedrock over millions of years (Nordstrom et al. 1989, Frape et al. 2003). These general hydrogeochemical features with depth result from subsequent paleo-recharge events related to alternation of glacial and postglacial periods (Figure 5-5) during the evolution of the Baltic Sea Basin since the Holocene (Laaksoharju et al. 1999b, Follin, 2008, Laaksoharju et al. 2008b, Waber et al. 2012).

Based on the conceptual hydrological understanding of the Baltic Sea Basin and of the region (Smellie et al. 1995, Laaksoharju et al. 1999a), five end-members related to important groundwater recharge events were identified and referred to as (1) Old-saline water, (2) Glacial water (Pleistocene origin), (3) Littorina Sea water (Past Baltic Sea water – mid-Holocene origin), (4) Meteoric water (past and modern origin) and (5) Baltic Sea water (modern origin). The Cl concentrations and $\delta^{18}O$ values are considered conservative in the groundwater system in fractured crystalline bedrock and thus constitute a fingerprint of the waters that once intruded and now compose the fracture groundwaters (Laaksoharju et al. 1999b, Mathurin et al. 2012, Gómez et al. 2014).

In order to semi-quantitatively relate the studied groundwater to the dominant source/origin of the groundwater and post-infiltration mixing phenomena, the groundwater classification system presented in Mathurin et al. (2012) was applied to the groundwater samples studied in this report. The classification system (Figure 5-6) is based on the conceptual hydrological understanding of the region and the values of Cl concentrations and $\delta^{18}O$ in groundwater samples. Five main groundwater

types (Figure 5-6) can be identified: (1) “deep saline” groundwater, which is made up of saline water located in the deepest part of the studied system, (2) “brackish glacial” groundwater, which is dominated by glacial melt water, often mixed with brackish to saline groundwater (Laaksoharju et al. 2008b, Gimeno et al. 2009), (3) “marine” groundwater, which is mainly of marine origin, (4) “meteoric” groundwater, which is predominantly of meteoric origin and (5) “thoroughly mixed” groundwater, which has no obvious dominant source and is interpreted as being made up of a thorough mixture of two or several of the other waters.

Such classification has previously been used in Mathurin et al. (2012) to study the impact of the significant pressure sink in the bedrock and related dynamic groundwater inflow towards the tunnel as well as the sources of recharging groundwater following the construction of the Äspö HRL in the early 1990s (Laaksoharju and Wallin 1997, Stanfors et al. 1999). A substantial flushing of the groundwater initially residing in the local fractures occurred, followed by a rapid intrusion of modern surficial seawater and regolith groundwater in the shallow-to-deep crystalline bedrock. Another process is active mixing of groundwater of past and modern origins, i.e. additional hydraulic mixing, within the fracture network surrounding the Äspö HRL (Banwart et al. 1994, Laaksoharju et al. 1999b, Pitkänen et al. 1999, Mathurin et al. 2012). In this report, the groundwater classification is applied to samples on scatter plots in order to study the possible effect of groundwater source and post-infiltration mixing phenomena on the nitrogen compounds.

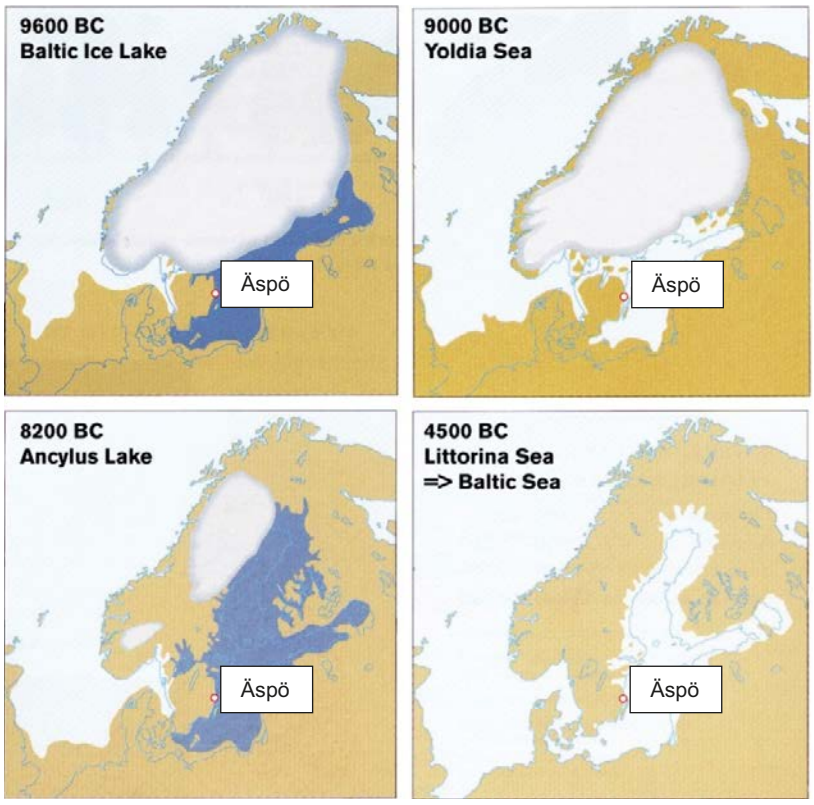

Figure 5-5. *Map of the Fennoscandia with some important stages during the Holocene period. Four main stages characterise the development of the aquatic systems in the Baltic basin since the latest deglaciation. Freshwater is symbolised with dark blue and marine/brackish water with light blue for the present shoreline. Adapted from Sohlenius and Hedenström (2008).*

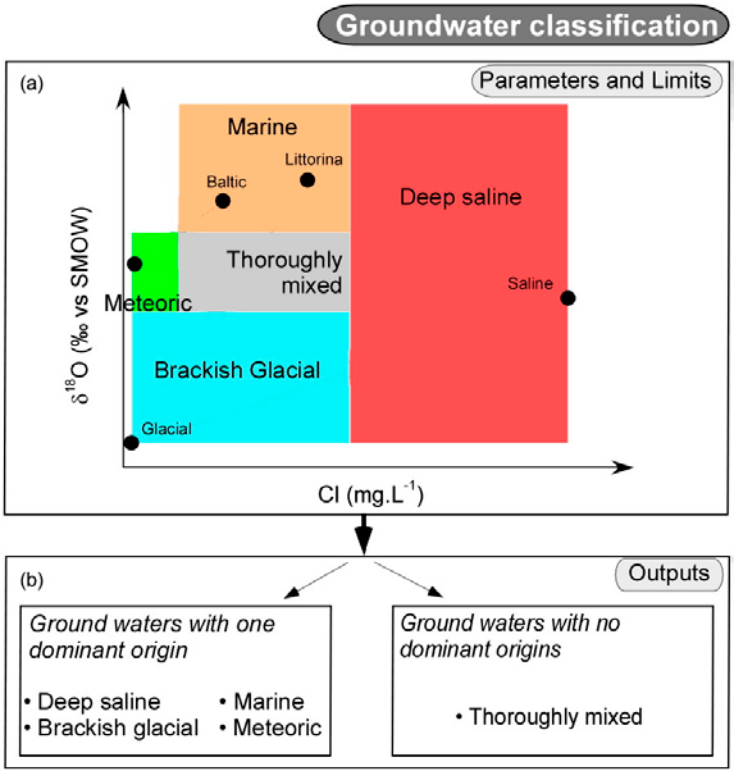

Figure 5-6. *Concept of the groundwater classification developed by Mathurin et al. (2012) for groundwater collected at the Äspö HRL. The background colours refer to the groundwater classes defined from the average Cl concentrations of two relevant end-member pairs (meteoric-Baltic and glacial-saline) and the average $\delta^{18}O$ values of another two relevant end-member pairs (meteoric-Baltic and glacial-Littorina).*

6 Natural variability of dissolved nitrogen compounds at Äspö

Nitrogen occurs in various oxidation states in natural waters from nitrate (+V) to ammonium (–III) and the transformation between these species is almost exclusively facilitated by microorganisms. Under reduced conditions, organic nitrogen is converted to ammonium (NH_4^+) (ammonification process). Under oxidising conditions, ammonium is oxidised to nitrite (NO_2^-) or further oxidised to nitrate (NO_3^-) by specialised nitrifying bacteria (two-step nitrification process). Analytical data are available for NO_2^- (as NO_2-N mg L^{-1}), NO_3^- (as NO_3-N mg L^{-1}) and NH_4^+ (as NH_4-N mg L^{-1}), although all the nitrogen species were not systematically determined for every sample (Nilsson et al. 2013). Ammonium is, by far, the most abundant species of the nitrogen compounds in the 286 groundwater samples, i.e. in the entire set of samples used to illustrate the natural variability of nitrogen compounds over time for the selected years. Such NH_4^+ predominance is favoured by the prevailing reducing redox characteristics (Eh: −140 to −380 mV) and the neutral-to-slightly basic pH (7 to 8.6) of the studied groundwaters (depth >50 m) in the Äspö area (Smellie et al. 1995, Auque et al. 2008, Gimeno et al. 2014).

6.1 Natural variability of NH_4^+

The NH_4^+ concentration (i.e. NH_4-N) is above the detection limit in all samples, showing a median concentration of 0.18 mg L^{-1}. Before the construction of the Äspö HRL, the NH_4-N concentrations ranged between 0.006 and 1.1 mg L^{-1} (Figure 6-1). After the completion of the excavated Äspö HRL, the NH_4-N concentrations have varied by two order of magnitude (from 0.01 to 9.6 mg L^{-1}), mainly at depths shallower than 200 m below sea level (Figure 6-2). Below this depth, the NH_4-N concentrations varies less substantially, mainly from 0.3 to 1.3 mg L^{-1}, although slightly higher concentrations (up to 1.8 mg L^{-1}) were determined at the bottom of the tunnel (i.e. −460 m.a.s.l.).

The NH_4^+ concentrations strongly relate to the dominant origin of the groundwater at Äspö, as previously reported by Mathurin et al. (2014). The highest concentrations were observed in the marine groundwater, with intermediate concentration in the thoroughly mixed type (Figure 6-3). The lowest concentrations appeared in the meteoric and deep saline groundwater types. The systematic association of high NH_4^+concentration to brackish marine groundwater was also reported in the Olkiluoto area and in the Forsmark area, although the maximum concentrations are substantially more moderate: Olkiluoto: up to 0.9 mg L^{-1} (Pitkänen et al. 2004); Forsmark: 1-4 mg L^{-1} (Gimeno et al. 2008). The main difference between the Äspö area and the Olkiluoto and Forsmark areas are the origin of the marine groundwater. In the Äspö area, the Cl concentrations of the marine groundwater (exhibiting relatively high NH_4^+ concentration) vary between 2750 and 3650 mg L^{-1} (Figure 6-1) and are therefore equivalent to the Cl concentration of the modern Baltic Sea in the bays around Äspö. By contrast, the Cl concentrations of the marine groundwater in Formark generally reach 5000 to 5500 mg L^{-1} (Gimeno et al. 2008). These highly saline marine groundwater types correspond to samples with the highest identified contributions of relict Baltic Sea water (Gimeno et al. 2008) which intruded during the Littorina Sea stage (8–6 ka BP), and showed twice the salinity of the modern Baltic Sea (Punning et al. 1988; Gustafsson and Westman, 2002; Emeis et al. 2003).

The existence of enhanced NH_4-N concentrations at depths above −200 m.a.s.l. (Figure 6-2) is in agreement with the influence of the marine groundwater. Borehole sections at such depths are mainly distributed in the second part of the tunnel ramp, which is located below the Baltic Sea in the bay around the Äspö Island (Figure 6-4). This particular part of the tunnel, together with the North-Eastern part of the tunnel spiral, intersect major deformation zones, where the modern Baltic Sea rapidly intruded during the excavation of the Äspö HRL and has prevailed there ever since (Laaksoharju et al. 1999b, Laaksoharju and Gurban 2003, Mathurin et al. 2012). The spatial distribution of the NH_4-N concentrations (Figure 6-4) is therefore related to the extent of connecting flow paths to the Baltic Sea surrounding Äspö (Gimeno et al. 2008). These preferential flow paths for intrusion of modern Baltic Sea water have been (re)activated by the artificial water inflow toward the tunnel induced by the tunnel excavation.

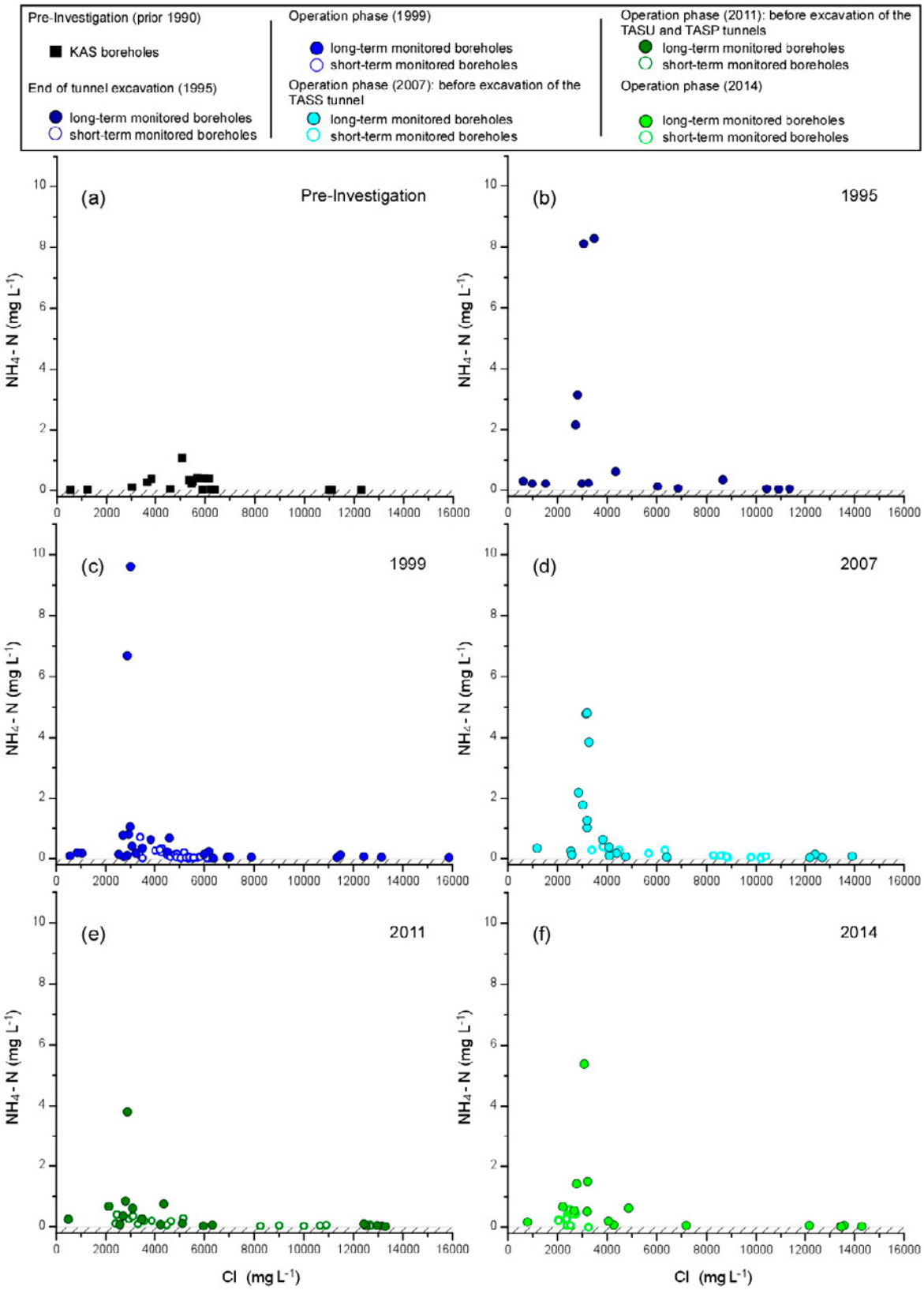

Figure 6-1. *NH_4-N concentrations versus Cl concentrations in the Äspö groundwaters during (a) years 1988–1989, (b) year 1995, (c) year 1999, (d) year 2007, (e) year 2011 and (f) year 2014. Samples with concentrations within the dashed area are below the limit of detection.*

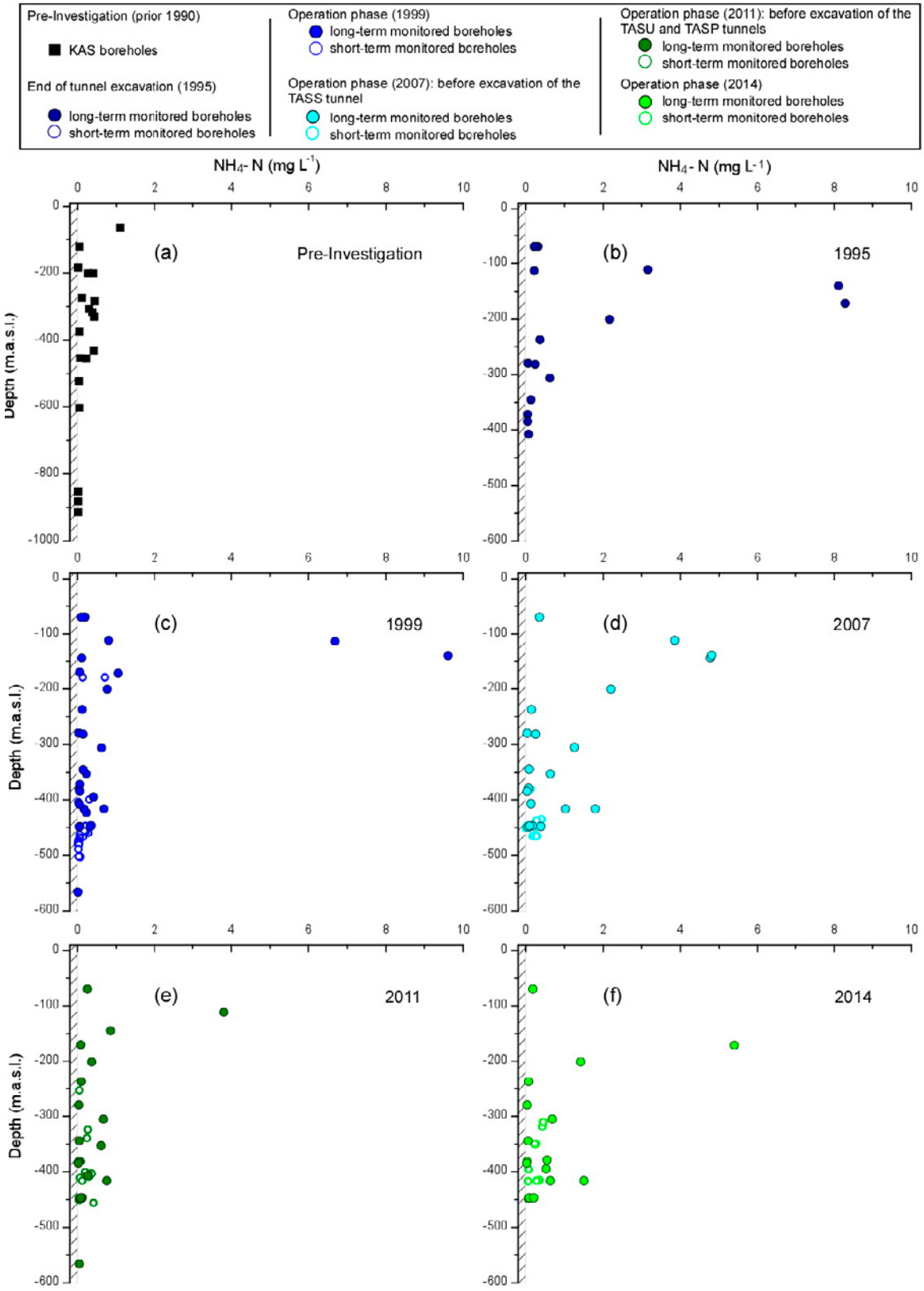

Figure 6-2. *Depth distribution of NH_4-N concentration in the Äspö groundwaters during (a) years 1988–1989, (b) year 1995, (c) year 1999, (d) year 2007, (e) year 2011 and (f) year 2014. Samples with concentrations within the dashed area are below the limit of detection. Note that the depth scale reaches up to −1 000 m on figure a and −600 m on the other figures.*

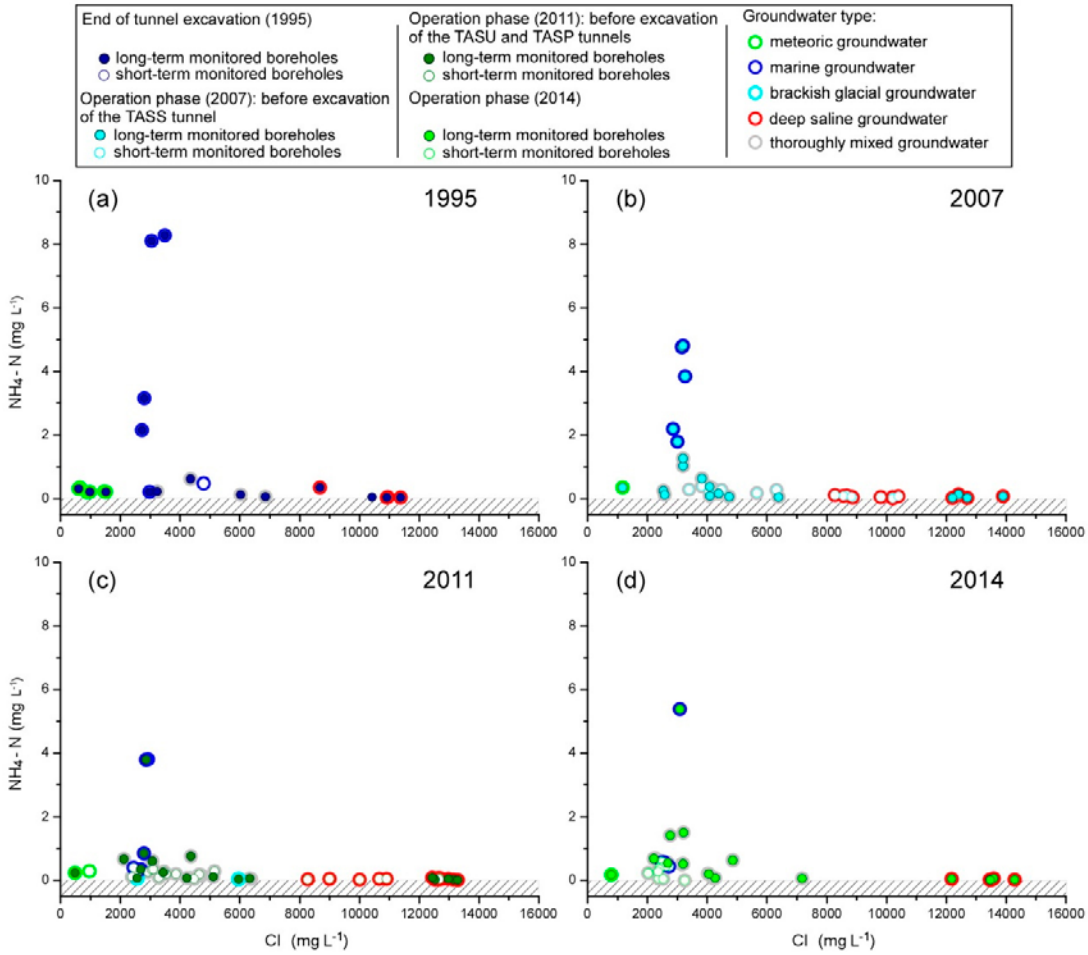

Figure 6-3. *NH_4-N concentrations versus Cl concentrations in the Äspö groundwaters during (a) year 1995, (b) year 2007, (c) year 2011 and (d) year 2014. The outermost colour of the dots refers to the groundwater source defined by Mathurin et al. (2012).*

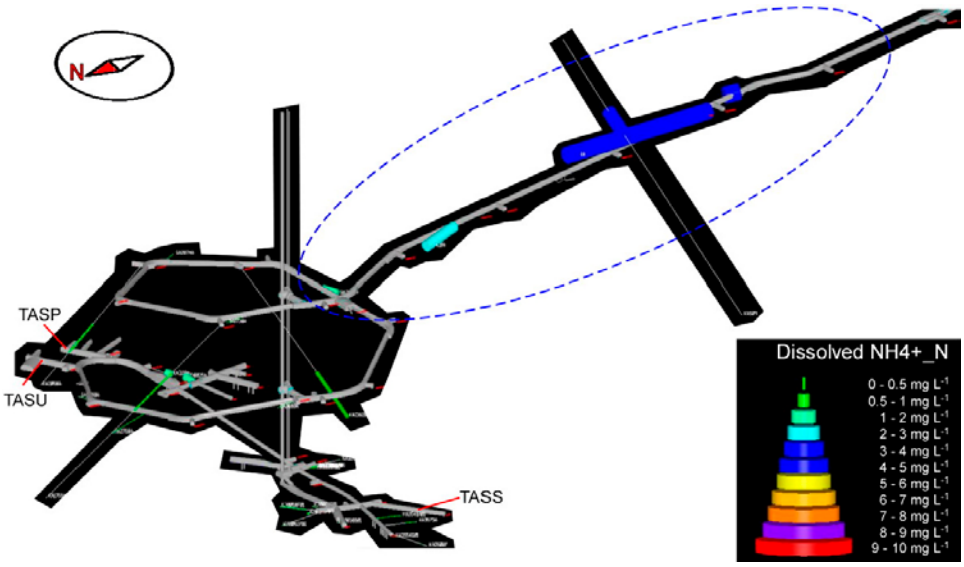

Figure 6-4. *3D distribution of the concentration of NH_4-N in fracture groundwater collected in borehole sections in surface boreholes and boreholes drilled along the Äspö HRL during year 2007. The colours and diameters of the cylinders, representing the packed-off borehole sections along the Äspö HRL, vary according to the dissolved NH_4-N concentrations. The beginning of the first spiral corresponds to 200 m depth, whereas the tunnel bottom corresponds to 460 m depth. The dashed blue oval symbolises the area with identified fracture zones with groundwater of marine origin (Mathurin et al. 2012).*

The water in the present Baltic Sea shows very low NH_4-N concentrations (0.004–0.21 mg L^{-1}; Table 1 in Mathurin et al. 2014). However, the NH_4-N concentrations in the sea sediment pore waters increase substantially with depth, both in the open sea (9.3–36 mg L^{-1}) and in the bay around Äspö (11–39 mg L^{-1}) as reported by Engdahl et al. (2008). In the marine sediments with organic matter, bacterial activity promotes the transformation of organic nitrogen compounds and the formation of NH_4^+ (Carman and Rahm 1997). This could justify important increments in dissolved NH_4^+ during infiltration of the seawater through marine sediments (Pitkänen et al. 2004, Gimeno et al. 2009). However, Mathurin et al. (2014) question the natural influx of high concentrations of NH_4^+ in the water conductive fractures at Äspö, and propose instead that the observed high concentrations could result either from ongoing and temporal biochemical processes or from the transient hydrogeological state (i.e. decades time scale) and the associated intrusion of shallow groundwater (enriched in NH_4^+) induced by the Äspö HRL.

6.2 Natural variability of NO_2^- and NO_3^-

Very few nitrite and nitrate data (as NO_2-N mg L^{-1} and NO_3-N mg L^{-1}, respectively) are available from the pre-investigation period, no determinations exist between years 1991–2003 and only a moderate number of analyses were conducted year 2004 and thereafter. The concentrations of nitrite and nitrate are very low and often below the limits of detection (LOD). The number of groundwater samples with NO_2 -N values below LOD are 71 % for the pre-investigation period (n_{tot} = 14), 61 % for year 2007 (n_{tot} = 41), 37 % for year 2011 (n_{tot} = 46) and 37 % for year 2014 (n_{tot} = 41). The number of groundwater samples with NO_3-N values below LOD were 85 % during the pre-investigation period (n_{tot} = 13), 66 % for year 2007 (n_{tot} = 41), 89 % for year 2011 (n_{tot} = 45) and 88 % for year 2014 (n_{tot} = 40).

Before construction of the Äspö HRL, the median concentrations (for samples above LOD) of NO_2-N and NO_3-N were 0.001 and 0.01 mg L^{-1}, respectively (Figure 6-5). Since the completion of the Äspö HRL, the median concentrations (for samples above LOD) of NO_2-N and NO_3-N were 0.0003 and 0.0009 mg L^{-1}, respectively (Figure 6-5). These extremely low contents of nitrite and nitrate have also been observed in other crystalline environments such as the crystalline batholith of Lac du Bonnet, Canada (Gascoyne 2004), Olkiluoto (Pitkänen et al. 2004) and Forsmark (Gimeno et al. 2008).

The maximum NO_2-N concentration observed was 0.003 mg L^{-1}. This concentration was measured in a saline groundwater with a Cl concentration of 8520 mg L^{-1} at -446 m.a.s.l. during year 2007 and in a brackish groundwater with a Cl concentration of 2500 mg L^{-1} at −281 m.a.s.l. in a newly drilled borehole along the TASU tunnel during year 2014 (Figure 6-5; Figure 6-6). The maximum NO_3-N concentration in the dataset was 0.024 mg L^{-1}. This concentration was also measured in the same brackish groundwater at −281 m.a.s.l. during year 2014 (Figure 6-6; Figure 6-7). These concentrations are quite similar to the maximum contents of dissolved NO_2^- and NO_3^- found in the groundwater in Forsmark, which are around 0.025 mg L^{-1} and 0.005 mg L^{-1}, respectively (Gimeno et al. 2008).

Although the maximum NO_2^- and NO_3^- concentrations are found in marine and saline groundwater, there is no significant correlation between the NO_2^- and NO_3^- concentrations and the groundwater type (Figure 6-7). Moreover, the maximum NO_2^- and NO_3^- concentrations are sporadic and thus not repeated over the years. Overall, these results are in agreement with nitrite and nitrate instability at the reducing conditions found in these groundwaters and with the aforementioned usual depletion of nitrogen species in anaerobic groundwater systems (Gimeno et al. 2008).

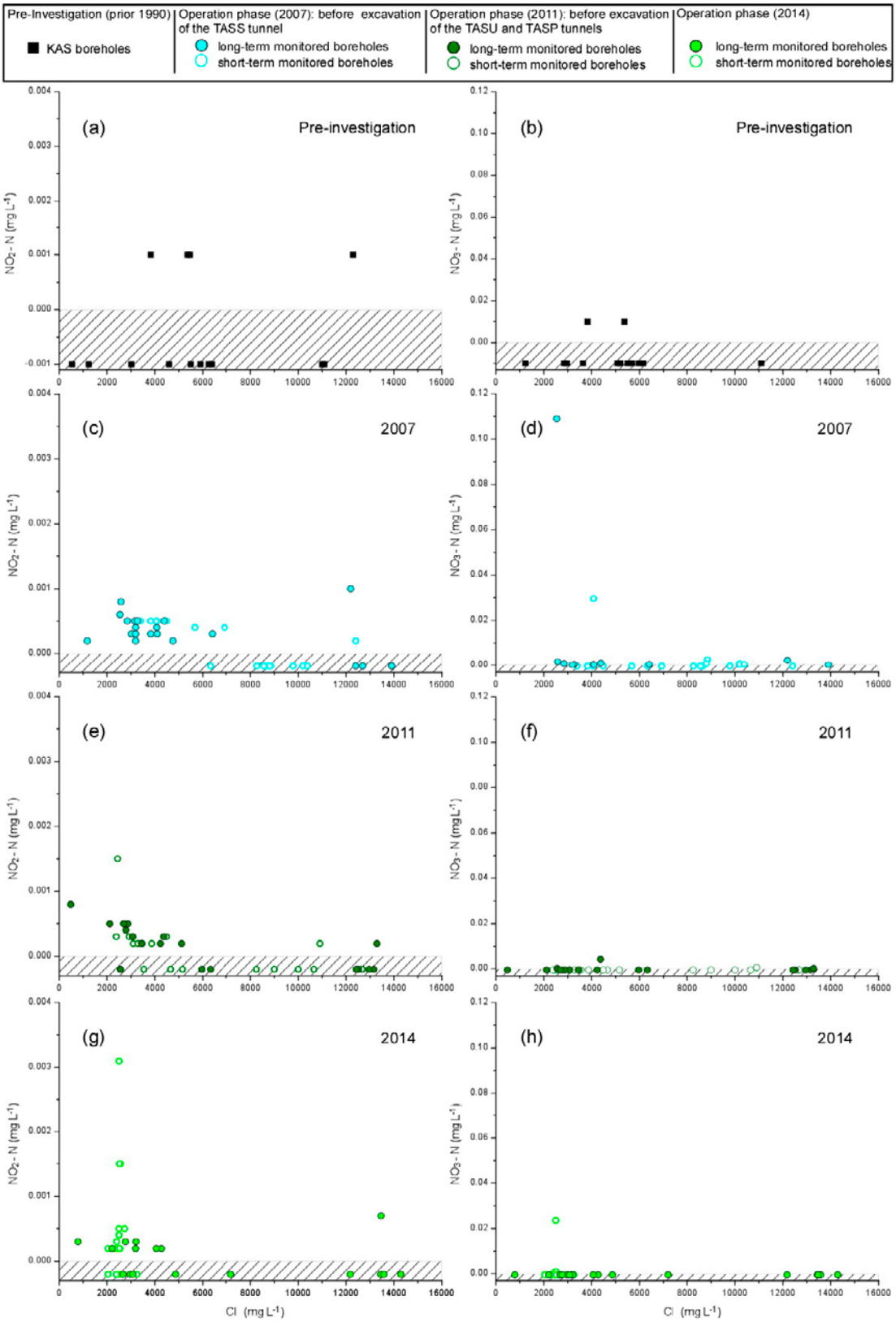

Figure 6-5. *NO_2-N (left) and NO_3-N (right) concentrations versus Cl concentrations in the Äspö groundwaters during years 1988–1989, year 2007, year 2011 and year 2014. Samples with concentrations within the dashed area are below the limit of detection (LOD).*

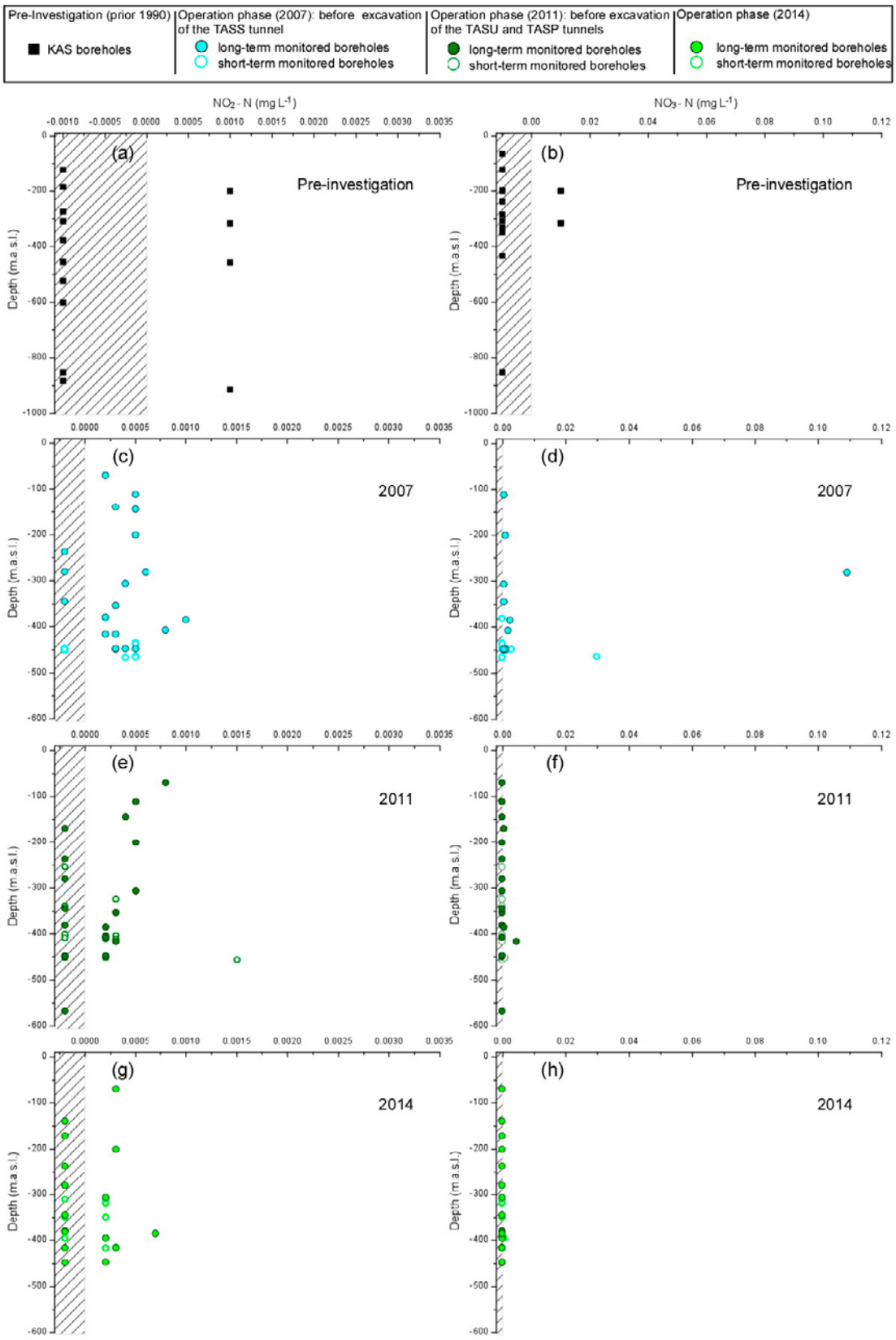

Figure 6-6. *Depth distribution of NO_2-N (left) and NO_3-N (right) concentrations in the Äspö groundwaters during years 1988–1989, year 2007, year 2011 and year 2014. Samples with concentrations within the dashed area are below the limit of detection (LOD).*

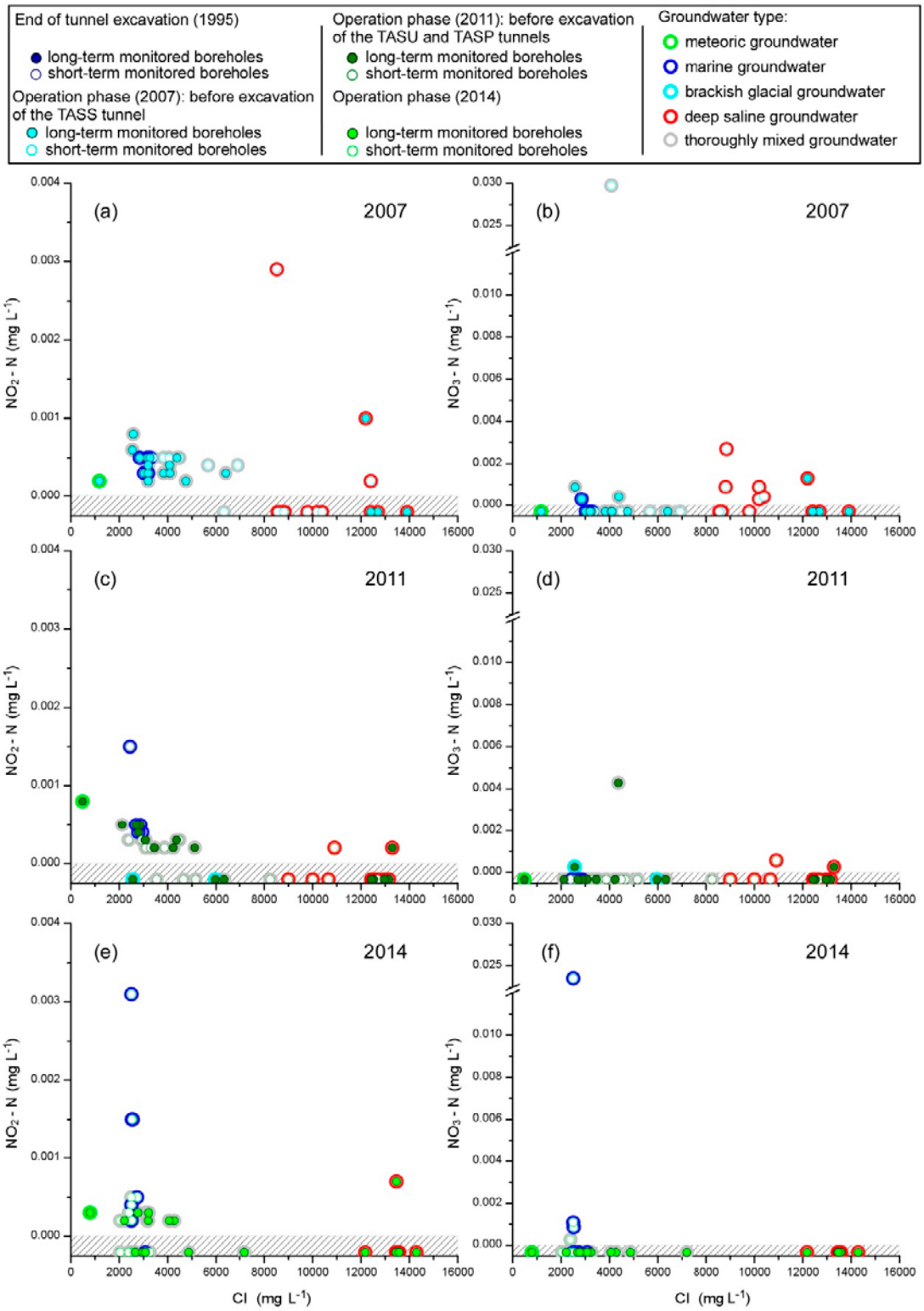

Figure 6-7. *NO_2-N (left) and NO_3-N (right) concentrations versus Cl concentrations in the Äspö groundwaters during year 2007 (top), year 2011 (middle) and year 2014 (bottom). The frame colour around the dots refers to the groundwater source defined by Mathurin et al. (2012).*

7 Evolution of dissolved nitrogen compounds following the expansions of the Äspö HRL

The successive phases of the expansion of the Äspö HRL are divided in two parts, including first the excavation of the TASS tunnel in 2008 and secondly the excavation of the TASU and TASP tunnels together with the related niches in 2012. The TASS tunnel and TASU and TASP tunnels are located in different parts of the Äspö HRL, therefore the evolution of the concentrations with time of the different compounds are presented separately.

7.1 Evolution close to the TASS tunnel

The groundwater samples from the packed-off borehole sections in the pilot boreholes represent the rock volume close to the projected TASS tunnel prior to the excavation. Before the blasting events the dissolved NH_4^+-N concentrations varied between 0.36 and 0.52 mg L^{-1} (Figure 7-1), the dissolved NO_2-N concentrations were around 0.5 µg L^{-1} and the NO_3-N concentrations were generally below detection limit or below 1.5 µg L^{-1} (Figure 7-2).

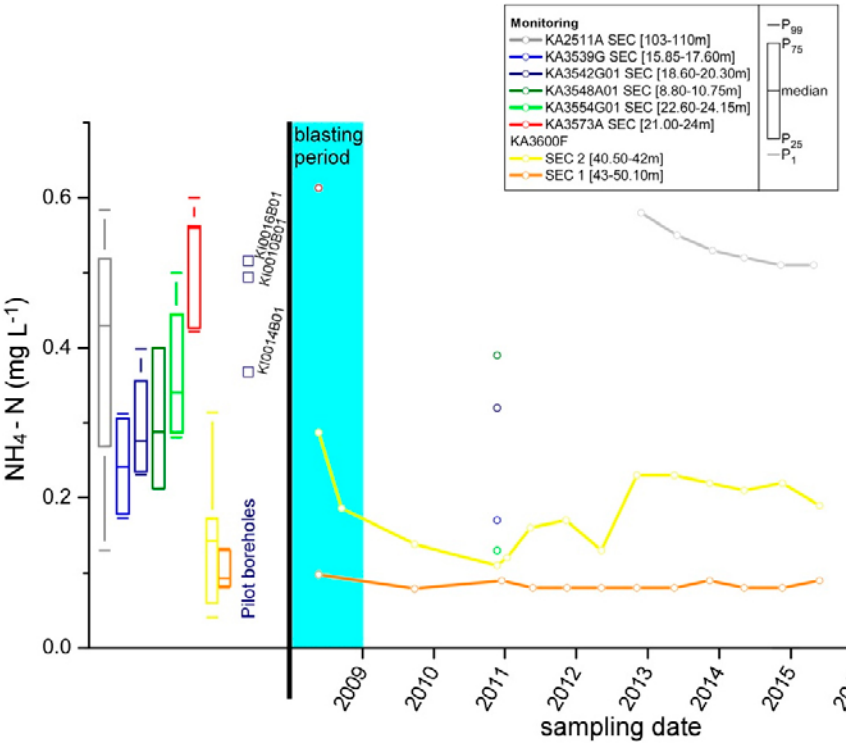

Figure 7-1. *Box-and-whisker plot (left part) and evolution with time (right part) of NH_4-N concentrations in groundwater collected in borehole sections nearby the TASS tunnel. The box-and-whisker plots show the statistical distribution of NH_4-N concentrations before the excavation of the TASS tunnel by blasting (years 1999–2007). The evolution with time of NH_4-N concentrations is shown during the blasting period (year 2008 – blue area) and after, for borehole sections included within the groundwater chemical monitoring programme.*

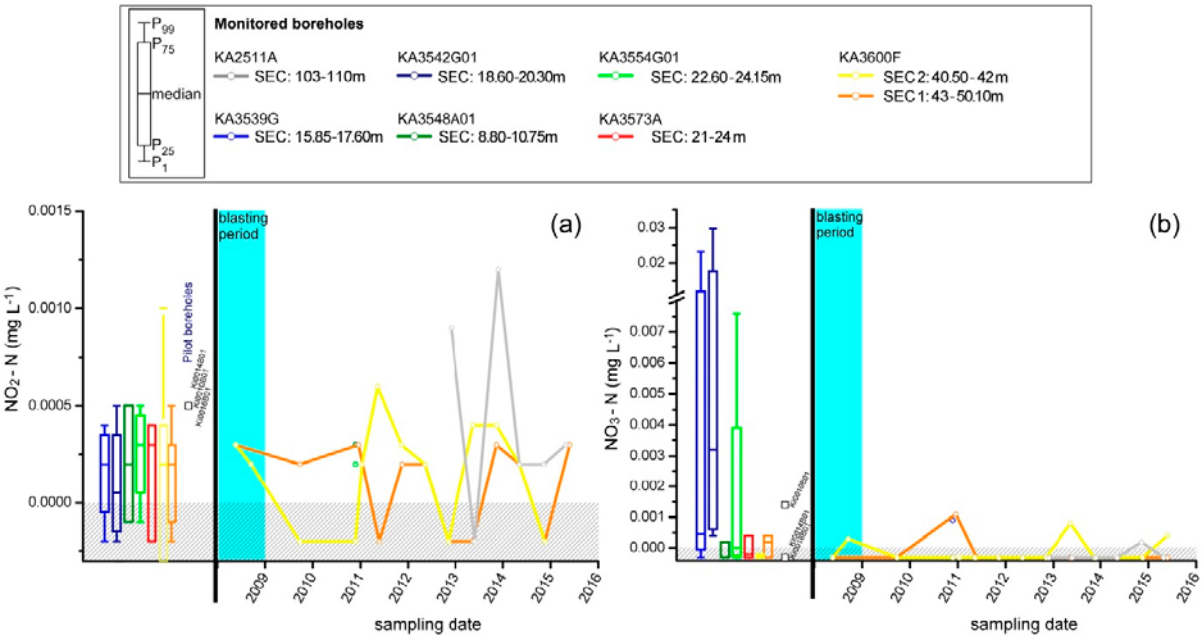

Figure 7-2. *Box-and-whisker plot (left part) and evolution with time (right part) of (a) NO_2-N and (b) NO_3-N concentrations in groundwater collected in borehole sections nearby the TASS tunnel. The box-and-whisker plots show the statistical distribution of NO_2-N and NO_3-N concentrations before the excavation of the TASS tunnel by blasting (years 2003–2007). The evolution with time of NO_2-N and NO_3-N concentrations is shown during the blasting period (year 2008 – blue area) and after, for borehole sections included within the groundwater chemical monitoring programme. Samples with concentrations within the dashed area are below the limit of detection.*

The concentrations of the nitrogen compounds (NH_4-N, NO_2-N, NO_3-N) in the pilot boreholes were generally similar to the natural variability, before the TASS tunnel excavation. The highest NH_4-N concentrations (0.6 mg L^{-1}) were found in the section in borehole KA3573A and the lowest (0.06 mg L^{-1}) in sections in borehole KA3600F (Figure 7-1). The highest NO_3-N concentrations (23–29 µg L^{-1} – unexpectedly high for a reduced deep environment) were found in the sections in boreholes KA3539G1 and KA3542G01 and the lowest in the sections in boreholes KA3600F and KA3548A01 (Figure 7-2). In contrast to NO_3-N, the NO_2-N concentrations in the pilot boreholes were generally corresponding to the maximum concentrations (0.5 µg L^{-1} in these other selected boreholes; Figure 7-2).

The few groundwater samples collected during the TASS blasting (spring 2008, blue area in Figure 7-1 and Figure 7-2) generally showed high dissolved NH_4-N and NO_2-N concentrations in comparison with the overall natural variability prevailing before the blasting period. The dissolved NO_3-N concentrations were systematically below the limit of detection.

Focussing on the NH_4-N concentrations (Figure 7-1), the evolution of the concentrations with time during the TASS blasting may be characterised from only one closely located borehole, KA3600F, which was included among the limited number of selected boreholes following the twice a year monitoring strategy. The groundwater sampling in section no. 2 suggests a progressive decrease of the dissolve NH_4-N concentrations from 0.29 mg L^{-1} to about 0.10 mg L^{-1} which prevails until year 2011, i.e. 2 years after the end of the TASS blasting and excavation. Section no.1, on the other hand, shows a stable concentration of approximately 0.10 mg L^{-1} during the entire period 2008 to 2015. The general decrease observed in section no. 2 during the 3 year period resulted in dissolved NH_4-N concentrations of only one third of the concentration originally determined during spring 2008. A hypothetical artificial peak of dissolved NH_4-N caused by the blasting should be very significant, and such a peak was not observed. The peak could have been missed due to low sampling frequency, however, the observed NH_4-N concentrations still display a progressive decrease and the increase of the Cl concentrations excludes a general dilution process (Figure 7-3) but suggest inflow of a more brackish to saline groundwater. In other words, the natural flushing of groundwater towards the tunnel seems to prevent any hypothetical persistent nitrogen contamination.

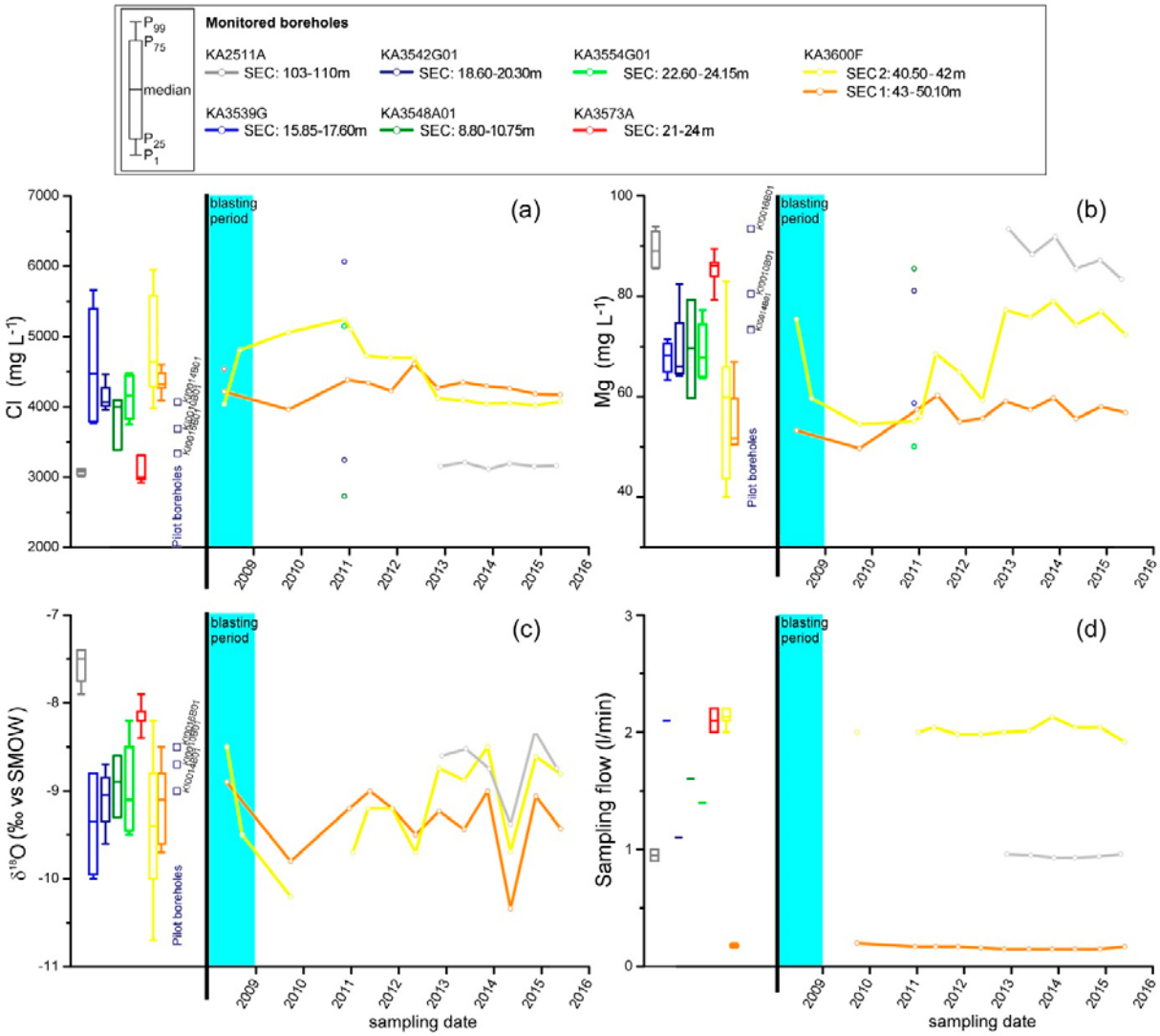

Figure 7-3. *Box-and-whisker plot (left part) and evolution with time (right part) of (a) Cl and (b) Mg concentration, (c) δ18O values and (d) sampling flow in groundwater collected in individual borehole sections nearby the TASS tunnel. The box-and-whisker plots show the statistical distribution of variables before the excavation of the TASS tunnel by blasting (years 1999–2007). The evolution with time of the variable is shown during the blasting period (year 2008 – blue area) and after, for borehole sections included within the groundwater chemical monitoring programme.*

Four additional boreholes (KA3539G, KA3542G01, KA3548A01 and KA3554G01), representing the groundwater volume close to the TASS tunnel, allow comparison of the NH_4-N concentrations in the groundwater before and 2 years after the blasting (Figure 7-1). By the end of year 2010, groundwaters collected in boreholes KA3542G01 and KA3548A01 displayed NH_4-N concentrations near or in the third percentile of those measured before the TASS blasting while the groundwater in borehole KA3539G showed NH_4-N concentrations within the first percentile and groundwater in borehole KA3554G01 displayed NH_4-N concentrations drastically lower than the natural variability observed before the TASS blasting and excavation. Taken together, this rough characterisation gives no evidence of significant and persistent nitrogen contamination. Instead, there are signs of significant decreases of the natural nitrogen concentrations, especially, in the sampled section in borehole KA3554G01.

Focusing on the entire period of monitoring, i.e. also after year 2010, the NH_4-N concentrations, together with the Cl and Mg concentrations, returned to the original concentrations measured during the blasting period in section no. 2 of borehole KA3600F, whereas the concentrations remain overall stable during the entire time period in section no. 1, certainly influenced by a constant low transmissivity (i.e. sampling flow; Figure 7-3) of the sampled fractures. Accordingly, the artificial drainage occurring in the rock volume surrounding the TASS tunnel seems to have a limited temporal effect on the NH_4-N concentrations and on the groundwater chemistry in general after a decade, although the limited number of monitored sections obstructs the observation of general trends.

7.2 Evolution close to the TASU and TASP tunnels

Before the blasting and excavation, the NH_4-N concentrations in the groundwater collected from the pilot boreholes and representing the rock volume close to the future locations of the TASU and TASP tunnels, varied between 0.06 and 0.37 mg L^{-1} (Figure 7-4). The dissolved NO_2-N concentrations varied from below LOD to 4 µg L^{-1} (Figure 7-5a) and the NO_3-N concentrations were generally below LOD and at maximum 1.3 µg L^{-1} (Figure 7-5b).

If the groundwater of a larger bedrock volume is considered (including other boreholes than the pilot boreholes), the available and relevant data on nitrogen (NH_4-N, NO_2-N, NO_3-N) before the TASU and TASP tunnel excavation showed either narrower or larger variabilities than those shown by the pilot boreholes (see Section 5.1.2).

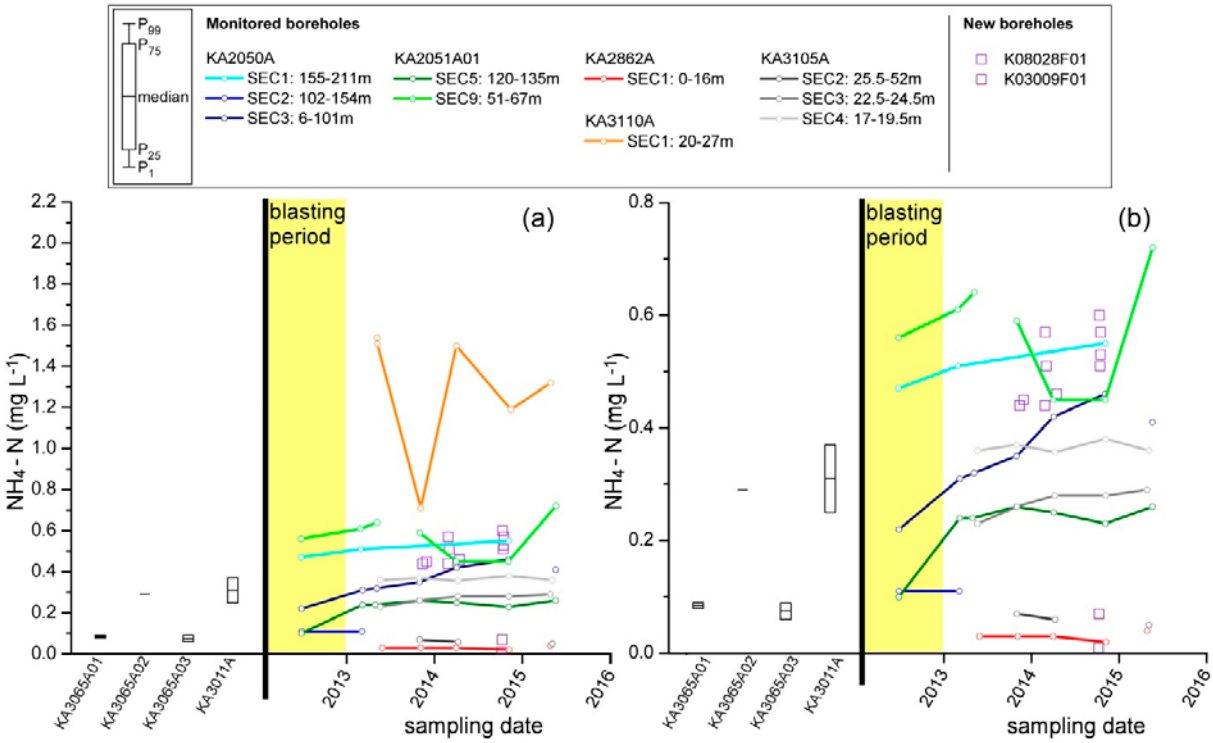

Figure 7-4. *Box-and-whisker plot (left part) of NH_4-N concentrations in groundwater collected in borehole sections of pilot boreholes before the excavation of the TASU and TASP tunnels (year 2011). Evolution with time (right part) of NH_4-N concentrations in groundwater collected in borehole sections close to the TASU and TASP tunnels during the blasting period (year 2012 – yellow area) and after, for borehole sections included within the groundwater chemical monitoring programme. Note that NH_4-N concentrations are unrestricted in plot (a) and restricted to 0.8 in plot (b) for increased resolution of the evolution of concentrations with time.*

The NO_2-N concentrations in all borehole sections near TASU and TASP displayed a narrower natural variability than the pilot boreholes. The highest concentrations amounted to 0.7 µg L^{-1} which is unexpectedly high for a reduced deep environment. This value was observed in one section in each one of the boreholes KA2050A and KA2051A01. Concentrations below LOD were found in boreholes KA2862A and KA3110A (Figure 7-6a). Also the NO_3-N concentrations displayed a narrower natural variability than the pilot boreholes, with the highest NO_3-N concentrations amounting to 0.8 µg L^{-1} which also is unexpectedly high for a reduced deep environment. This value was measured in boreholes KA3110A and KA2050A. Most other borehole sections showed concentrations below LOD (Figure 7-6b). The variations in the NO_2-N, and NO_3-N concentrations were significant not only within individual boreholes but also within the individual isolated sections from the same borehole considering the analytical uncertainty, being 2 % for NO_2^- and 5 % for NO_3-N (Nilsson 2008). The variability is a result of the often very limited number of data from each section (n = 1 in many sections, see Table 5-2).

In contrast, the dissolved NH_4-N concentrations in all borehole sections near the future TASU and TASP locations displayed a larger range of natural variability than found for the pilot boreholes. The highest concentration amounted to 2 mg L^{-1} in borehole KA3110A (Figure 7-7a) and the lowest (0.017 mg L^{-1}) was measured in borehole KA2862A (Figure 7-7b). The substantially larger range of NH_4-N concentrations is mainly caused by the data from borehole KA3110A (Figure 7-7a). All other sampling locations showed NH_4-N concentrations similar to those found in the pilot boreholes. With respect to the qualitative tracers for water origin (Figure 7-8), including chloride, magnesium and $\delta^{18}O$ values, the groundwaters collected in borehole KA3110A (i.e. with the highest NH_4-N concentrations) showed substantially higher Mg concentrations (113–150 mg L^{-1}) and $\delta^{18}O$ values (−8.9 to −6.9 ‰ vs SMOW), which is typical for groundwater with a higher proportion of water of marine origin. On the contrary, the groundwater collected in borehole KA2862A (i.e. with the lowest NH_4-N concentrations) displayed the highest Cl concentration (up to 16 140 mg L^{-1}) and the lowest $\delta^{18}O$ values (−11.5 to −12.4 ‰ vs SMOW), characteristic of a deep saline groundwater.

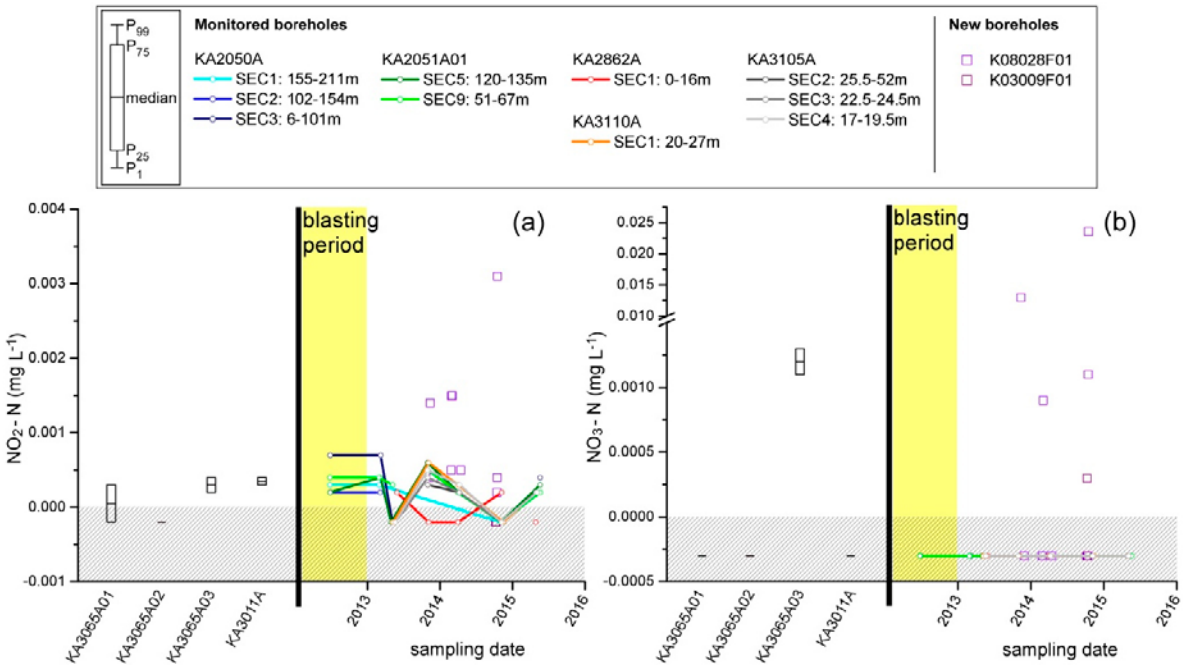

Figure 7-5. *Box-and-whisker plot (left part) of (a) NO_2-N and (b) NO_3-N concentrations in groundwater collected in borehole sections of pilot boreholes before the excavation of the TASU and TASP tunnels (year 2011). Evolution with time (right part) of NO_2-N and NO_3-N concentrations in groundwater collected in borehole sections nearby the TASU and TASP tunnels during the blasting period (year 2012 – yellow area) and after, for borehole sections included within the groundwater chemical monitoring programme. Samples with concentrations within the dashed area are below the limit of detection.*

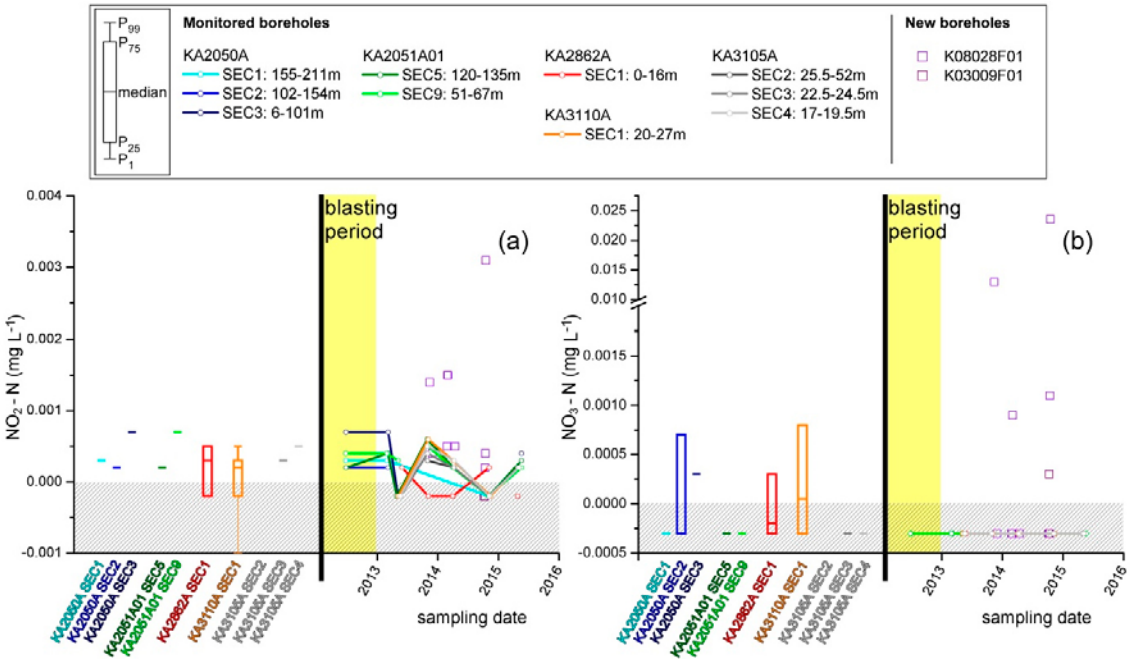

Figure 7-6. *Box-and-whisker plot (left) and evolution with time (right) of (a) NO_2-N and (b) NO_3-N concentrations in groundwater collected in individual borehole sections nearby the TASU and TASP tunnels. The box-and-whisker plots show the statistical distribution of NO_2-N and NO_3-N concentrations before the excavation of the TASU and TASP tunnels by blasting (years 2009–2011). The evolution with time of NO_2-N and NO_3-N concentrations is shown during the blasting period (year 2012 – yellow area) and after, for borehole sections included within the groundwater chemical monitoring programme. Samples with concentrations within the dashed area are below the limit of detection.*

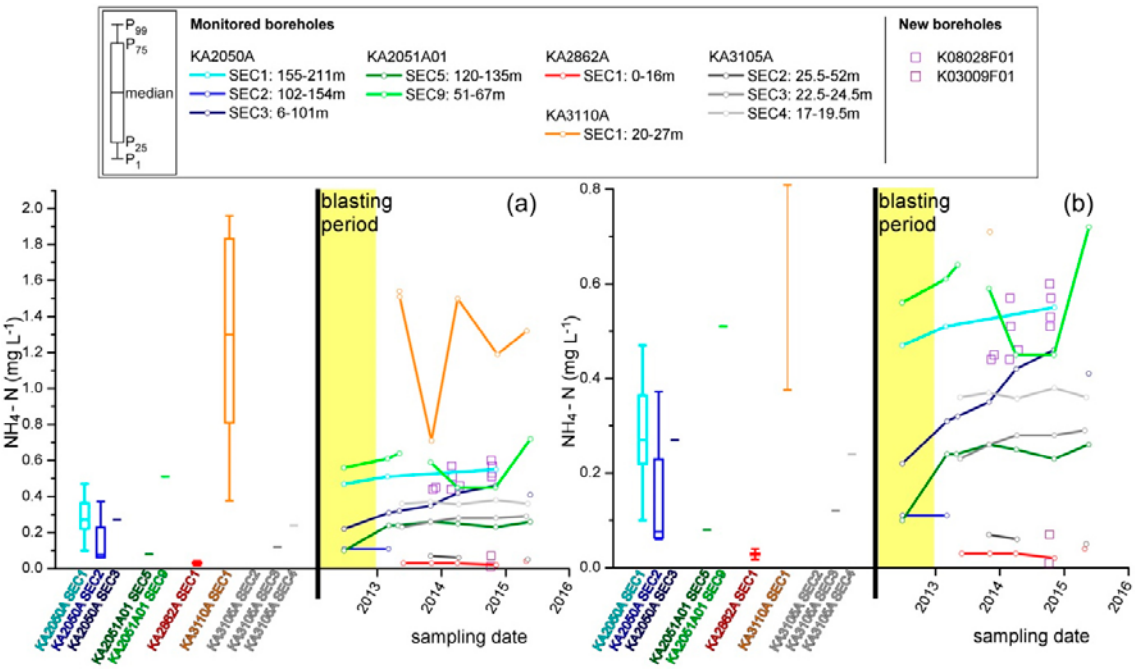

Figure 7-7. *Box-and-whisker plot (left) and evolution with time (right) of NH_4-N concentrations in groundwater collected in individual borehole sections nearby the TASU and TASP tunnels. The box-and-whisker plots show the statistical distribution of NH_4-N concentrations before the excavation of the TASU and TASP tunnels by blasting (years 2009–2011). The evolution with time of NH_4-N concentrations is shown during the blasting period (year 2012 – yellow area) and after, for borehole sections included within the groundwater chemical monitoring programme. Note that NH_4-N concentrations are unrestricted in plot (a) and restricted to 0.8 in plot (b) for increased resolution of the evolution of concentrations with time.*

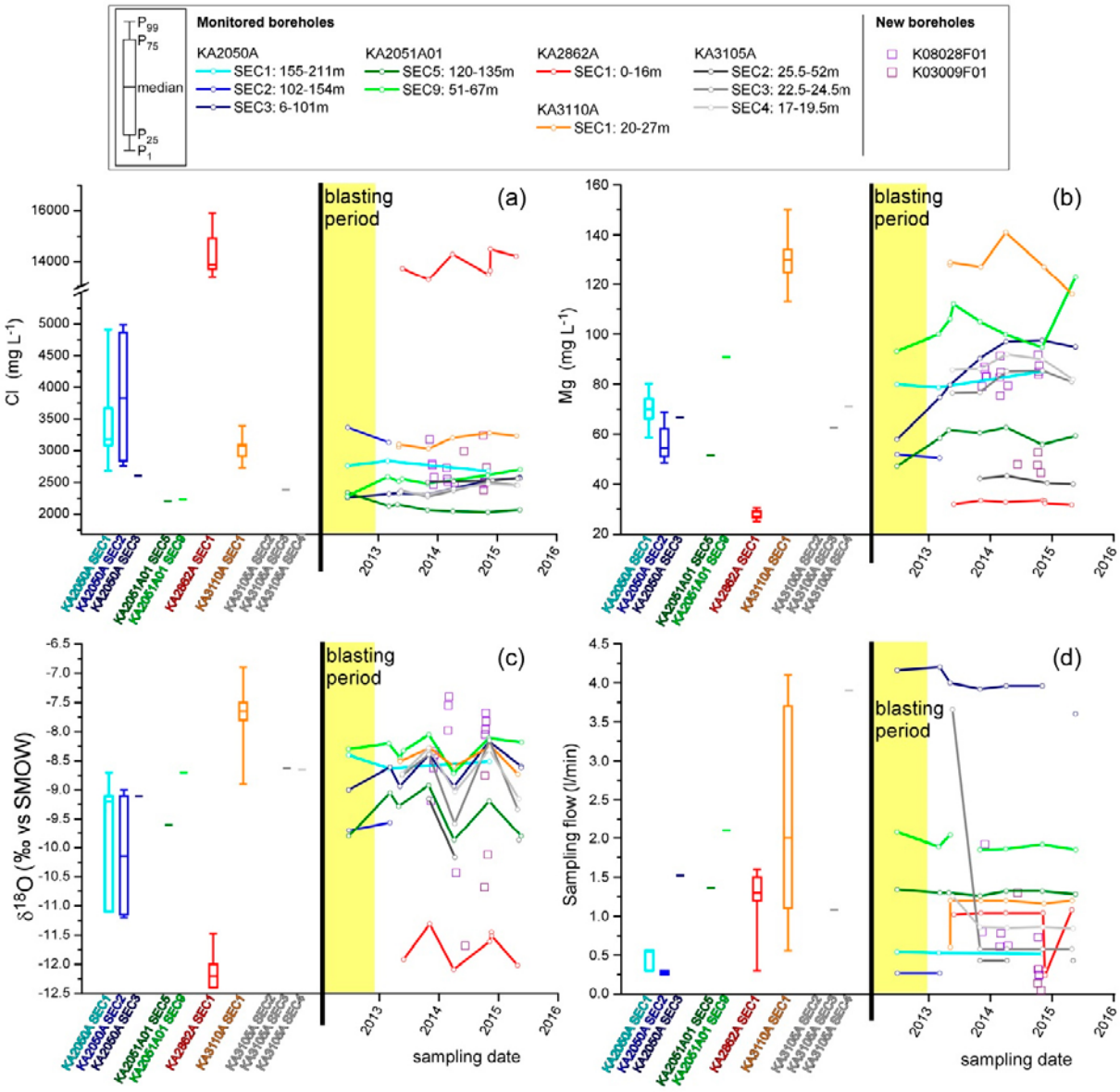

Figure 7-8. *Box-and-whisker plot (left part) and evolution with time (right part) of (a) Cl and (b) Mg concentration, (c) $\delta^{18}O$ values and (d) sampling flow in groundwater collected in individual borehole sections nearby the TASU and TASP tunnels. The box-and-whisker plots show the statistical distribution of variables before the excavation of the TASU and TASP tunnels by blasting (years 2009–2011). The evolution with time of the variables is shown during the blasting period (year 2012 – yellow area) and after, for borehole sections included within the groundwater chemical monitoring programme.*

Five sections from boreholes KA2050A and KA2051A01 were sampled at one occasion each during the TASU and TASP blasting in year 2012. The NH_4-N and NO_2-N concentrations were similar to the natural concentrations – or within the analytical uncertainty (Figure 7-6; Figure 7-7). The dissolved NO_3-N concentrations were systematically below LOD. The generally constant concentrations of nitrogen compounds before and during the blasting period are in line with the lack of evolution of the Cl and Mg concentration, as well as of the $\delta^{18}O$ values (Figure 7-8). Taken together, the available data do not suggest contamination/emission of nitrogen compounds in the vicinity of the bedrock volume excavated during the construction period of the TASU and TASP tunnels. The only possible apparent evidence of increased nitrogen concentrations in fracture groundwater during the blasting period might be in the borehole section no. 1 in borehole KA2050A, where the observed NH_4-N concentration was similar to the highest concentration measured before the blasting period (Figure 7-7b).

On a longer time scale, if the NO_2-N and NO_3-N concentrations remains constant several years after the completion of the blasting and excavation of the TASU and TASP tunnel (Figure 7-7), the dissolved NH_4-N concentrations generally increased during the year 2013 in most of the sections in the semi vertical boreholes KA2050A and KA2051A01 (Figure 5-2). The extent of the increase, after the year 2013 was specific to each packed-off section. For instance, in borehole KA2050A, the dissolved NH_4-N concentrations remained fairly constant (around 0.11 mg L^{-1}) in section no. 2, whereas it rapidly rose in the sections no. 1 and no. 3 (Figure 7-7). In section 3, i.e. the section closest to the tunnel wall, the dissolved NH_4-N concentration increased continuously over the period of time covered by the available data, to reach concentrations up to 0.46 mg L^{-1}. In section 1, i.e. not only the most distant section from the tunnel wall, but also the section with higher NH_4-N concentration during the blasting period (0.47 mg L^{-1}), the ammonium concentration increased more moderately than in section no. 3 during the same 2.5 year period, to reach 0.55 mg L^{-1}. Although increases of the NH_4-N concentrations are also exhibited in the two borehole sections of borehole KA2051A01 (section no. 5 and section no. 9), the rise is limited in time (i.e. one year period) in both sections. In section no. 5, the dissolved NH_4-N concentration increased sharply, and then stabilised at around 0.25 mg L^{-1}. In section no. 9, i.e. the section with higher NH_4-N concentration, the moderate rise (to 0.64 mg L^{-1}) was followed by a sharp decrease at the end of the year 2013 to stabilise around 0.45 mg L^{-1} for one year, before increasing again to reach its maximum value of 0.72 mg L^{-1}. Among other boreholes (KA2862A, KA3110A and KA3105A), the boreholes KA2862A and KA3105A displayed fairly stable NH_4-N concentrations from May 2013 to April 2015, but in borehole KA3110A the NH_4-N concentration varied considerably (Figure 7-7).

The rise of NH_4-N concentrations that was expected after the blasting of the TASU and TASP tunnels, i.e. since the beginning of 2013 is generally significant in most of the borehole sections in boreholes KA2050A and KA2051A. However, when comparing concentrations in these boreholes before and during the blasting period with the natural variability of the nitrogen compounds in all boreholes in the rock volume near the TASU and TASP tunnels, the maximum dissolved NH_4-N concentrations remained lower than the concentrations previously determined in borehole KA3110A, see Figure 7-7. The natural occurrence of such relatively high NH_4-N concentrations in the groundwater (i.e. 1–2 mg L^{-1}) in the vicinity of the excavated tunnel cannot exclude a possible natural NH_4-N enrichment of the groundwater in the studied rock volume induced by an artificial drawdown of modern Baltic Sea water taking place after the excavation of the TASU and TASP tunnels. The common rise of NH_4-N and Mg concentrations in the borehole sections in the boreholes KA2050A and KA2051A (Figure 7-7; Figure 7-8b) tend to support the Baltic Sea drawdown hypothesis, although a more complex scenario, involving both drawdown and mixing of marine water with more dilute water is suggested by the stable Cl concentration and $\delta^{18}O$ values and the moderate NH_4-N concentrations (< 1 mg L^{-1}) found in the groundwaters (Figure 7-7; Figure 7-8b).

A pronounced decrease of NH_4-N concentrations was observed during year 2014 in borehole KA2051A01 (Figure 7-7). This specific period coincided with the drilling phase of new boreholes (K08028F01 and K03009F01) along the TASU tunnel wall (Wallin 2016). Such a temporary decrease suggests a possible hydrogeological connection between the fractures intersected by the newly drilled boreholes and the identified hydro-structures monitored in the isolated borehole sections in borehole KA2051A01. In such a case the orientation and location of the borehole KA2051A01 allows groundwater from the hydro-structures to be drawn towards the newly drilled boreholes causing a drainage effect. The two newly drilled boreholes displayed NH_4-N concentrations relatively similar to those determined in the section no. 9 in borehole KA2051A (Figure 7-7). However, the NO_3-N and NO_2-N concentrations from the new borehole K03009F01 were unexpectedly high (NO_3-N up to 24 µg L^{-1}; NO_2-N up to 3.1 µg L^{-1}) (Figure 7-6).

8 Influence of drawdown and mixing on ammonium concentrations

8.1 Evolution of mixing induced by the tunnel expansions

Mixing is the dominant process imposing the composition of the major constituents in the fractured bedrock (see Section 5.2). Because of the multiple origin and residence time of the waters composing the groundwater in the bedrock, several approaches have been developed to characterise groundwater mixing, including qualitative and quantitative methods. The qualitative method relies on conservative variables (e.g. groundwater classification; Figure 5-6) and allows identifying the dominant component/origin of the groundwater. Quantitative method relies on Principal Component Analysis (PCA) to study variations in groundwater compositions so that the mixing components, their proportions, and chemical reactions can be identified (Laaksoharju et al. 1999a, Laaksoharju et al. 2008a, Gómez et al. 2014). The PCA method identifies the principal components in terms of linear combinations of the concentrations of those species analysed that best explain the spread in data. The method quantifies the contribution to hydrochemical variations by mixing of groundwater masses in a flow system by comparing groundwater compositions with identified end-member waters. There is however an uncertainty in the mixing proportions which is associated to the uncertainty in the composition of the end-members.

In the tunnel excavation environment, where intense flush-out of groundwater and partial to total replacement of past groundwater by rapidly intruding modern surficial water, the PCA method has difficulties in finding mixing proportions including both past and modern waters (e.g. Nilsson et al. 2011). Accordingly, in this work, the PCA method is not used in the attempts to quantify the mixing proportions between the end-members in the studied borehole sections. Instead the PCA is regarded as a method allowing comparing the composition of the groundwater in the studied borehole sections with respect to the groundwater dataset of the entire site and the identified end-members. This aims (1) to track the dominant multiple origins of the groundwaters in a context of complex mixing, (2) to identify whether significant changes of the groundwater composition has occurred since the excavation of the tunnels, i.e. before and during/after the blasting period at a local scale (near the excavated rock volume), and (3), if possible, to allow identification of co-variation between NH_4^+ and other ions.

Figure 8-1 and Figure 8-2 show the result of the principal component analysis in the three main principal component planes of the entire groundwater dataset collected at Äspö during year 2007 and year 2011, respectively. Here the data for Na, K, Ca, Mg, HCO_3, Cl, SO_4, NH_4-N and $\delta^{18}O$ have been included in the PCA. The first principal component, points in the direction of the maximum variability of the dataset, the second principal component points in the perpendicular direction with the second-largest variability and so on for the principal components. From a general point of view, the groundwater dataset of the entire site collected during year 2007 (Figure 8-1) and collected during year 2011 (Figure 8-2) displays similar distribution along the 3 main principal components. This means that the PCA transformation performed with the dataset for these two specific years is similar and thus groundwater in borehole sections near the TASS tunnel (Figure 8-1) and near the TASU and TASP tunnels (Figure 8-2) can be compared with each other's in term of mixing. More central are the samples along the three main axes since they represent the more complex groundwater origins to estimate (Laaksoharju and Gurban 2003, Mathurin et al. 2012).

With respect to the isolated borehole sections near the TASS tunnel (Figure 8-1), the groundwater samples remain distributed near the axes, and thus near none of the identified end-members. The groundwaters occurring near the TASS tunnel thus originate from a complex mixing, involving at least three end-members or more. Only the systematic distribution of the groundwater samples on the other side of the deep saline end-member along the PC1 axis suggest some contribution of deep saline groundwater. Littorina Sea (past Baltic Sea) water and glacial melt-water seem to be the main origins of this groundwater, combined with a minor portion of deep saline groundwater. Contribution from modern Baltic Sea and meteoric groundwater are more difficult to identify from the nine variables used for the PCA. For the borehole sections in borehole KA3105A, which are the only sections with hydro-chemical monitoring performed both before and after blasting of the rock volume, no

significant change was noticed in term of composition (major anions and cations). In spite of an expected artificial drainage of groundwater towards the tunnel during and after its excavation, the impact of the blasting and TASS tunnel construction did not lead to major changes in groundwater composition nor in groundwater mixing/origin. The relatively low transmissivity (10^{-7} to 10^{-8} m^2 s^{-1}; Table 4-1) of the hydro-structures near the TASS tunnel (i.e. TRUE Block Scale model) may limit the hydrogeochemical evolution that has been observed in other parts of the Äspö HRL during its construction.

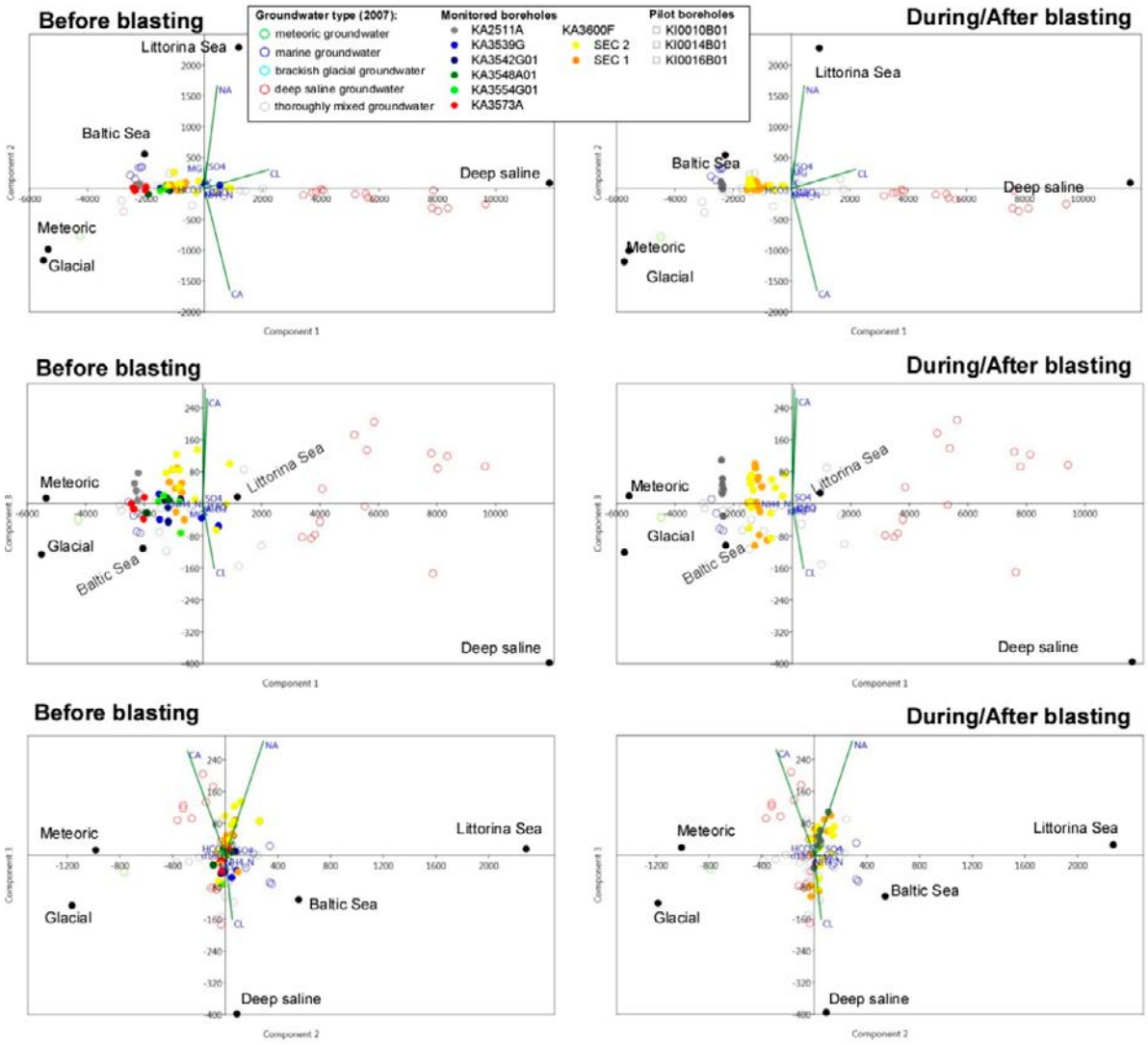

Figure 8-1. *Distribution of the groundwater after principal component analyses of 9 variables (Na, K, Ca, Mg, HCO_3, Cl, SO_4, NH_4-N and $\delta^{18}O$) along the three main component planes: PC1 vs PC2 (top), PC1 vs PC3 (middle), PC2 vs PC3 (bottom). Data include Äspö groundwaters collected during year 2007 colour labelled by groundwater type (based on the groundwater classification by Mathurin et al. (2012), see Section 5.2), and groundwaters in the rock volume near the TASS tunnels before (left) and during/ after (right) blasting. The black dots indicate the composition of the end-members reported in the Äspö area (Laaksoharju and Gurban 2003, Mathurin et al. 2012). The axe orientations of the 8 variables are represented in green.*

With respect to the borehole sections near the TASU and TASP tunnels (Figure 8-2), the groundwater collected in borehole KA2862A was distributed near the deep saline end-member (PC1), whereas groundwater collected in borehole KA3110A water distributed near the (modern) Baltic Sea end-member (PC1 and PC3). Groundwater in boreholes KA2050A and KA2051A01, monitored before and after blasting, as well as in borehole KA3105A, result from a more complex mixing, with a general distribution near the Baltic Sea type groundwater characterised in borehole KA3110A (along the PC1), even if a significant contribution from a meteoric end-member appears to be present in the mixture.

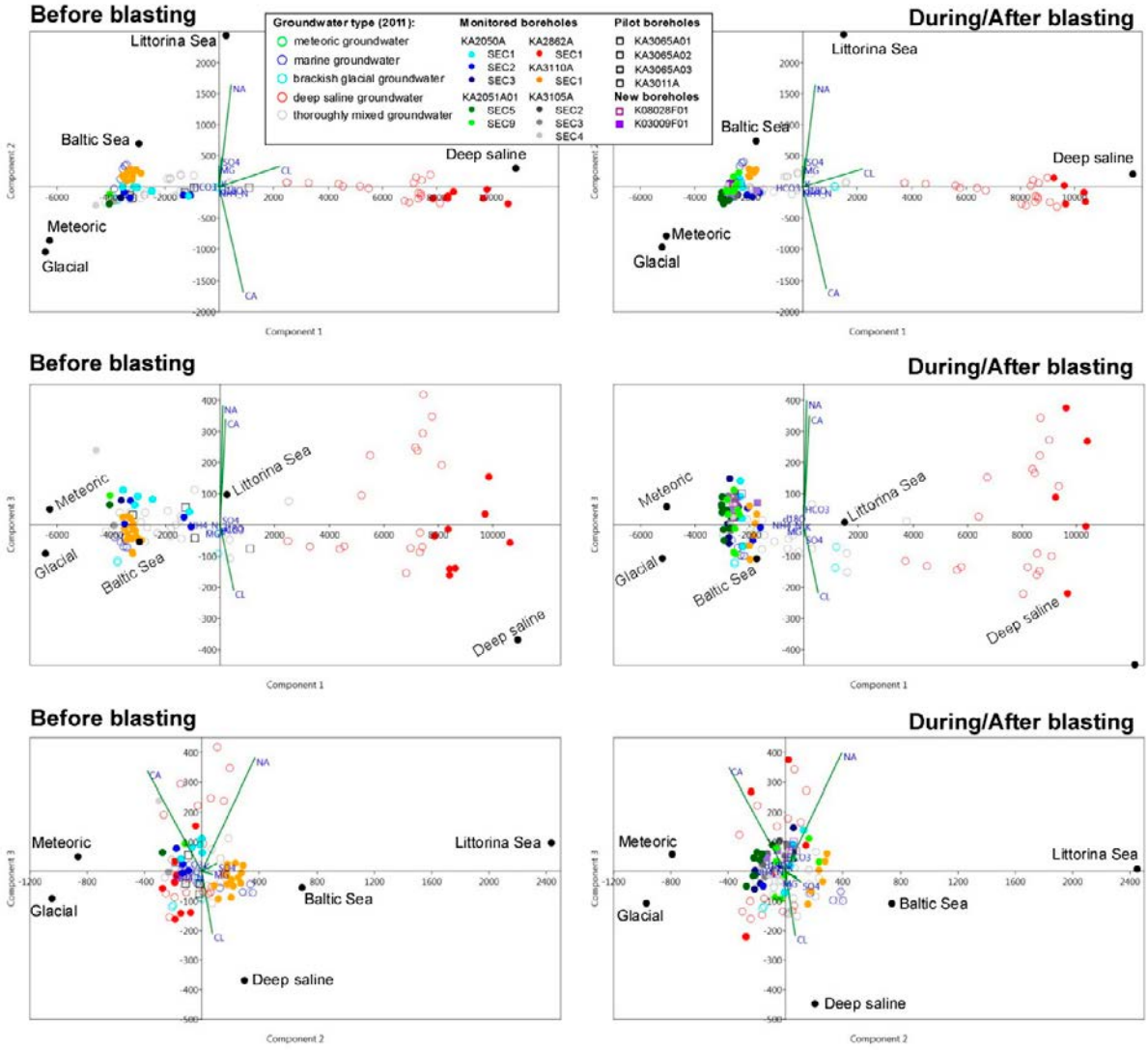

Figure 8-2. *Distribution of the groundwater after principal component analyses of 9 variables (Na, K, Ca, Mg, HCO_3, Cl, SO_4 NH_4-N and $\delta^{18}O$) along the three main components: PC1 vs PC2 (top), PC1 vs PC3 (middle), PC2 vs PC3 (bottom). Data include Äspö groundwaters collected during year 2011 colour labelled by groundwater type (based on the groundwater classification by Mathurin et al. (2012), see Section 5.2), and groundwaters in the rock volume near the TASU and TASP tunnels before (left) and during/after (right) blasting. The black dots indicate the composition of the end-members reported in the Äspö area (Laaksoharju and Gurban 2003, Mathurin et al. 2012). The axe orientations of the 8 variables are represented in green.*

In contrast to the TASS tunnel, the excavation of the TASU and TASP tunnels induced a hydrogeochemical disturbance in the surrounding rock volume. This disturbance was noticeable from the evolution of the concentrations of the major cations and anions and suggests an evolution of the groundwater, corresponding to the enrichment of modern water such as Baltic Sea water and meteoric groundwater. The occurrence of deep saline groundwater (KA2862A) and marine groundwater (KA3110A) indicates the presence of groundwater of various origins in the rock volume before the excavation. Accordingly, the evolution of the groundwater is certainly not induced by a massive drawdown of surficial water (or upconing of deep groundwater) resulting from the excavation of the TASU and TASP tunnel, but may result from partial drainage towards the tunnels and mixing of modern groundwaters already present in the local rock volume after the construction of the main Äspö HRL tunnel in the early 1990's. However, the partial enrichment of water with marine origin in the rock volume cannot be related to the occurrence of marine groundwater in the structures of borehole KA3110A due to a lack of direct evidence of hydraulic connections (from the existing hydro-structural model) with the structures of boreholes KA2050A, KA2051A01, KA3105A. Moreover, the location and orientation of borehole KA3110A, i.e. at distance and in the opposite direction, and thus not towards the TASU and TASP tunnels (Figure 5-2) indicate that hydraulic connection is unlikely at the depth of investigation. This does not exclude the occurrence of connectivity at shallower or deeper depth considering the dominant sub-vertical dipping of the hydraulic structures at Äspö (Figure 4-2; Ericsson et al. 2015).

The hydraulic connections between some of the water yielding structures sampled in boreholes KA2050A, KA2051A01, and KA3105A, identified in the conceptual M2 model (Morosini M 2012, personal communication; Table 5-3), could explain the observed similar hydrochemical evolution (Na, Ca and Cl) along the third component of the PCA during and after blasting (Figure 8-2). The transmissivity of the hydro-structures near the TASU and TASP tunnels (10^{-6} to 10^{-7} m^2 s^{-1}; Table 4-2), is generally one order of magnitude larger than the hydro-structures near the TASS tunnel (Table 4-1), which may favour the artificial drainage and the related local hydrochemical changes.

8.2 Natural enrichment of dissolved ammonium concentrations related to seawater drawdown

The variance of the NH_4-N concentration is insignificant compared to the variance of the major constituents used in the PCA. The highest NH_4-N concentrations measured in the groundwater in the Äspö area are related to the groundwater with a strong marine component (Figure 6-3). Since the PCA method suggests an evolution of the groundwater composition before and after blasting involving a partial enrichment in a marine component, the evolution of the NH_4-N concentrations was compared with variables positively related to the marine enrichment. Accordingly, the NH_4-N concentrations are compared with the Mg and the SO_4^{2-} concentration in binary plots (Figure 8-3).

The patterns between the NH_4-N and Mg show a common (non-linear) increase with the progressive enrichment of the marine component in the groundwater (Figure 8-3). This suggests one main and similar origin of the Mg and NH_4-N in the groundwater system associated to a seawater drawdown. On the other hand, there is substantial spreading of the samples for SO_4^{2-} concentrations within the range of 250–400 mg L^{-1} (Figure 8-4). In a hydro system where the hydrogeochemistry is dominated by mixing of groundwater of multiple origins, the linearity between two chemical variables is meaningless, except if the two elements display a similar co-variance. The observed patterns between the NH_4-N and SO_4^{2-} (Figure 8-4) are characteristic of the evolution of the SO_4^{2-} sources in the mixing, rich in modern Baltic and Littorina Sea waters but also composed partially of deep saline groundwater, which is naturally rich in SO_4^{2-} but relatively poor in NH_4-N and Mg.

8.3 Ammonium sources during Sea water infiltration

Although groundwater of marine origin has been identified as a natural source of NH_4^+ in Section 8.2, the marine origin of the NH_4^+ itself in the fractures near the TASS, TASU and TASP tunnels remains to be confirmed.

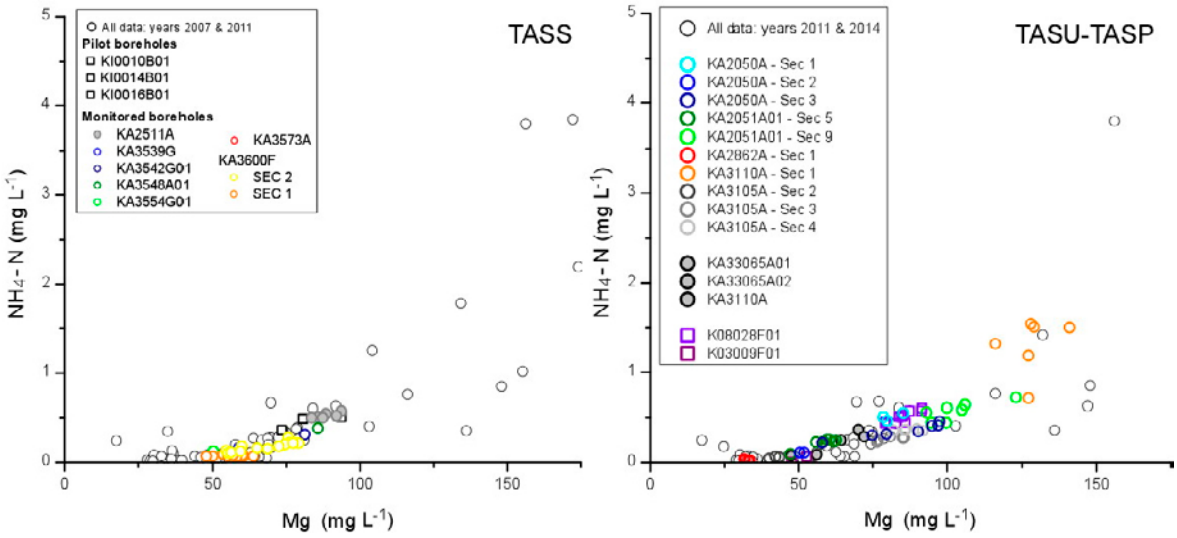

Figure 8-3. *NH_4-N concentrations versus Mg concentrations in borehole sections near the TASS tunnel and in the entire Äspö HRL during years 2007 and 2011 (left), and in borehole sections near the TASU and TASP tunnel and in the entire Äspö HRL during years 2011 and 2014 (right).*

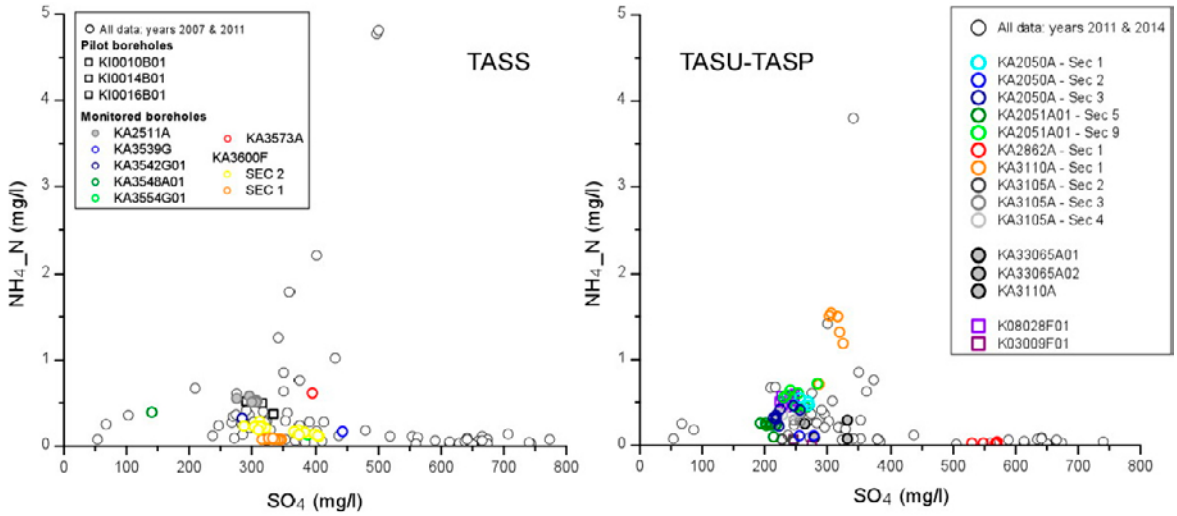

Figure 8-4. *NH_4-N concentrations versus SO_4^{2-} concentrations in borehole sections near the TASS tunnel and in the entire Äspö HRL during years 2007 and 2011 (left), and in borehole sections near the TASU and TASP tunnel and in the entire Äspö HRL during years 2011 and 2014 (right).*

Modern Baltic Sea water shows very low NH_4 concentrations, usually well below 0.05 mg L^{-1} (Engdahl et al. 2008, Mathurin et al. 2014). Enrichment in NH_4^+ occurs during the process of seawater intrusion along the flow path connecting the surface (Baltic Sea bay) and the characterised groundwater with a strong marine signature at depth. Along the preferential flow path, the marine sediment, usually rich in organic matter and bacterial activity, is believed to be the compartment where conditions are favourable for the transformation of organic nitrogen compounds and the formation of NH_4^+ thus increasing the ammonium concentrations (Carman and Rahm 1997, Gimeno et al. 2008). Such processes have notably been characterized in the present sediments of the Baltic Sea, where ammonium-N concentrations from 8 to 31 mg L^{-1} are frequent (Engdahl et al. 2008). If NH_4^+ is produced by the decomposition of organic debris in seabed sediments, this cation could be easily removed from groundwater by cation exchange processes along the flow path (Mathurin et al. 2014). Therefore, the concentration of ammonium will probably be below the detection limit, except if the seawater intrusion has reached the sampled depth fairly quickly. The role of mixing and drawdown of modern Baltic Sea water during the construction of the Äspö HRL have, therefore,

certainly contributed to the concentration of NH_4^+ observed in the groundwater along the flow paths during the intrusion. The exponential trend between Mg and NH_4^+ (Figure 8-3), especially in samples with Mg concentrations higher than 100 mg L^{-1}, reminds the strong influence of the bacterial activity on nitrogen concentrations in the marine rich fracture groundwater.

The bacterial activity inducing the high NH_4^+ concentrations may also promote significant increases in other elements that may be used as marine indicators in the present groundwaters. This is the case for dissolved manganese, SiO_2 and bicarbonate which were identified in previous studies (Gimeno et al. 2008, 2009). Each one of these chemical components is reactive to different extent within the fractures, which means that if the enrichment results from sources and reactions within the sea sediments, the inherited concentrations can be altered along the flow paths within the fracture network in the crystalline bedrock. Based on the known implication of the sea sediment on the high NH_4^+ concentrations found in the marine groundwater type, the evolution of other elements related to reactions in the sea sediment could provide additional confidence with respect to the identification of a single dominant source combined with groundwater mixing or multiple sources of dissolved nitrogen compounds, including contamination from blasting.

If the Mg concentrations are considered quasi-conservative in the fracture groundwater (i.e. mainly influence by mixing), the trend between Mg and the studied elements resulting from the production of NH_4^+ in the sea sediment can be used to qualitatively estimate the influence of mixing vs reactions (additional sources or sinks) in the crystalline bedrock. In the Baltic Sea bay around the Äspö Island, the average HCO_3^- concentrations are around 94 mg L^{-1}, the average Mn concentrations are approximately 0.045 mg L^{-1} and the SiO_2 concentrations are around 1.10 mg L^{-1}. During infiltration of the marine waters through sediments, biological activity promotes an important increase in HCO_3^- and Mn contents. For example, Engdahl et al. (2008) report HCO_3^- concentrations as high as 80–154 mg L^{-1} and Mn concentrations as high as 0.18 mg L^{-1} just 10 cm below the water-sediment interface in the shallow sea sediment in the bay around Äspö. In a similar way, enrichment of the silica concentrations may be promoted when marine water infiltrates through the sea sediment composed of highly soluble diatom skeletons. For the pore water of the sea sediment, SiO_2 concentrations as high as 6.6–10 mg L^{-1} were reported in the bay around Äspö (Engdahl et al. 2008).

The HCO_3^- concentrations in the groundwaters at Äspö varied greatly from 10 to 280 mg L^{-1} (Figure 8-5). The HCO_3^- concentrations remained very low for Mg concentration below 50 mg L^{-1} and generally increased sharply (with a large data scattering) within the Mg range 50–100 mg L^{-1}, reaching a plateau (i.e. around 200 ± 50 mg L^{-1}) for Mg concentrations higher than 100 mg L^{-1} (Figure 8-5). Generally, the Mn concentrations also increased with the Mg, despite of an increasing scattering, until a Mg concentration of 100 mg L^{-1} was reached (Figure 8-6). Above this concentration, the increase in Mn with the Mg concentration is declining (Figure 8-6). By contrast, the SiO_2 concentrations in groundwater displayed a substantial scattering (5–10 mg L^{-1}) for Mg concentrations below 100 mg L^{-1} (Figure 8-7) and a moderate scattering (5–7 mg L^{-1}) for Mg concentration higher than 100 mg L^{-1}. In other words, the HCO_3^- and Mn concentrations tend to increase to reach maximum concentration in marine rich groundwater, supporting a (partial or total) primary origin from the sea sediment in the groundwater. By contrast, the SiO_2 concentrations are not correlated to the Mg concentration, suggesting additional primary sources (e.g. silicate minerals) to the enrichment in the sea sediment and/or involvement of SiO_2 in reactive processes (i.e. control by mineral equilibrium).

With respect to the NH_4^+ concentrations, similar trends to those described for Mg can be observed between NH_4-N and HCO_3^- (Figure 8-5), Mn (Figure 8-6) or SiO_2 (Figure 8-7), although the plateau for the HCO_3^- concentrations or the gradient of the Mn rise were reached at lower NH_4-N concentrations (i.e. above 1 mg L^{-1}). Most of groundwater samples collected in the borehole sections near the studied tunnels have Mg concentration in the range of 50–100 mg L^{-1} and NH_4-N concentrations in the range of 0–0.75 mg L^{-1}. Therefore they distribute along the trend corresponding to the increase of HCO_3^- and Mn concentrations. The similarities observed in the general trends displayed by the two binary scatter plots support a similar origin for Mg and NH_4^+ and a similar behaviour along the flow path in the fracture network.

The large scattering observed along the trend is coherent with mixing including multiple end-members. The larger scattering observed in the binary scatter plots for HCO_3 than for Mn is induced by the reported substantial occurrence of calcite in the fractures (Landström and Tullborg 1995, Drake et al. 2006), which affects dissolved bicarbonate concentrations through control by calcite mineral equilibrium (pH dependent), together with biological activity (that promotes an increase in HCO_3^- contents; Gimeno et al. 2014). Among the elements inherited from reactions in the sea sediment, Mn appears to be the best proxy to $NH4^+$. This despite the fact that the dissolved carbonate system is also connected to the dissolved Mn concentration through equilibrium with respect to rhodochrosite. Marine groundwaters will be especially affected since autogenesis of Mn-carbonates is an active process in the Baltic Sea for the past 7 000–8 000 years (Gimeno et al. 2014). Such control by Mn-carbonate minerals would explain the common plateau observed for dissolved HCO_3^- and Mn concentrations in groundwater with Mg and NH_4-N concentration higher than 100 mg L^{-1} (Figure 8-5) and 1 mg L^{-1} (Figure 8-6), respectively.

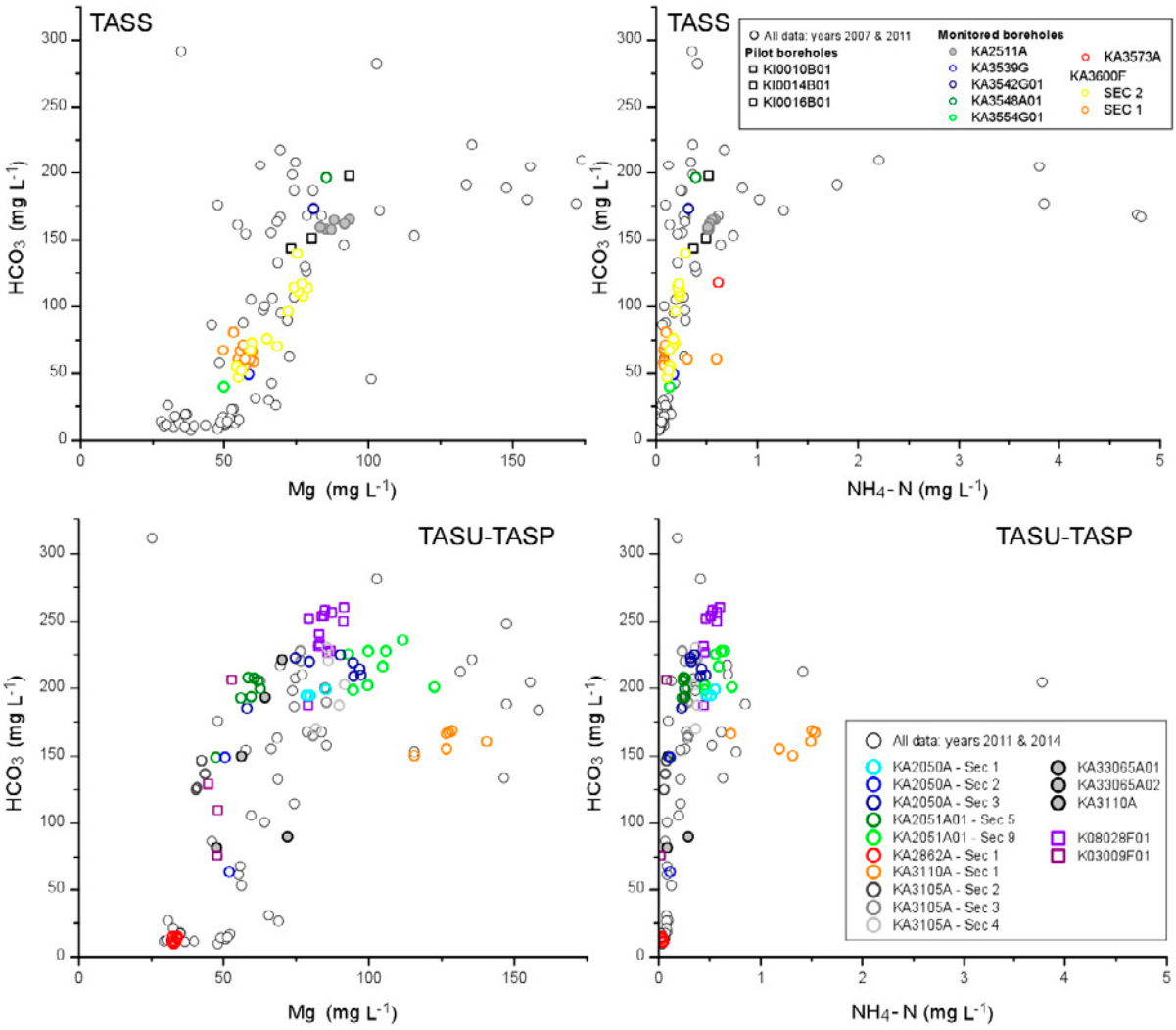

Figure 8-5. *HCO_3- concentrations versus Mg (left) and versus NH_4-N (right) concentrations in borehole sections near the TASS tunnel and in the entire Äspö HRL during years 2007 and 2011 (top), and in borehole sections near the TASU and TASP tunnel and in the entire Äspö HRL during years 2011 and 2014 (bottom).*

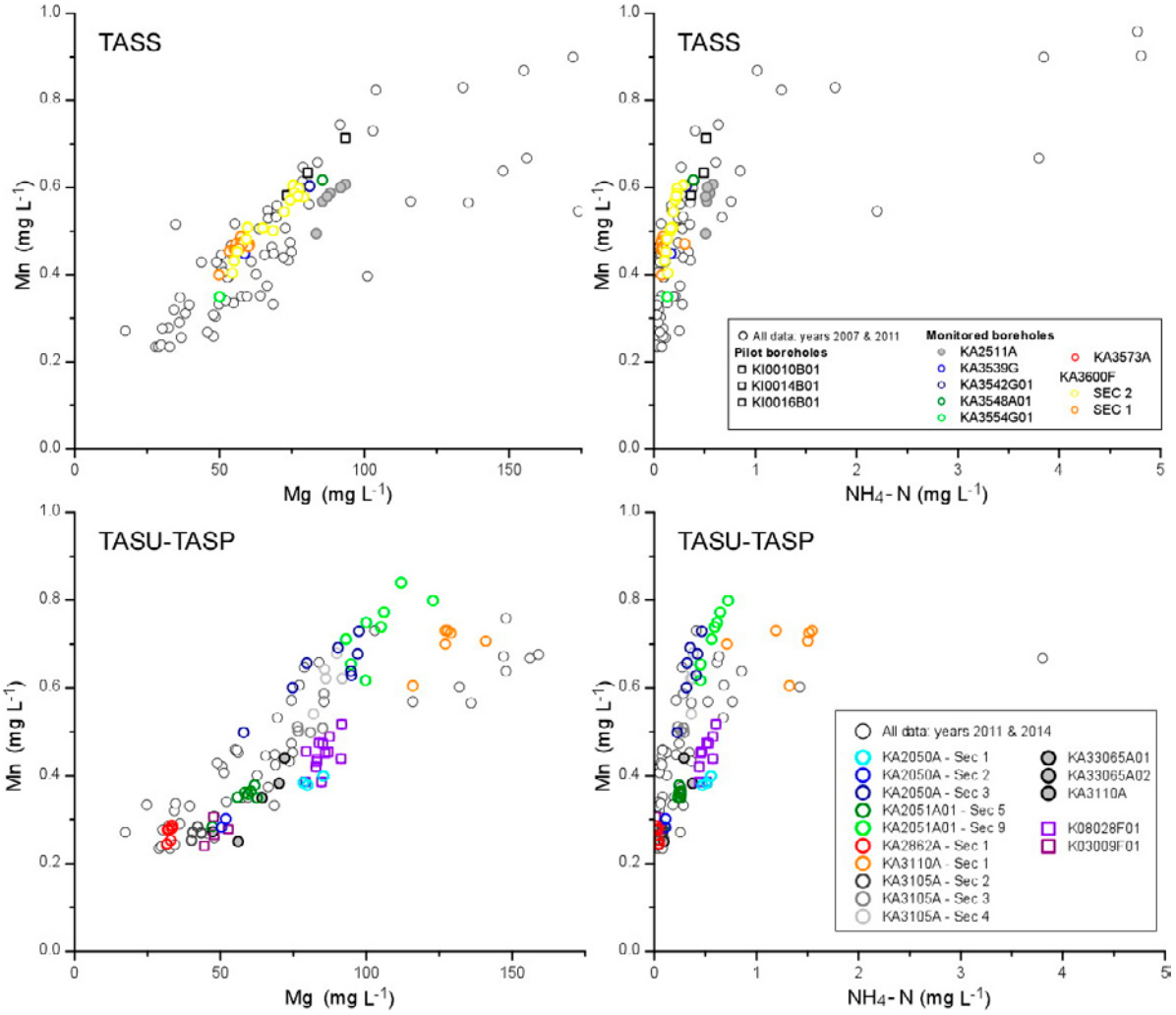

Figure 8-6. *Mn concentrations versus Mg (left) and versus NH_4-N (right) concentrations in borehole sections near the TASS tunnel and in the entire Äspö HRL during years 2007 and 2011 (top), and in borehole sections near the TASU and TASP tunnel and in the entire Äspö HRL during years 2011 and 2014 (bottom).*

Taken together, the comparison between each of these chemical components (i.e. HCO_3^-, SiO_2 and Mn) and NH_4-N emphasizes the role of mixing and drawdown of modern Baltic Sea water during the construction of the Äspö HRL. The groundwater data collected from the borehole sections in the bedrock close to the TASS, TASP and TASU tunnels display coherent concentrations of NH_4^+ and other dissolved elements inherited from the interaction in the sea sediment, both before and after the blasting activity compared to the entire set of data selected as representative for the Äspö site. The dissolved HCO_3^- and (to some extent) the dissolved Mn concentrations are controlled by mineral equilibrium (i.e. calcite and rhodochrosite, respectively), which induce their non-conservative behaviour. Accordingly, the observed scattering between NH_4-N and Mn (Figure 8-6) cannot be attributed to unusual NH_4^+ concentrations caused by possible contamination of the groundwater samples resulting from the blasting activity near the tunnel expansion.

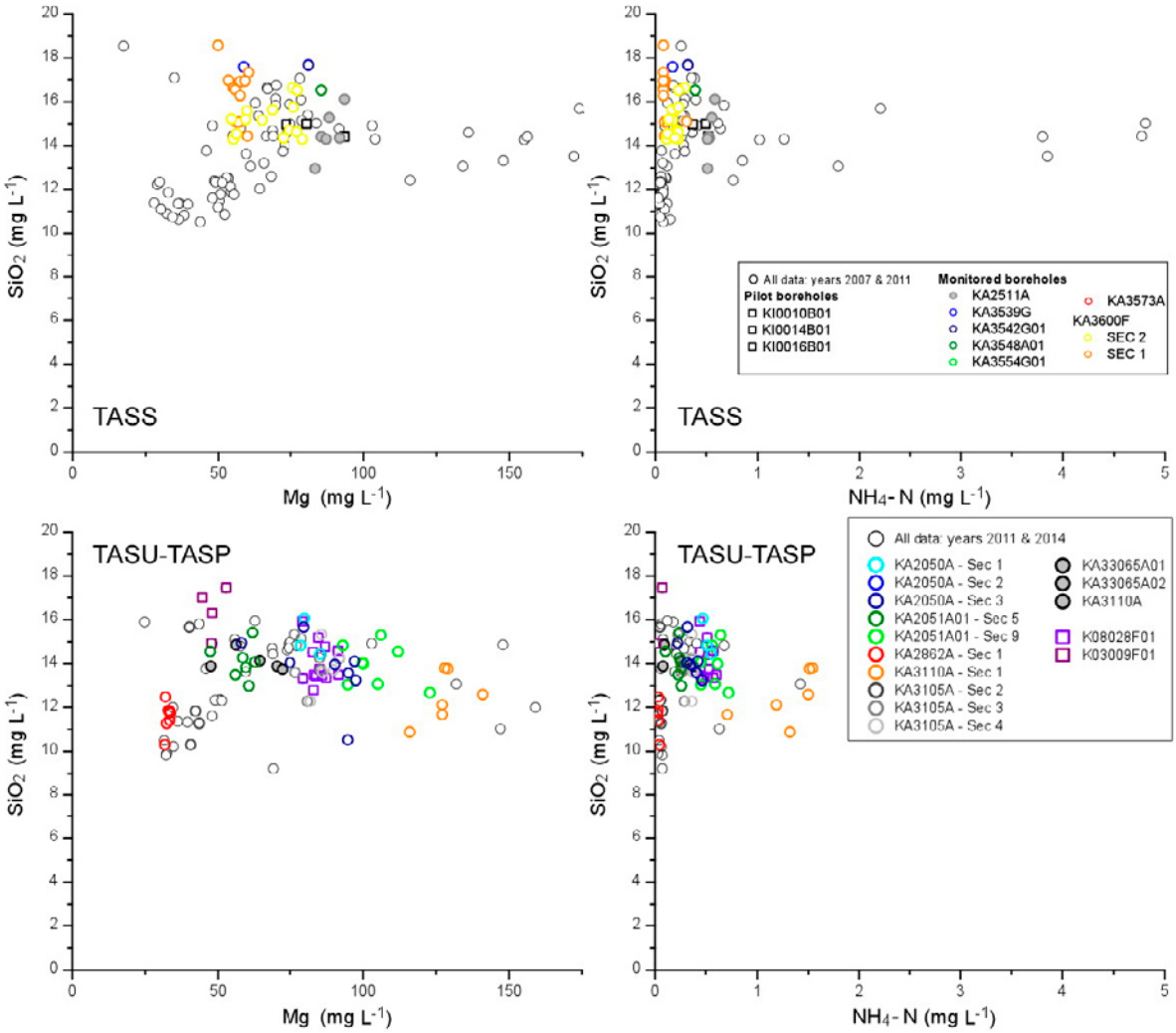

Figure 8-7. *SiO_2 concentrations versus Mg (left) and versus NH_4-N (right) concentrations in borehole sections near the TASS tunnel and in the entire Äspö HRL during years 2007 and 2011 (top), and in borehole sections near the TASU and TASP tunnel and in the entire Äspö HRL during years 2011 and 2014 (bottom).*

9 Discussion

The dissolved nitrogen in the rock volume close to the TASS, TASU and TASP tunnels is preferably present as ammonium (NH_4^+), while the amounts of nitrite (NO_2^-) and nitrate (NO_3^-) are comparatively low. The available data are too limited to allow a straightforward assessment of possible emission/contamination from the blasting activity. The limited data obtained during the blasting period, i.e. up to two samples in a few packed-off borehole sections, prevent the monitoring of short term changes (if any) induced in the fracture groundwater. Moreover, the sampled borehole sections during and after the blasting period are generally located far (>20m) from the excavated rock volume. The limitations are due to security reasons during tunnel construction work involving loading of explosives and the lack of borehole sections (as part of the monitoring program or other specially equipped boreholes) near the blasted tunnels suitable for assessment of possible nitrogen emission and propagation into the fracture groundwater. Consequently, the possible contamination assessed in this report can only be characterised in the broad volume of the blasted rock (Figure 5-1; Figure 9-1). The compiled nitrogen data in the rock volume close to the new tunnels illustrate, therefore, the general disturbance/change caused by dissolved nitrogen compounds induced by the blasting as well as by the new hydraulic conditions as a consequence of the excavation of new tunnels.

Leaching of nitrogenous compounds from explosives to the environment depends on several factors, such as solubility of the explosive or the hydrogeological conditions present at the mine site (Revey 1996). Whereas the nitrogen compounds that originate from explosives usually appear dominantly as nitrate and ammonium or ammonia in mine waters (Håkansson 2016, Karlsson and Kauppila 2016), the in situ redox (Eh: −260 to −400 mV; Auque et al. 2008) and pH (7.5 to 8.45; Smellie and Laaksoharju 1992) conditions in the groundwater system, together with the biological activity (Pedersen 2001, Hallbeck and Pedersen 2008a), induce a predominant (reduced) ammonium form of nitrogen compounds. If nitrogen contamination occurred in groundwater during the blasting activity, such a contamination adds to the natural concentrations of ammonium prevailing in the groundwater near the studied tunnels. Considering that the concentrations of nitrate and nitrite determined in the studied groundwaters are systematically negligible as compared to ammonium, no evidence of an active reduction process can be characterized and thus no emitted/anomalous nitrate or nitrite can be defined.

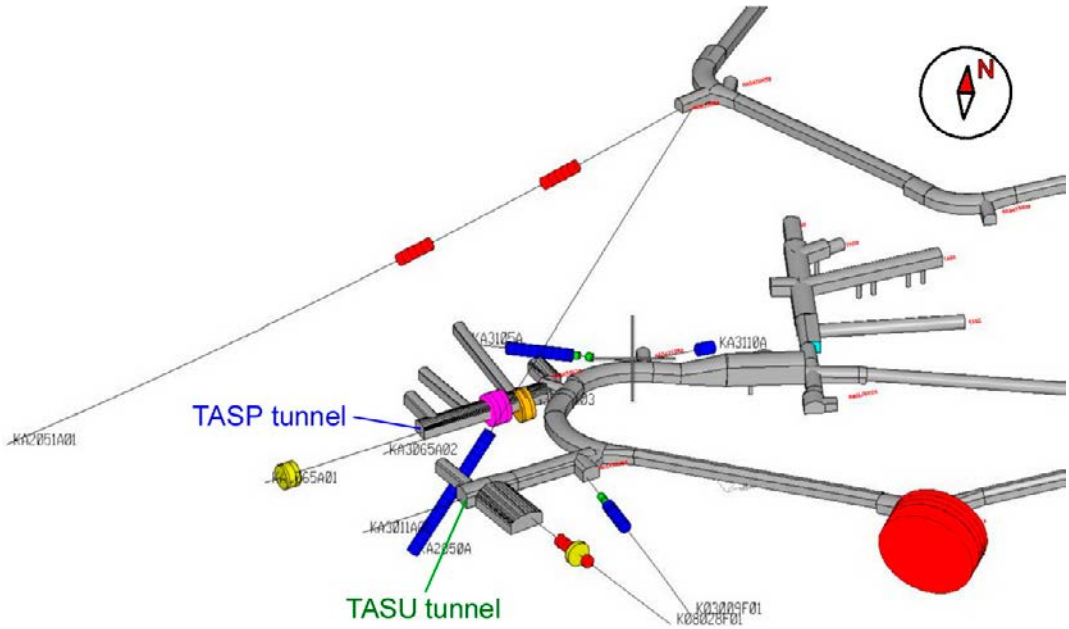

Figure 9-1. *3D distribution of the packed-off borehole sections hydrochemically monitored during and/or after blasting near the TASU and TASP tunnels (profile view). Only section 1 in borehole KA2050A is represented; sections 2 and 3 are represented in Figure 5-2. The packed-off borehole sections are symbolized by cylinders of different colours and/or diameters mainly for visualisation purposes.*

The two boreholes drilled after the completion of the TASU tunnel (boreholes K08028F01 and K03009F01) and perpendicular to the wall displayed anomalously high nitrate and nitrite concentrations in comparison to the prevailing natural variability ("new boreholes" in Figure 7-6). Although anomalous for groundwaters, the nitrate and nitrite concentrations remain substantially low in the two boreholes (up to 0.025 mg L^{-1} for NO_2-N; Figure 7-6) in contrast to the concentration of ammonium (around 0.5 mg L^{-1}; Figure 7-7). The groundwater samples from boreholes K08028F01 and K03009F01 were partly collected during the drilling procedure, in order to obtain point-wise fingerprints of the groundwater along the whole borehole length, i.e. *"first strike"* sample of the formation water (Wallin 2016), also regarded as pristine groundwater in the fractures intersected by the drilling equipment. In other words, the water sampled during the drilling is a mixture of returning drilling water and formation groundwater in the water-bearing fractures intersected along the drilled distance. The hydrogeochemical samples collected at two different occasions during drilling of borehole K03009F01 in year 2013 showed the highest nitrate and nitrite concentrations (NO_3-N: 13 µg L^{-1}; NO_2-N: 1.4 µg L) at 0.34–2.55 m borehole length corresponding to the part of the borehole closest to the TASU tunnel wall. These anomalous high concentrations of nitrate and nitrite can be due to contamination from remains of the blasting activity in the bedrock near the excavated rock volume. However, there can also be several other causes for the contamination than blasting.

The content of drilling water must be considered as a possible reason for contamination of borehole K03009F01. However, the drilling water content in this particular borehole was low (<2 % calculated from addition of uranine dye to the drilling water as a tracer) during drilling as well as after completion of the borehole (Wallin 2016). Therefore, the drilling water source can be excluded. The persistent high NO_3^- after completion of the borehole (NO_3-N up to 24 µg L^{-1}; NO_2-N up to 3.1 µg L^{-1}) observed in one borehole section relatively far from the tunnel wall (borehole length: 21.5–24.5) rule out a possible contamination from the drilling equipment. If the high nitrate and nitrite concentrations are due to contamination, the source of the contamination is uncertain. Contamination from blasting cannot be excluded in the first samples as they correspond to water samples collected in the shortest sections (while drilling) including natural and blast induced fractures near the tunnel wall. However, microbial activity leading to nitrification in the section or during sampling is also likely, as similar outlier values were also found in data from the monitoring program during years 2007 and 2014 (Figure 6-5; Figure 6-6). Duplicate samples or sample series from section 5 of borehole K03009F01 including NO_3-N and NO_2-N could have been used to exclude sampling contamination, but such additional samples were not taken. It is not possible to estimate or simply assess a possible occurrence of nitrogen related to blasting from the available dissolved NO_3-N and NO_2-N data. Assessment of hydraulic transmissivity in the fractures and/or the characterisation of the microbial community active within the packed-off section 5 of borehole KA3009F01 may be useful for the interpretation of the observed outliers, if the hypothetical role of nitrate/nitrite reducing bacterial activity can be clarified.

The only possible evidence of impacts on the nitrogen content in groundwater by the tunnel expansion is the moderate increase in NH_4^+ concentrations, which started some months after the beginning of the TASU and TASP tunnel excavation in many packed off-sections located close to the blasted rock volumes (Figure 7-7). The increase remains evident even when compared to the natural variability of NH_4^+ in groundwater close to the TASU and TASP tunnels (Figure 7-7). The dissolved NH_4^+ reached a higher concentration range compared to the corresponding values in each selected packed-off borehole sections before blasting. The use of the PCA methods did not allow a direct identification of the role of mixing on the evolution of the NH_4^+ concentrations (see Chapter 8), due to a negligible variance of the NH_4^+ concentrations in comparison to the other variables (i.e. major dissolved elements). However, the noticeable enrichment of the marine component in several borehole sections near the TASU and TASP tunnel, inducing a common rise of Mg and NH_4^+ concentrations, suggests a natural evolution of the nitrogen compounds related to the artificial drainage caused by the tunnel excavation and a partial enrichment of the marine component of the groundwater. Such process was not observed in the borehole sections near the TASS tunnel, where less explosives were used for the blasting. Although only a few packed-off borehole sections were monitored, the relatively constant values (around 0.1 mg L^{-1}) or the progressive decreases of the dissolved NH_4^+ concentrations (0.29 to 0.13 m L^{-1}) compared to the initial concentrations (Figure 7-1) are likely due to the lower transmissivity of the hydro-structures in the vicinity of the investigated rock volume, and possibly also due to the limited occurrence of groundwater of marine origin in the rock volume near the TASS tunnel before tunnel excavation.

Generally most of the groundwater in the isolated borehole sections in the rock volume near the TASS, TASU and TASP tunnels, displayed NH_4-N concentrations lower than 1 mg L^{-1}. Accordingly, the samples were distributed along the lower part of the increasing trend of Mg and NH_4-N concentrations (Figure 8-3) observed from the natural variability of groundwater collected at the Äspö site. This indicates that the extent of the contamination from blasting is limited (if any) as no extreme (i.e. outlier) NH_4^+ concentrations can be identified from the data when compared to the overall body of data for the Äspö site. Additionally, the hydro-structures near the TASS tunnel displayed relatively low hydraulic transmissities, and thus lower potential for the nitrous gases to penetrate into the rock volume. The overall low NH_4^+ concentrations in the packed-off borehole sections intersecting the hydro-structures near the TASS tunnel tend to support the absence of apparent contamination from the blasting with respect to nitrogen compounds. Near the TASU and TASP tunnels, the overall low to moderate NH_4^+ concentrations in the packed-off borehole sections near the blasted rocks indicate that the use of explosives has indirectly contributed to the partial increase of the NH_4^+ concentrations. However, the observed increasing trend appears to result from a partial drawdown of groundwater of marine origin already present in the rock volume/hydro structures (i.e. before blasting of the TASU and TASP tunnels) and likely induced from the construction of the Äspö HRL in the early 1990's (Figure 6-3) and the associated substantial regional drainage.

It is likely that possible contaminated groundwater from blasting will be flushed out from the water-bearing rock volume near the excavated tunnels relatively soon due to the artificial flow. The present study therefore concludes that no apparent contamination of nitrogen compounds from blasting and by the use of explosives in the rock volume relatively near the excavated TASS, TASU and TASP tunnels could be identified. Considering the large natural range of NH_4^+ found at the Äspö site, the low to moderate NH_4^+ concentrations appear to be related to the portion of the marine component, naturally enriched with respect to NH_4^+ by bacterial activity in the sea sediment, in the groundwater. The hydraulic transport process and changed proportions of groundwater with marine origin may obstruct the possibilities to identify possible minor contamination from the blasting.

10 Conclusions

The possible influence of blasting has been investigated in two rock volumes of the Äspö HRL during the two successive expansion phases of the Äspö tunnel, corresponding to the excavation of the TASS tunnel (450 m.b.s.l.) during year 2008 and the TASU and TASP tunnels (410 m.b.s.l.) during year 2012. The characterisation of the dissolved nitrogen compounds in fracture groundwater of the entire Äspö site and the evolution of the dissolved nitrogen compounds before, during and after the blasting activity in the rock volume close to the TASS, TASU and TASP tunnels indicate that:

(1) NH_4^+ was the dominant dissolved nitrogen compound in the investigated rock volumes, in agreement with the prevailing reducing redox conditions of the groundwater at the investigation depth.

(2) the variability of the NH_4-N concentrations of the Äspö site ranged 0.006 to 1.1 mg L^{-1} before the construction of the Äspö HRL and 0.3 to 1.3 mg L^{-1} after the construction of the Äspö HRL at depth greater than 200 m.b.s.l.

(3) with respect to the evolution of the nitrogen compounds in groundwater close to the excavated rock volumes:
- during the TASS blasting, the dissolved NH_4^+ and NO_2^- concentrations remained generally among the highest percentile measured before the blasting period (NH_4-N: 0.06 to 0.6 mg L^{-1}; NO_2-N: up to 0.5 µg L^{-1}), whereas the dissolved NO_3-N concentrations were systematically below the limit of detection.
- during the TASU and TASP blasting period, the dissolved NH_4-N and NO_2-N concentrations were generally similar to the natural concentrations (NH_4-N 0.017 to 0.55 mg L^{-1}; NO_2-N: up to 0.7 µg L^{-1}) - or within the analytical uncertainty for sections with only one sample - determined before the blasting period, whereas the dissolved NO_3-N concentrations were systematically below the limit of detection.
- The variability of the NH_4-N concentrations (i.e. before, during and after blasting) close to the excavated tunnels remained within the natural variability of the Äspö site.

(4) with respect to potential contamination of nitrogen compounds from blasting:
- in the rock volume near the TASS tunnel, no anomalous concentration peaks, if they occurred, could be identified (from the biannual monitoring program) along the time series of NH_4 concentrations.
- the moderate increases in NH_4^+ concentrations, which appeared some months after the beginning of the TASU and TASP tunnel excavation in many borehole sections close to the blasted rock volumes, could be signs of potential contamination of the groundwater at depth by nitrogen from blasting.
- if the use of explosives may have contributed to the partial increase of the NH_4^+ concentrations near the TASU and TASP tunnels, the extent of the potential contamination would be very limited (i.e. increase <0.3 mg L^{-1})
- anomalously high nitrate and nitrite concentrations (NO_3-N up to 24 µg L^{-1}; NO_2-N up to 3.1 µg L^{-1}), compared to the natural concentration range, were found in the K030009F01 borehole drilled along the TASU tunnel wall (i.e. after completion of the TASU excavation).

The general understanding of the site, supported by a principal component analyse and the identified correlation between the Mg and the NH_4^+ concentrations trends in the studied isolated borehole sections, suggests a natural evolution of the NH_4^+ concentrations related to the artificial drainage in the TASU and TASP tunnels caused by their excavation. The drawdown of groundwater of marine origin, already present in the rock volume/hydro structures (i.e. before blasting), may have induced the temporary increases of NH_4^+ concentrations a few months after blasting and excavation. The use of explosives and the following rock excavation would therefore have indirectly contributed to the partial and very limited increase of the NH_4^+ concentrations, which cannot be considered as a contamination. Such process was not observed in the borehole sections near the TASS tunnel, probably due to the lower transmissivity of the hydro-structures in the vicinity of the investigated rock volume, and possibly also due to less contribution of groundwater of marine origin in the rock volume near the TASS tunnel.

The anomalously high concentrations of nitrate and nitrite found in the K030009F01 borehole are evidences of contamination of the natural nitrogen pool available in the presented data. However, the origin of the contamination can be multiple. Although the contamination from blasting in the fracture cannot be excluded, microbial activity leading to nitrification in the section or in the samples remains likely. Because the isotopic composition for nitrogen compounds is a powerful tool for improved process understanding and to identify the nitrogen sources (e.g. Aravena and Robertson 1998, Denk et al. 2017), a detailed characterisation of the isotopic composition of the nitrogen compounds, in addition to duplication of the sampling in the packed-off section of concern, are therefore recommended in order to clarify the origin of the potential contaminations. Such strategy is also recommended to be applied in groundwater sampling programmes for future expansion projects at the Äspö HRL.

References

SKB's (Svensk Kärnbränslehantering AB) publications can be found at www.skb.com/publications.

Andersson P, 1999. TRUE Block Scale project. Analysis of needs for re-instrumentation of boreholes KA2511A, KA2563A and Kl0025F. SKB IPR-01-49, Svensk Kärnbränslehantering AB.

Andersson P, Byegård J, Dershowitz B, Doe T, Hermanson J, Meier P, Tullborg E-L, Winberg A (ed), 2002. Final report of the TRUE Block Scale project. 1. Characterisation and model development. SKB TR-02-13, Svensk Kärnbränslehantering AB.

Andersson P, Byegård J, Billaux D, Cvetkovic V, Dershowitz W, Doe T, Hermanson J, Poteri A, Tullborg E-L, Winberg A (ed), 2007. TRUE Block Scale Continuation project. Final report. SKB TR-06-42, Svensk Kärnbränslehantering AB.

Aravena R, Robertson W D, 1998. Use of multiple isotope tracers to evaluate denitrification in ground water: study of nitrate from a large-flux septic system plume. Ground Water 36, 975–982.

Arilahti E, Bojinov M, Mäkelä K, Laitinen T, Saario T, 2000. Stress corrosion cracking investigation of copper in groundwater with ammonium ions. Posiva Working Report 2000-46, Posiva Oy, Finland.

Auqué L, Gimeno M J, Gómez J, Nilsson A-C, 2008. Potentiometrically measured Eh in groundwaters from the Scandinavian Shield. Applied Geochemistry 23, 1820–1833.

Banwart S, Gustafsson E, Laaksoharju M, Nilsson A-C, Tullborg E-L, Wallin B, 1994. Large-scale Intrusion of shallow water into a vertical fracture zone in crystalline bedrock: initial hydrochemical perturbation during tunnel construction at the Äspö Hard Rock Laboratory, southeastern Sweden. Water Resources Research 30, 1747–1763.

Carman R, Rahm L, 1997. Early diagenesis and chemical characteristics of interstitial water and sediments in the deep deposition bottoms of the Baltic proper. Journal of Sea Research 37, 25–47.

Degnan J R, Böhlke J K, Pelham K, Langlais D M, Walsh G J, 2016. Identification of groundwater nitrate contamination from explosives used in road construction: isotopic, chemical, and hydrologic evidence. Environmental Science & Technology 50, 593–603.

Denk T R A, Mohn J, Decock C, Lewicka-Szczebak D, Harris E, Butterbach-Bahl K, Kiese R, Wolf B, 2017. The nitrogen cycle: a review of isotope effects and isotope modeling approaches. Soil Biology and Biochemistry 105, 121–137.

Drake H, Sandström B, Tullborg E-L, 2006. Mineralogy and geochemistry of rocks and fracture fillings from Forsmark and Oskarshamn: Compilation of data for SR-Can. SKB R-06-109, Svensk Kärnbränslehantering AB.

Ekblad A, 1995. Kvävespridning från bergtäkt: en förstudie. Publikation B 418, Chalmers University of Technology, Sweden. (In Swedish.)

Emeis K-C, Struck U, Blanz T, Kohly A, Voss M, 2003. Salinity changes in the central Baltic Sea (NW Europe) over the last 10 000 years. Holocene 13, 411–421.

Engdahl A, Rådén R, Borgiel M, Omberg L-G, 2008. Oskarshamn and Forsmark site investigation Chemical composition of suspended material, sediment and pore water in lakes and sea bays. SKB P-08-81, Svensk Kärnbränslehantering AB.

Ericsson L O, Thörn J, Christiansson R, Lehtimäki T, Ittner H, Hansson K, Butron C, Sigurdsson O, Kinnbom P, 2015. A deonstration project on controlling and verifying the excavation-damaged zone. Experience from the Äspö Hard Rock Laboratory. SKB R-14-30, Svensk Kärnbränslehantering AB.

Follin S, 2008. Bedrock hydrogeology Forsmark. Site descriptive modelling, SDM-Site Forsmark. SKB R-08-95, Svensk Kärnbränslehantering AB.

Fox A, Dershowitz W, Ziegler M, Uchida M, Takeuchi S, 2005. Äspö Hard Rock Laboratory. TRUE Block Scale continuation project. BS2B experiment: Discrete fracture and channel network modeling of solute transport modeling in fault and non-fault structures. SKB IPR-05-38, Svensk Kärnbränslehantering AB.

Frape S K, Blyth A, Blomqvist R, McNutt R H, Gascoyne M, 2003. Deep fluids in the continents: II. Crystalline rocks. In Holland H D, Turekian K K (eds). Treatise on geochemistry. Vol. 5. Oxford: Pergamon, 541–580.

Fritz P, 1997. Saline groundwater and brines in crystalline rocks: the contributions of John Andrews and Jean-Charles Fontes to the solution of a hydrogeological and geochemical problem. Applied Geochemistry 12, 851–856.

Gascoyne M, 2004. Hydrogeochemistry, groundwater ages and sources of salts in a granitic batholith on the Canadian Shield, southeastern Manitoba. Applied Geochemistry 19, 519–560.

Gimeno M J, Auqué L F, Gómez J, Acero P, 2008. Water–rock interaction modelling and uncertainties of mixing modelling. SDM-Site Forsmark. SKB R-08-86, Svensk Kärnbränslehantering AB.

Gimeno M J, Auqué L F, Gómez J B, Acero P, 2009. Water–rock interaction modelling and uncertainties of mixing modelling. Site descriptive modelling SDM-Site Laxemar. SKB R-08-110, Svensk Kärnbränslehantering AB.

Gimeno M J, Auqué L F, Acero P, Gómez J B, 2014. Hydrogeochemical characterisation and modelling of groundwaters in a potential geological repository for spent nuclear fuel in crystalline rocks (Laxemar, Sweden). Applied Geochemistry 45, 50–71.

Gómez J B, Gimeno M J, Auqué L F, Acero P, 2014. Characterisation and modelling of mixing processes in groundwaters of a potential geological repository for nuclear wastes in crystalline rocks of Sweden. Science of the Total Environment 468–469, 791–803.

Gustafsson B G, Westman P, 2002. On the causes for salinity variations in the Baltic Sea during the last 8500 years. Paleoceanography and Paleoclimatology 17, 12-1–12-14.

Hallbeck L, Pedersen K, 2008a. Characterization of microbial processes in deep aquifers of the Fennoscandian Shield. Applied Geochemistry 23, 1796–1819.

Hallbeck L, Pedersen K, 2008b. Explorative analyses of microbes, colloids, and gases together with microbial modelling. Site description model, SDM-Site Laxemar. SKB R-08-109, Svensk Kärnbränslehantering AB.

Hardenby C, Sigurdsson O, 2010. Äspö Hard Rock Laboratory. The TASS-tunnel. Geological mapping. SKB R-10-35, Svensk Kärnbränslehantering AB.

Hardenby C, Sigurdsson O, Hernqvist L, Bockgård N, 2008. Äspö Hard Rock Laboratory. The TASS-tunnel project "Sealing of tunnel at great depth". Geology and hydrogeology – Results from the pre-investigations based on the boreholes Kl0010B01, Kl0014B01 and Kl0016B01. SKB IPR-08-18, Svensk Kärnbränslehantering AB.

Hermansson J, 1998. Äspö Hard Rock Laboratory. TRUE Block Scale projekt. October 1997 structural model; update using characterisation data from KA2511A and KI0025F. SKB IPR-01-41, Svensk Kärnbränslehantering AB.

Håkansson K, 2016. Kvävehalter i berg. Kunskapssammanställning bakgrundshalter. Fallstudie och vattenprovtagningar TASS, Äspö. SKB R-10-32, Svensk Kärnbränslehantering AB. (In Swedish.)

Högström K, Olin M, 1990. Studie av grundvattnets kväveinnehåll i en bergtäkt. Publikation B 352, Chalmers University of Technology, University of Gothenburg, Sweden.

Johansson E, Stenberg L, Olofsson I, Karlzén R, 2015. Utbyggnaden av Äspölaboratoriet 2011–2012. Karakterisering, projektering och tunneldrivning. SKB R-13-28, Svensk Kärnbränslehantering AB. (In Swedish.)

Jonsson J, 2012. Uppföljning av kvalitét på sprängning inom bergentreprenaden vid SKB:s Äspölaboratorium. Luleå University of Technology, Sweden. (In Swedish.)

Karlsson T, Kauppila T, 2016. Explosives-originated nitrogen emissions from dimension stone quarrying in Varpaisjärvi, Finland. Environmental Earth Sciences 75, 834.

Karlzén R, Johansson E, 2010. Slutrapport från drivningen av TASS-tunneln. SKB R-10-31, Svensk Kärnbränslehantering AB. (In Swedish.)

King F, Ahonen L, Taxén C, Vuorinen U, Werme L, 2001. Copper corrosion under expected conditions in a deep geologic repository. SKB TR-01-23, Svensk Kärnbränslehantering AB.

King F, Lilja C, Pedersen K, Pitkänen P, Vähänen M, 2010. An update of the state-of-the-art report on the corrosion of copper under expected conditions in a deep geologic repository. SKB TR-10-67, Svensk Kärnbränslehantering AB.

King F, Lilja C, Vähänen M, 2013. Progress in the understanding of the long-term corrosion behaviour of copper canisters. Journal of Nuclear Materials 438, 228–237.

Laaksoharju M, Gurban I, 2003. Äspö Hard Rock Laboratory. Update of the hydrogeochemical model 2002. SKB IPR-03-36, Svensk Kärnbränslehantering AB.

Laaksoharju M, Wallin B (eds), 1997. Evolution of the groundwater chemistry at the Äspö Hard Rock Laboratory, Proceedings of the second Äspö International Geochemistry Workshop, June 6–7, 1995. SKB ICR-97-04, Svensk Kärnbränslehantering AB.

Laaksoharju M, Skarman C, Skarman E, 1999a. Multivariate mixing and mass balance (M3) calculations, a new tool for decoding hydrogeochemical information. Applied Geochemistry 14, 861–871.

Laaksoharju M, Tullborg E-L, Wikberg P, Wallin B, Smellie J, 1999b. Hydrogeochemical conditions and evolution at the Äspö HRL, Sweden. Applied Geochemistry 14, 835–859.

Laaksoharju M, Gascoyne M, Gurban I, 2008a. Understanding groundwater chemistry using mixing models. Applied Geochemistry 23, 1921-1940.

Laaksoharju M, Smellie J, Tullborg E-L, Gimeno M, Molinero J, Gurban I, Hallbeck L, 2008b. Hydrogeochemical evaluation and modelling performed within the Swedish site investigation programme. Applied Geochemistry 23, 1761–1795.

Landström O, Tullborg E-L, 1995. Interactions of trace elements with fracture filling minerals from the Äspö Hard Rock Laboratory. SKB TR 95-13, Svensk Kärnbränslehantering AB.

Louvat D, Michelot J L, Aranyossy J F, 1999. Origin and residence time of salinity in the Äspö groundwater system. Applied Geochemistry 14, 917–925.

Mathurin F A, Åström M E, Laaksoharju M, Kalinowski B E, Tullborg E-L, 2012. Effect of tunnel excavation on source and mixing of groundwater in a coastal granitoidic fracture network. Environmental Science & Technology 46, 12779–12786.

Mathurin F A, Drake H, Tullborg E-L, Berger T, Peltola P, Kalinowski B E, Åström M E, 2014. High cesium concentrations in groundwater in the upper 1.2km of fractured crystalline rock – Influence of groundwater origin and secondary minerals. Geochimica et Cosmochimica Acta 132, 187–213.

Nilsson A-C, 2008. Laxemar site investigation. Quality of hydrochemical analyses (DF version 2.3) In Kalinowski B E (ed), Background complementary hydrogeochemical studies. Site descriptive modelling SDM-Site Laxemar. SKB R-08-111, Svensk Kärnbränslehantering AB, 131–148.

Nilsson A-C, Tullborg E-L, Smellie J, Gimeno M J, Gòmez J, Auqué L F, Sandstrom B, Pedersen K, 2011. SFR site investigation. Bedrock hydrogeochemistry. SKB R-11-06, Svensk Kärnbränslehantering AB.

Nilsson A-C, Gimeno M J, Tullborg E-L, Mathurin F A, Smellie J, 2013. Hydrogeochemical data report. Site descriptive modelling Äspö SDM. SKB R-13-26, Svensk Kärnbränslehantering AB.

Nordstrom D K, Lindblom S, Donahoe R J, Barton C C, 1989. Fluid inclusions in the Stripa granite and their possible influence on the groundwater chemistry. Geochimica et Cosmochimica Acta 53, 1741–1755.

Olofsson I, Christiansson R, Holmberg M, Carlsson A, Martin D, 2014. Application of the observational method in the Äspö expansion project. SKB R-13-44, Svensk Kärnbränslehantering AB.

Olsson M, Niklasson B, Wilson L, Andersson C, Christiansson R, 2004. Äspö HRL. Experiences of blasting of the TASQ tunnel. SKB R-04-73, Svensk Kärnbränslehantering AB.

Olsson M, Markström I, Pettersson A, Sträng M, 2009. Examination of the Excavation Damaged Zone in the TASS tunnel, Äspö HRL. SKB R-09-39, Svensk Kärnbränslehantering AB.

Patel S, Dahlström L-O, Stenberg L, 1997. Äspö Hard Rock Laboratory. Characterisation of the rock mass in the prototype repository at Äspö HRL, Stage 1. SKB PR HRL-97-24, Svensk Kärnbränslehantering AB.

Pedersen K, 2001. Diversity and activity of microorganisms in deep igneous rock aquifers of the Fennoscandian Shield. In Fredrickson J K, Fletcher M (eds). Subsurface microbiology and biogeochemistry. Chichester: Wiley, 97–139.

Pitkänen P, Löfman J, Koskinen L, Leino-Forsman H, Snellman M, 1999. Application of mass-balance and flow simulation calculations to interpretation of mixing at Äspö, Sweden. Applied Geochemistry 14, 893–905.

Pitkänen P, Partamies S, Luukkonen A, 2004. Hydrogeochemical interpretation of baseline groundwater conditions at the Olkiluoto site. Posiva 2003-07, Posiva Oy, Finland.

Punning J-M, Martma T, Kessel H, Vaikmäe R, 1988. The isotope composition of oxygen and carbon in the subfossil mollusc shells of the Baltic Sea as an indicator for paleosalinity. Boreas 17, 27–31.

Revey G F, 1996. Practical methods to reduce ammonia and nitrate levels in mine water. Mining Engineering 48, 61–64.

SKB, 2006. Long-term safety for KBS-3 repositories at Forsmark and Laxemar – a first evaluation. Main report of the SR-Can project. SKB TR-06-09, Svensk Kärnbränslehantering AB.

Smellie J, Laaksoharju M, 1992. The Äspö Hard Rock Laboratory: Final evaluation of the hydrogeochemical pre-investigations in relation to existing geologic and hydraulic conditions. SKB TR 92-31, Svensk Kärnbränslehantering AB.

Smellie J A T, Laaksoharju M, Wikberg P, 1995. Äspö, SE Sweden: a natural groundwater flow model derived from hydrogeochemical observations. Journal of Hydrology 172, 147–169.

Sohlenius G, Hedenström A, 2008. Geological development during the Quaternary period. In Söderbäck B (ed). Geological evolution, palaeoclimate and historical development of the Forsmark and Laxemar-Simpevarp areas. Site descriptive modelling. SDM-Site. SKB R-08-19, Svensk Kärnbränslehantering AB, 89–134

Stanfors R, Rhen I, Tullborg E-L, Wikberg P, 1999. Overview of geological and hydrogeological conditions of the Aspo Hard Rock Laboratory site. Applied Geochemistry 14, 819–834.

Tilly L, Ekvall J, Borg G C, Ouchterlony F, 2006. Vattenburna kväveutsläpp från sprängning och sprängstensmassor. SveBeFO Rapport 72, SveBeFo (Swedish Rock Engineering Research). (In Swedish.)

Waber H N, Gimmi T, Smellie J A T, 2012. Reconstruction of palaeoinfiltration during the Holocene using porewater data (Laxemar, Sweden). Geochimica et Cosmochimica Acta94, 109–127.

Wallin B, 2016. KBS-3H – DETUM Large fractures. Compilation of hydrogeochemical data from groundwater sampling in boreholes K08028F01 and K03009F01 at Äspö HRL. SKB P-15-10, Svensk Kärnbränslehantering AB.

Winberg A, Andersson P, Byegård J, Poteri A, Cvetkovic V, Dershowitz W, Doe T, Hermanson J, Gómez-Hernández J J, Hautojärvi A, Billaux D, Tullborg E-L, Holton D, Meier P, Medina A, 2003. Final report of the TRUE Block Scale project. 4. Synthesis of flow, transport and retention in the block scale. SKB TR-02-16, Svensk Kärnbränslehantering AB.

Arkitektkopia AB, Bromma, 2018

SKB is responsible for managing spent nuclear fuel and radioactive waste produced by the Swedish nuclear power plants such that man and the environment are protected in the near and distant future.

skb.se